National Technical University of Athens
School of Chemical Engineering

Department: Department of Process Analysis and Plant Design
Laboratory: Thermodynamics and Transport Phenomena Laboratory

Evaluation of Mercury Distribution Models in Process Simulators

DIPLOMA THESIS OF
Andreas Gompos

Supervisor: Epaminondas Voutsas, Associate Professor, NTUA

Athens, September 2015

Acknowledgements

This thesis would not have been possible without the guidance and the help of several individuals who in one way or another contributed to the completion of this study. Therefore, I would like to thank my supervisor at NTNU Even Solbraa as well as my co-supervisors Efstathios Skouras-Iliopoulos from Statoil and Epaminondas Voutsas from NTUA for their continuous guidance and support. I would like to thank Eleni Panteli from Statoil for the advice and encouragement she provided during this project and Christos Boukouvalas for the help that he so willingly provided. Last but not least, I would like to thank my parents for the unceasin encouragement, support and attention.

Περίληψη

Ο υδράργυρος είναι ένα στοιχείο που μπορεί να βρεθεί σε ίχνη σε όλα τα ορυκτά καύσιμα. Η ύπαρξη υδραργύρου σε υδρογονάνθρακες εγείρει ανησυχίες σχετικά με την υποβάθμιση εξοπλισμού, με την υγιεινή και ασφάλεια του προσωπικού πεδίου και με το περιβάλλον. Η υποβάθμιση του εξοπλισμού που προκαλείται λόγω του υδραργύρου, είναι μεγάλης σημασίας, ιδιαιτέρως για την βιομηχανία φυσικού αερίου, καθώς μπορεί να οδηγήσει σε αστοχία των εναλλακτών θερμότητας από αλουμίνιο έχοντας καταστροφικές συνέπειες.

Τόσο το γεγονός ότι ο υδράργυρος υπάρχει σε πολύ μικρές συγκεντρώσεις στα ορυκτά καύσιμα όσο και το ότι μπορεί να προκαλέσει σοβαρά ατυχήματα στην βιομηχανία του φυσικού αερίου, οδηγεί στην ανάγκη ύπαρξης μοντέλων υδραργύρου υψηλής ακρίβειας. Ως εκ τούτου, η αξιολόγηση των διαθέσιμων μοντέλων υδραργύρου είναι απαραίτητη. Σκοπός αυτής της διπλωματικής εργασίας είναι η αξιολόγηση διαφορετικών μοντέλων υδραργύρου συγκρίνοντάς τα με δεδομένα διαλυτότητας και εφαρμόζοντάς τα σε διάφορους προσομοιωτές ώστε να γίνει προσομοίωση δύο διαφορετικών εγκαταστάσεων επεξεργασίας φυσικού αερίου με στόχο την σύγκριση των μοντέλων με πειραματικά δεδομένα πεδίου.

Για το σκοπό αυτό, πραγματοποιήθηκε βιβλιογραφική ανασκόπηση ώστε να βρεθούν όλα τα διαθέσιμα μοντέλα υδραργύρου. Όλα τα μοντέλα που βρέθηκαν χρησιμοποιούν τις καταστατικές εξισώσεις Peng-Robinson(PR) και Soave-Redlich-Kwong(SRK) με διαφορετικές εκφράσεις για την συνάρτηση άλφα καθώς και διαφορετικούς συντελεστές αλληλεπίδρασης. Διαθέσιμο για αξιολόγηση ήταν επίσης ένα μοντέλο που αναπτύχθηκε από την Statoil, που αναφέρεται ως SRK-Twu(Hg), όπως επίσης και το UMR-PRMC που αναπτύχθηκε από τον Βουτσά και τους συνεργάτες του.

Τα μοντέλα που επιλέχθηκαν για αξιολόγηση περιλαμβάνουν τα μοντέλα PR και SRK χωρίς συντελεστές αλληλεπίδρασης για τον υδράργυρο. Επίσης αξιολογήθηκαν τα μοντέλα PR και SRK του πακέτου PRO/II. Αυτά τα δύο μοντέλα χρησιμοποιούν συντελεστές αλληλεπίδρασης και επομένως βελτιώνουν την ικανότητα πρόβλεψης του μοντέλου στην υγρή φάση. Επιπλέον, αξιολογήθηκαν τα μοντέλα SRK-Twu και PRMC. Αυτά τα μοντέλα χρησιμοποιούν προηγμένες εκφράσεις για την συνάρτηση άλφα, κάτι που οδηγεί σε σημαντική βελτίωση της ικανότητας πρόβλεψης του μοντέλου για την αέρια φάση. Το μοντέλο SRK-Twu(Hg) της Statoil χρησιμοποιεί τόσο μία προηγμένη έκφραση της συνάρτησης άλφα όσο και συντελεστές αλληλεπίδρασης. Τέλος, το UMR-PRMC χρησιμοποιεί την καταστατική εξίσωση PRMC αλλά αντί των κλασσικών κανόνων ανάμιξης χρησιμοποιεί τις «universal mixing rules». Αυτοί οι κανόνες ανάμιξης χρησιμοποιούν τις παραμέτρους συνεισφοράς ομάδων Unifac αντί των παραμέτρων αλληλεπίδρασης. Τα δύο τελευταία μοντέλα βελτιώνουν την ικανότητα πρόβλεψης τόσο για την υγρή όσο και για την αέρια φάση.

Τα μοντέλα επιλέχθηκαν έτσι ώστε να αξιολογηθεί η συμπεριφορά των μοντέλων όταν διορθώνεται η ικανότητα πρόρρησης για την αέρια φάση(SRK-Twu and PRMC), για την υγρή φάση (SRK PRO/II default, PR PRO/II default), για καμία φάση (SRK and PR) και για τις δύο φάσεις(SRK-Twu(Hg), UMR-PRMC). Διαπιστώθηκε ότι αν διορθωθεί η ικανότητα πρόρρησης μόνο για μία από τις δύο φάσεις τότε είναι πιθανό η ικανότητα πρόρρησης για την κατανομή υδραργύρου να χειροτερέψει. Ως εκ τούτου, συνίσταται η ταυτόχρονη χρήση διόρθωσης και για τις δύο φάσεις.

Τα αποτελέσματα της αξιολόγησης που έγινε υποδεικνύουν ότι το μοντέλο που αναπτύχθηκε από την Statoil καθώς και το UMR-PRMC είναι τα ακριβέστερα μοντέλα από αυτά που δοκιμάστηκαν και θεωρούνται αξιόπιστα. Το επόμενο καλύτερο μοντέλο βρέθηκε ότι είναι το PR PRO/II default του πακέτου PRO/II αλλά συνίσταται να χρησιμοποιείται με προσοχή. Κανένα από τα υπόλοιπα μοντέλα δεν ήταν ικανά για πρόρρηση της κατανομής υδραργύρου ενώ τα χειρότερα μοντέλα βρέθηκαν να είναι τα SRK και SRK PRO/II default.

ΛΕΞΕΙΣ ΚΛΕΙΔΙΑ: υδράργυρος, μοντέλο υδραργύρου, κατανομή υδραργύρου, προσομοίωση, φυσικό αέριο

Abstract

Mercury is a trace component that can be found in all fossil fuels. Mercury's existence in hydrocarbons raises concerns about equipment degradation, about the health and safety of the field personnel and about the environment. Equipment degradation, caused by mercury, is of great importance, especially for the gas industry, because it can lead rapidly to catastrophic failures of the aluminum heat exchangers.

Both the fact that mercury exists at very low concentrations in fossil fuels and that it can cause major accidents in the natural gas industry, leads to the need of very accurate models for mercury. Therefore, an evaluation of the available models for mercury is necessary. The scope of this thesis is to evaluate different models by comparing them to solubility data and by implementing them in different process simulators, to simulate two natural gas processing plants, in order to compare the predictions given by the simulations to field data.

To this purpose, a literature review was conducted to find all the available models for mercury. All the models found, use the Peng-Robinson(PR) and Soave-Redlich-Kwong(SRK) equations of state as their basis with varying expressions for the alpha function and different binary interaction parameters. A model developed by Statoil, referred to as SRK-Twu(Hg), was alos available for evaluation as was UMR-PRMC proposed by Voutsas et al.

The models that were selected for evaluation included the PR and SRK models with no binary interaction parameters for mercury. Also, the PR and SRK models found in the PRO/II software package were evaluated. These two models use binary interaction parameters and therefore they improve the prediction ability of the model for the liquid phase. Additionally, the SRK-Twu and PRMC models were tested. These models use advanced expressions for the alpha function, which results in a major improvement of the predictive ability for the vapor phase. The SRK-Twu(Hg) by Statoil uses both an advanced expression for the alpha function and binary interaction parameters. Finally, the UMR-PRMC uses the PRMC model, but instead of the classical mixing rules, it introduces the universal mixing rules. These mixing rules use the Unifac contribution group parameters instead of binary interaction parameters. The two last models improve the prediction ability for both the liquid and vapor phase.

These models were selected in such a way, in order to evaluate how the models behave when vapor phase correction is used (SRK-Twu and PRMC), when liquid phase correction is used(default PRO/II SRK and PR), when no correction is used (SRK and PR) and finally when both corrections are used (SRK-Twu(Hg), UMR-PRMC). It was found that if one uses for their model only vapor phase correction or only liquid phase correction they could possibly get worse results for mercury's distribution. Therefore, it is recommended that both vapor phase and liquid phase corrections should be applied at the same time.

The results of the evaluation indicate that the model developed by Statoil and the UMR-PRMC model are the most accurate of the models tested and are considered reliable. The next best model was found to be the PR PRO/II default model, but it is recommended to be used with caution. All the other models, were found unable to predict mercury's distribution, with the worst models being the SRK and the SRK PRO/II default models.

KEY WORDS: mercury, mercury model, mercury distribution, simulation, natural gas

Table of Contents

List of Tables

List of Figures

Nomenclature

Latin Letters

α	Attractive parameter of a cubic EoS
b	Co-volume parameter of a cubic EoS
k	Interaction parameter
m	Parameter in α parameter of EoS
P	Pressure
R	Gas constant
T	Temperature
V	Volume
x	Molar fraction for the liquid phase
y	Molar fraction for the vapor phase

Greek Letters

γ	Activity coefficient
ω	Acentric factor

Subscripts

ij	Cross parameter (defined by the combining rules)
c	Critical

Abbreviations

CN	Carbon Number
EoS	Equation of State
MC	Mathias Copeman expression for the alpha function
NG	Natural Gas
PR	Peng-Robinson cubic EoS
SRK	Soave-Redlich-Kwong cubic EoS
THg	Total mercury
UMR	Universal Mixing Rules

1. Introduction

Mercury is a trace component that can be found in all fossil fuels including natural gas, gas condensates, crude oil, coal, tar sands and other bitumens. The concentration of mercury in crude oil and natural gas is highly dependent on geologic location and issues associated with it have become more apparent as deeper and hotter reservoirs are exploited.

Mercury's existence in hydrocarbons raises concerns about equipment degradation, about health and safety matters of the field personnel and about the environment, since it is designated as a persistent, bioaccumulative and toxic pollutant. Equipment degradation, caused by mercury, is of great importance, especially for the gas industry, because it can lead rapidly to catastrophic failures of the aluminum heat exchangers (Cold Boxes). One such accident happened in 1973, when a catastrophic failure of an aluminium heat exchanger occurred at Skikda LNG plant in Algeria and led to a plant explosion [1]. It is, therefore, of great importance for operators to have models that are able to accurately predict mercury's distribution in a processing plant. However, very limited data are available on mercury modelling in the literature, since the models developed by different companies have not been published.

Both the fact that mercury exists at very low concentrations in fossil fuels and the fact that it can cause major accidents in the natural gas industry, leads to the need of very accurate models for the prediction of its distribution in a processing facility. Therefore, an evaluation of the available models for mercury is necessary and in this work this evaluation is made by comparing different models to solubility data and using them in different process simulators, in order to simulate two natural gas processing plants.

In Chapter 2, the theoretical background about mercury and the concerns associated with it will be discussed. Then, in Chapter 3, all the considered models will be presented and some of these models will be selected for further evaluation. In Chapter 4, the evaluation of the selected models will be presented and discussed. All the models are used in Chapter 5, for the simulation of one natural gas processing plant where no field data are available to further evaluate the models. Then, the most accurate model is used, for the simulation of another natural gas processing plant, where it is compared to field data, since they are now available. Finally, in Chapter 6 and Chapter 7, conclusions and future work proposals will be given respectively.

2. Theoretical Background

The U.S. EPA designates mercury and its common chemical forms as persistent, bioaccumulative and toxic pollutants. Mercury enters the global mercury cycle from both natural sources, such as volcanic activity and dissolution of mercury mineral in oceans, and human activities such as industrial activities and combustion of fossil fuels.

Mercury occurs mostly in the elemental form or in the inorganic form. Mercury in the atmosphere is mostly elemental, but most of the mercury in water, soil, sediments, plants and animals is in the form of inorganic mercury salts and organometallics (mostly methylmercury). [2]

Mercury is a trace component that can be found in all fossil fuels including natural gas, gas condensates, crude oil, coal, tar sands and other bitumens. The concentration of mercury in crude oil and natural gas is highly dependent on geologic location and varies between approximately 0.01 ppb and 10 ppm (wt.). Mercury deposits are often associated with geological plate boundaries fold belts and areas with volcanic or hydrothermal activity. Issues associated with mercury have become more apparent as deeper and hotter reservoirs are exploited, since higher levels of mercury are found there. In the following table regional estimated levels of mercury in natural gas and condensates are shown. [3, 4]

Table 2.1: Regional Estimated Levels of Mercury in Natural Gas and Condensates.[3]

Location	Estimated mercury in natural gas and condensate for world regions	
	Gas (μg/m^3)	Liquids (μg/kg)
Europe	100-150	-
South America	50-120	50-100
Gulf of Thailand	100-400	400-1200
Africa	80-100	500-1000
Gulf of Mexico (USA)	0.02-0.4	-
Overthrust Belt (USA)	5-15	1-5
North Africa	50-80	20-50
Malaysia	1-200	10-100
Indonesia	200-300	10-500

In addition to the contribution of geologic mercury to atmospheric pollution, mercury in oil and gas has a direct negative impact on petroleum processes. These impacts include equipment degradation, toxic waste generation, increased risk to the health and safety of workers and poisoning of catalysts. Mercury in plant feeds often requires process modifications to avoid the negative impacts and to comply with product specifications

2.1 Natural Gas

The evaluation made in this work has two main parts. The comparison of models against experimental solubility data of mercury in different components and the evaluation of the models in case studies for different natural gas processing facilities. Therefore, a short description will be made about natural gas and about the processing of natural gas in a processing plant.

Natural gas is a mixture of light hydrocarbon gases at ambient pressure and temperature. Natural gas is colorless, odorless, tasteless and lighter than air and is used primarily as a fuel and as a raw material in manufacturing. In home, it is used for furnaces, water heaters and cooking stoves and as an industrial fuel is used for generating steam in water boilers and as a clean heat source for sterilizing instruments and processing foods. As a raw material it is used for hydrogen, sulfur, carbon black and ammonia production.

Natural gas is considered environmentally friendly when comparing to other fossil fuels due to low sulfur dioxide, nitrous oxide and carbon dioxide emissions which help reduce acid rain, ozone layer and greenhouse gases. However, because of the storage difficulties and the lack of transporting structures the use of natural gas had remained limited until 1920s. [5]

Natural gas exists in nature under pressure in rock reservoirs, formed by organic matter degradation on the past millions of years, in the Earth's crust by itself or dissolved in heavier hydrocarbons and water. Natural gas consists mainly of methane. Other constituents include ethane, propane, butanes and small proportion of C_5+ hydrocarbons. Toxic compounds can also be present, such as benzene, toluene and xylenes while trace components include sulfur, nitrogen, halogen and heavy metal compounds, like mercury. Although the composition of natural gas varies depending on the field from which it is extracted a typical composition of natural gas can be found below:

Table 2.2: Typical Composition of Natural Gas

Name	Volume (%)
Methane	>85
Ethane	3-8
Propane	1-2
Butane	<1
Pentane	<1
Carbon Dioxide	1-2
Hydrogen Sulfide	<1
Nitrogen	1-5
Helium	<0.5

2.2 Natural Gas Processing

Raw natural gas must be processed before its distribution to end consumers in order to separate natural gas, condensate, noncondensable, acid gases and water. The plant is also necessary to control excess hydrocarbon liquid and to control delivery pressure. The typical process operation modules can be found at the figure below.

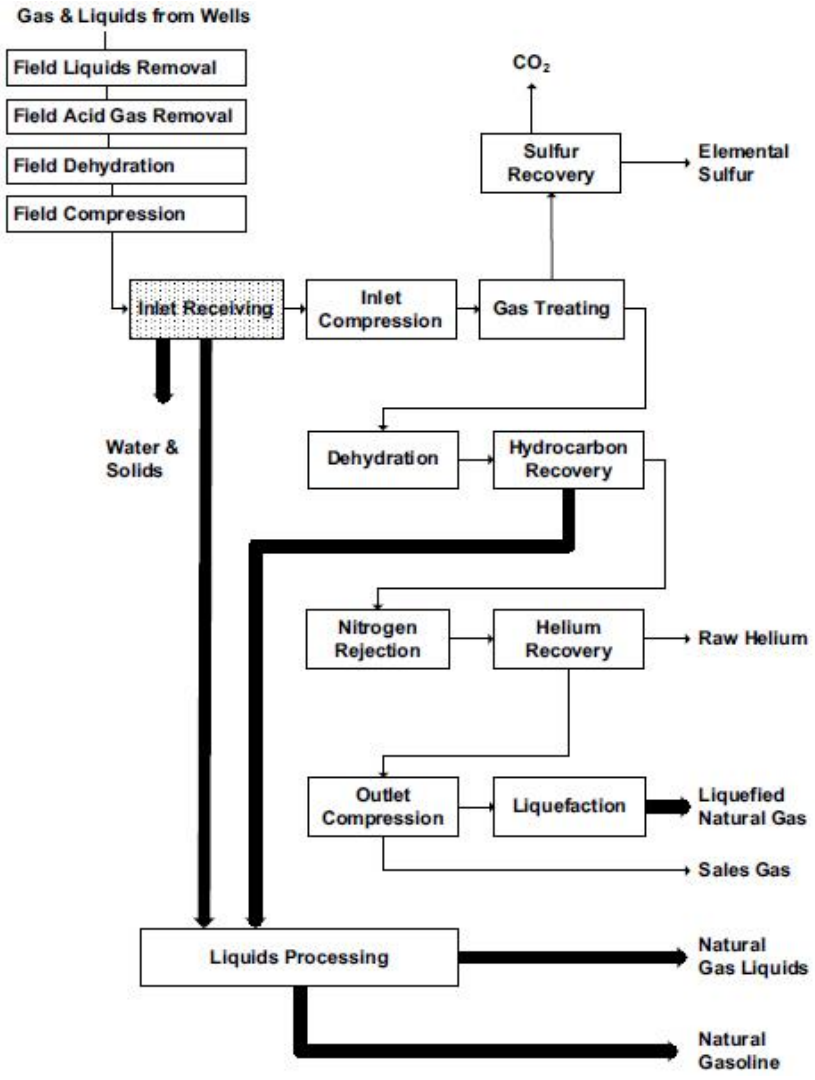

Figure 2.1: Typical Process Operation Modules for a Gas Processing Facility[6]

Physical Separation

At a typical gas processing plant, the raw gas entering the facilities goes to the inlet receiving. There a physical separation of the distinct phases is made. In this process, liquid water, hydrocarbon liquids and solids are removed. Water and solids are processed for disposal and the hydrocarbon condensate is typically stabilized to produce a safe transportable liquid.

Acid Gas Treating Facilities

After the physical separation, the gas continues to the gas treating facilities where acid gas treating takes place and mercury is removed. During the acid gas treating carbon dioxide (CO_2),

hydrogen sulfide (H_2S) and other sulfur-containing species such as mercaptans are removed. These compounds must be removed since hydrogen sulfide and carbon dioxide, in the presence of water, form sulfuric acid and carbonic acid respectively. This raises corrosion and toxicity issues. Most plants use water-based absorbents to remove these impurities but in general, two processes are used for acid gas removal. The first is adsorption, carbon being the adsorbing medium. In this case, hot air or steam can be used for desorbing the captured gas for recovery or for thermal destruction. The second process is absorption. For this process water, aqueous amine solutions, caustic, sodium carbonate and nonvolatile hydrocarbon oils can be used as absorbing media depending on the type of gas to be absorbed. [6]

Mercury Removal

In the gas treating facilities, mercury removal units (MRU) can be used since mercury can often be present in natural gas. Mercury is known to damage aluminum heat exchangers to the point of catastrophic failure and therefore its removal is necessary. Both regenerative and nonregenerative processes are available for the removal of mercury from gas and liquid streams. Most of the nonregenerative processes use sulfur, impregnated on a support, such as activated charcoal or alumina, to provide a large surface area. This impregnated sulfur reacts with mercury to form a stable compound on the adsorbent surface. The regenerative processes utilize silver on molecular sieve to chemisorb elemental mercury while providing dehydration at the same time. The mercury-silver amalgam that is formed decomposes at typical regeneration temperatures for dehydration and essentially all of the mercury condenses with the water on regeneration and form a separate phase, which can easily be decanted. [7-9]

Dehydration

The gas leaving the gas treating facilities is usually water saturated, thus making the dehydration step necessary. The dehydration is necessary because natural gas in the right conditions can combine with liquid or free water to form solid hydrates that can plug valves fittings and pipelines. Water can also cause erosion and corrosion if condensed in the pipeline. Moreover, water vapor increases the volume and decreases the heating value of the gas. The most common methods for dehydrating natural gas are liquid desiccant (glycol) dehydration and solid desiccant dehydration. In these two methods water molecules are transferred into a liquid solvent (glycol solution) or a crystalline structure (dry desiccant). Another method is refrigeration. In this method the stream is cooled and water is condensed while an inhibitor to prevent hydrate formation is injected. [5, 6]

Hydrocarbon Recovery

Generally in a gas processing plant apart from the sales gas, which is rich in methane, liquid heavier products can be produced. These heavier hydrocarbon liquids, referred to as natural gas liquids (NGLs), include ethane, propane, butanes and natural gasoline (condensate). It should be noted that the recovery of NGL components yields a source of revenue, since NGLs normally have greater value as separate products than as part of the natural gas stream.

Pipeline quality natural gas specifications include apart from limits on sulfur and water content also a higher heating value specification(35400 to 42800 kJ/Sm^3) [10]. The heating value may be too high because of C_2+ fraction present in the treated gas, which makes the hydrocarbon recovery necessary. Hydrocarbon recovery is also required in field operations for fuel conditioning or dew point control. By controlling dew point, hydrocarbon condensation can be

prevented in cold spots, such as under rivers or lakes, where the liquid collect in the low areas and then move as a slug through the system.

NGL can be separated from the gas using many different processes. The separation can be done with refrigeration processes or even with lean oil absorption, solid bed adsorption and membrane separation processes. Then, the NGL can be sold as mixed product or it can be fractionated into its various components using a series of distillation columns. A general scheme of the fractionation part can be seen at the following figure. [5, 6]

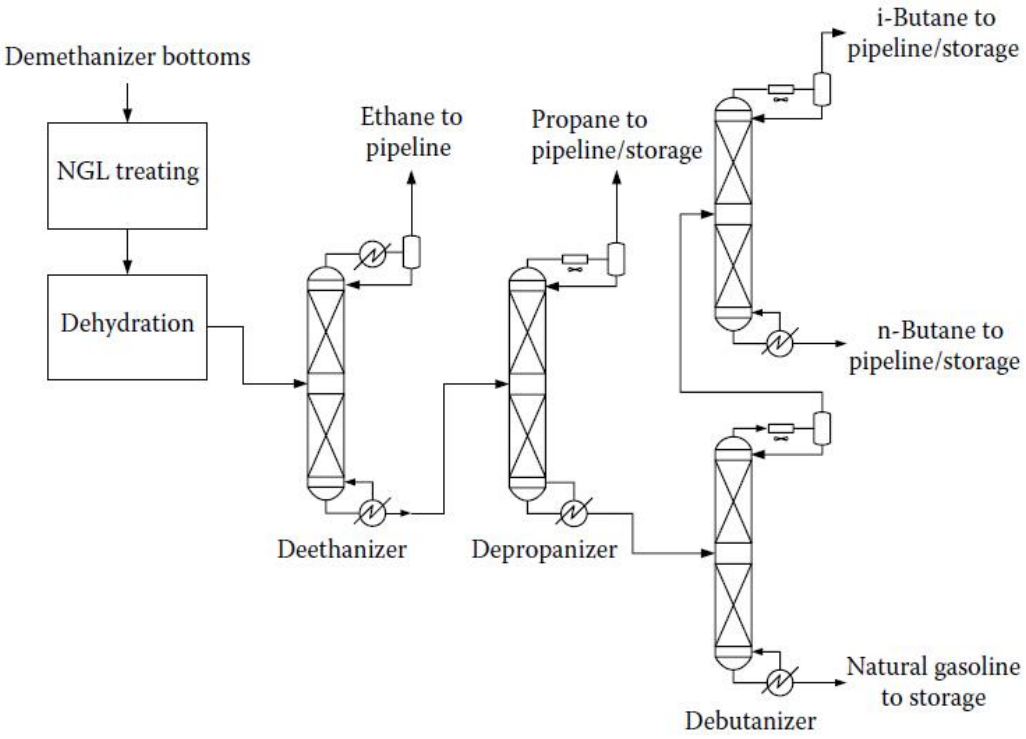

Figure 2.2: General Scheme of the Fractionation Part.[6]

Other processes

Other processes in a gas processing plant involve nitrogen rejection, helium and sulfur recovery. As regards nitrogen rejection, it is used for lower-quality gas feedstock in order to produce pipeline quality gas and the process used is typically cryogenic. The removed nitrogen from the natural gas can then be used in an enhanced oil recovery (EOR) operation, just like CO_2.

Helium recovery is used only if helium content is above 0.5 vol%. Helium is a valuable product from natural gas processing and therefore high concentrations are desirable.

As regards sulfur recovery, this process is required if venting the H_2S exceeds the environmental limits. The alternative way of dealing with H_2S is its disposal by injection into underground formations. [5, 6]

2.3 Mercury

Mercury is a chemical compound also known as quicksilver or hydrargyrum. It is a d-block element and is the only metallic element that is liquid at standard conditions for temperature and pressure. Mercury is a poor conductor of heat, but a fair conductor of electricity. Mercury behaves similarly to nobble gas elements, forming weak bonds and thus melting at relatively low temperatures, because of its electron configuration.

Mercury is a very rare element in the Earth's crust. However, mercury does not blend geochemically with the elements that contribute to the majority of the crustal mass and thus mercury ores can be concentrated extraordinarily considering the abundance of the element in ordinary rock [11].

Mercury's existence in hydrocarbons raises concerns about equipment degradation, about health and safety matters of the field personnel, mostly during opening equipment or during hot work, and about the environment. Mercury is designated as persistent, bioaccumulative and toxic pollutant. The different forms of mercury show different toxicity levels. Organic species of mercury are the most toxic form of mercury, while inorganic mercury (inorganic salts) are considered to be less toxic but they can also bioaccumulate.

2.3.1 Mercury Species

Mercury in most forms is toxic and contributes to health, safety, and environmental risks. In natural gas, mercury occurs as the metallic form. Various forms of mercury, elemental, organometallic, and inorganic salt, can be present in natural gas condensates, depending on the origin of the condensates [3]. Mercury can be found in nature in the zero (elemental), +1 (mercurous), or the +2 (mercuric) valence state. Mercurous compounds involve Hg-Hg bonds and are generally unstable and rare in nature.

Mercury's forms can be grouped in the following categories [2].

1. **Organic Mercury (dissolved)**
   In this species, a mercury atom has at least one bond to a carbon atom: R-Hg-R or R-Hg-X.
   Where R=CH_3 (most common), C_2H_5, etc. and X=Cl, nitrate, sulfate, hydroxide or another anion.

   The most prominent R-Hg-R compound is dimethylmercury. Mercury is difficult to oxidize and can be oxidized only by strong oxidants such as halogens, hydrogen, peroxide, nitric acid and concentrated sulfuric acid. Mercury can also be oxidized and methylated by sulfate-reducing bacteria in sediments. Under ambient conditions, elemental mercury readily forms amalgams with silver, gold, copper, zinc and aluminum.

2. **Inorganic Mercury Salt**
   Some of these species are water-soluble: $(HgX)^+$ or HgX_2, where X is an inorganic ion. The water-soluble group is also characterized like ionic mercury. However, some mercuric halides remain unionized in aqueous and organic solutions, like $HgCl_2^0$, which is soluble in oil. The most common insoluble forms of inorganic salts are mercury sulfide (HgS) and mercuric oxide (HgO).

3. **Elemental Mercury (Hg^0)**
   Elemental mercury may be present in dissolved or particulate form. It corresponds to metallic mercury and it is the most common specie in most hydrocarbon matrices. Elemental mercury has a high vapor pressure, comparing to the other forms of mercury and relatively low solubility in water, 0.05 ppm. Elemental mercury is soluble to liquid hydrocarbons to a few (1-3) ppm. Elemental mercury adsorbs on metallic surfaces and on solid materials (sand) suspended in liquids, and reacts with iron oxide corrosion products on pipe and equipment walls. The solubility of Hg^0 depends strongly on temperature, which could cause Hg^0's precipitation in equipment, when saturated liquids are cooled**.** Mercury in the atmosphere is most commonly found in the elemental form. [4]

2.3.2 Mercury in Hydrocarbons

Elemental mercury and mercury compounds occur naturally in geologic hydrocarbons including coal, natural gas, gas condensates and crude oil. As regards natural gas, mercury can be almost exclusively found only in its elemental form and at concentrations far below saturation, thus preventing the existence of liquid mercury phase formation in most reservoirs.

Several chemical forms of mercury are contained in crude oil and gas condensate [2]:

1. Dissolved elemental mercury (Hg^0): Elemental mercury is soluble in hydrocarbon liquids in atomic form to a few ppm. Elemental mercury adsorbs on metallic components, suspended wax and sand, and thus mercury concentration of dissolved elemental mercury typically decreases with distance from the wellhead due to adsorption, reaction with iron or conversion to other forms.
2. Dissolved organic mercury (RHgR and RHgX, where R=CH_3, C_2H_5, etc. and X = Cl or other inorganic anion): Dissolved organic mercury compounds are highly soluble in crude oil and gas condensate and are adsorptive similarly to elemental mercury.
3. Inorganic (ionic) mercury salts ($Hg^{2+}X$ or$Hg^{2+}X2$, where X is an inorganic ion): Mercury salts are soluble in oil and gas condensate but prefer to partition to the water phase. Mercuric chlorides have a reasonably high solubility in organic liquids and ionic salts also may be physically suspended in oil or may be adsorbed to suspended particles.[2]
4. Complexed mercury (HgK or HgK_2): Mercury can exist in hydrocarbons as a complex, where K is a ligand such as an organic acid, porphyrin or thiol.
5. Suspended mercury compounds (HgS, HgSe): Mercury in this form is insoluble to water and oil but could be present as suspended solid particles of very small particle size.
   HgS is formed in the presence of both mercury and hydrogen sulfide, which can settle out in tanks and deposit in equipment:
   $$Hg^0 + H_2S \leftrightarrow HgS(s)$$
6. Suspended adsorbed mercury: Elemental and organic mercury, in this form, is adsorbed on particles like sand or wax. Suspended mercury compounds can be separated from liquid feeds to the plant by physical separation techniques such as filtration or centrifugation.

An approximation of natural abundance of mercury compounds in hydrocarbons can be found at the following table.

Table 2.3: Approximation of Natural Abundance of Mercury Compounds in Hydrocarbons [2]

	Coil	Natural Gas	Gas Condensate	Crude Oil
Hg^0	Trace	Dominant	Dominant	Dominant
$(CH_3)_2Hg$	?	Trace	T, (Some?)	Trace, (Some?)
$HgCl_2$	Some?	None	Some	Some
HgS	Dominant	None	Suspended	Suspended
HgO	Trace?	None	None	None
CH_3HgCl	?	None	Trace?	Trace?

Where "?" indicates that data are not conclusive

2.3.3 Mercury's Partitioning during Processing

Very little data are available that could show how mercury distributes in a refining or in a gas process. Calculations of mercury's distribution could be made as long as experimental data and accurate models for mercury are available. The partitioning of mercury into product and effluent streams in petroleum processing is largely determined by solubility. Pressure and temperature changes during processing produce the major redistribution of mercury compounds in process separations. Predictive calculations are easier when low temperature processes are involved because chemical reactions to transform one mercury species to another typically occur less at low temperatures. On the other hand, some high temperature refinery processes make predictive calculations more difficult, because now chemical reactions exist.

Mercury is more soluble in heavier hydrocarbons compared to the lighter ones of the same type, meaning normal alkanes, cycloalkanes, aromatic hydrocarbons and branched Hg. The branched alkanes dissolve the least amount of Hg. For all hydrocarbons the order of their ability to dissolve Hg is as follows: branched alkanes<normal alkanes<cycloalkanes<aromatic hydrocarbons. For the hydrocarbons with six atoms there is a difference at the order of the aromatic hydrocarbons and the cycloalkanes. Aromatic hydrocarbons and cycloalkanes, at some cases, can dissolve more Hg than normal alkanes even if the normal alkanes have more carbon atoms than the aromatic hydrocarbons. In general, more Hg could be expected in the heavy hydrocarbon streams in a real process. [12]

Broad generalities about mercury distribution are possible:

During Extraction

The fluid produced at the wellhead contains both the dissolved and suspended forms of mercury. The fluid goes through separators so that a primary phase separation of hydrocarbon liquids, gas and water is accomplished. Most of the suspended mercury will be retained in the liquid phases that separate, strictly due to gravity or it will be retained in the separator as sludge. As regards dissolved forms of mercury, in general, purely ionic mercury should partition preferentially to the water phase while elemental and organic forms should be retained by the liquid hydrocarbon phase. [2]

During Transportation

During transportation of fluids, mercury is not lost as regards mercury in oil. This is not always the case for gas though. During transportation of wet gas in steel pipelines, a reaction between steel corrosion products and elemental mercury takes place and thus a mercury-rich layer is created on pipeline walls. Because of that, the time to detect mercury at the end of a pipeline is dependent on the length of that pipeline. The reaction is catalyzed by the presence of H_2S in trace quantities and driven by the following reactions. [2, 8]

$$H_2S + Fe_2O_3 \rightarrow FeO + S + H_2O$$

$$Hg + S \rightarrow HgS$$

During Refining

During oil refining, general rules apply to all operations but little is known about what happens to mercury during unit operations such as catalytic cracking or visbreaking. Crude oil goes through a desalting process where it is washed with water in order to remove soluble salts. During this process, suspended mercury and ionic species that have affinity for water are removed. Thus, downstream of the desalting unit, oil should contain higher percentages of the elemental and complexed species of mercury. The distribution of total mercury in crude oil to primary distillation products trends to be lower in heavier products [4]. If a crude feed contains large amounts of suspended mercury, then HgS would remain in heavier products and in the residue. HgS in residue could then find its way to the atmosphere after having been converted to Hg^0 or HgO, after its use as a fuel for combustion in a fire boiler.

In the following figure, mercury's separation in an oil field separation system is shown. The system is part of a mercury removal process applied to crude oil of Southern Argentina [13]. There it was found that during the lifting process the larger drops of mercury, being in ionic or elemental form, tend to separate towards the aqueous phase, while the smaller ones remained suspended inside the hydrocarbon phase. Elemental mercury was the primary form of mercury in the gas phase. Drops of elemental mercury condense and adhere to the walls of the pipelines and vessels, creating mud deposits in association with other solids, such as oxides, sand and clay. [13]

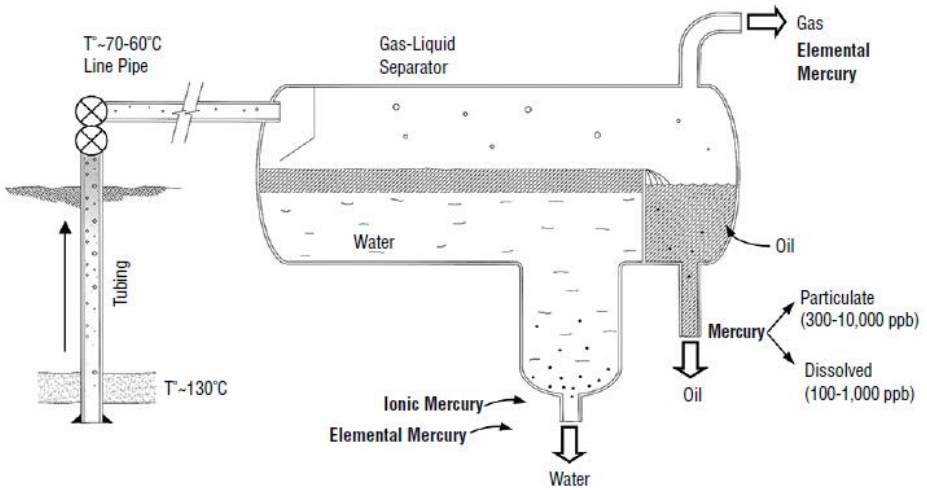

Figure 2.3: Mercury's distribution in an oil field separation system. [13]

Mercury's Fate in a Natural Gas Processing Facility

Mercury's distribution in gas processing is easier to predict, as the process is simpler and less inclined to cause species' transformations. Fluids from gas wells typically contain lesser amounts of suspended and ionic mercury compounds than those found in crude oil. Mercury is highly mobile and bonds to metal surfaces with which it comes into contact. The implication of this is that any mercury that enters a gas processing plant will be distributed across process and waste streams [8]. In general, organic mercury preferentially partition to heavy liquid fractions (condensate) and ionic compounds partition to water, while elemental mercury equilibrates between liquid and gas fractions [11, 14, 15]**.** Between the hydrocarbon and the aqueous phase, elemental mercury partitions predominantly to the hydrocarbon liquid phase except where the aqueous phase contains alcohols such as mono-ethylene glycol. [16]

The elemental mercury in gas will dissolve in the liquid glycol dehydrators during treatment for contaminants, but if the concentration of mercury is high enough, then elemental mercury vapor can condense in the glycol reboiler vapor condenser [2]. The lean glycol is put through heat exchangers to drive off accumulated impurities, which are either vented or flared. While the solubility of mercury in glycol is low, high concentrations are found in the vented gas. A potential explanation is that mercury is in suspension attached to fine sulphur particles, or alternatively that the gas contains hydrocarbon residues [8].

In amine systems, mercury can react with the H_2S scavenged by the amine to transform into HgS, which could then be found in the amine filters [2]. Elemental mercury could condense during cryogenic separation processes especially when mercury in feeds is in excess of approximately 10-20 ug/m^3. Mercury is also known to concentrate on molecular sieves, since mercury is absorbed onto metals [8]. In a report by Johnson Matthey Catalysts [17], it is stated that up to half of the mercury present in the raw gas is likely to be removed on the acid gas removal and drying stages, due to mercury's high volatility.

2.3.4 Concerns about Mercury

In natural gas processing plants considerable quantities of mercury can collect in the cryogenic heat exchangers. The substantial amounts of mercury are derived from traces of mercury present in natural gas which can condense and collect in cold parts of the system. Typically mercury would condense onto surfaces in the solid form (i.e. at temperatures less than -39 ^{0}C) and would only melt during shut down periods when it would be expected to collect in low points in the manifolds and pipework in the heat exchanger system. [18]

Deposition of liquid elemental mercury in aluminium heat exchangers can compromise their structural integrity. The equipment degradation is a particular concern for LNG plants and since the level of mercury that can be tolerated is not established, most operators want to remove it "all", meaning to remove it to a level where it cannot be detected with the available analytical capability. At this moment, this level is 0.01 μg/Nm^3 and this limit is the desirable maximum concertation at the feed. [19]

Mercury creates a risk of corrosion and liquid metal embrittlement of Al, Zn and Cu and can cause cracking of welded aluminum heat exchangers, as it tends to deposit in cryogenic equipment. Mercury is also responsible for contamination of molecular sieves and glycol dehydration units, amine acid gas removal systems and catalysts. Mercury could also cause health and safety risk because of potential personnel exposure to mercury vapor in vents or in

waste sludge where mercury is accumulated, even in small amounts**.** Furthermore, waste-water streams containing high levels of mercury must be treated before disposal thus adding costs to plant's expenses. Environmental risk also exists because of mercury contamination in produced water disposal and because of the combustion of fossil fuels within the processing facility.

2.3.4.1 Technical Problems

The main concern about mercury is aluminium equipment degradation, especially in aluminium heat exchangers or cold boxes where mercury can condense. However, it should be noted that mercury in the form of $HgS_{(s)}$ could cause problems such as fouling and plugging of compact equipment. Mercury can also cause catalyst poisoning in different catalysts such as the hydrotreating catalysts due to metal amalgamation. Following, there is a description of the mechanisms that can lead to equipment degradation because of the presence of mercury.

Mercury's Mechanism for Aluminum Degrading

Mercury in natural gas occurs at very low levels, but it can accumulate and cause severe attack and failure in cryogenic aluminum heat exchangers, which are typically aluminum plate-fin heat exchangers. Condensation or precipitation of solid mercury can occur in heat exchanger passes, even with functional mercury removal systems in place [18]. Solid deposits become liquid when heat exchangers warm during a shutdown or when a trip is triggered, leading to a catastrophic failure of aluminum heat exchangers. Implications of the effect of mercury in natural gas were first reported in 1973, when a catastrophic failure of an aluminium heat exchanger occurred at LNG plant in Algeria. There, it was found that a combination of mercury and water temperatures around 0 ^{0}C caused corrosion in the aluminium tubes [1].

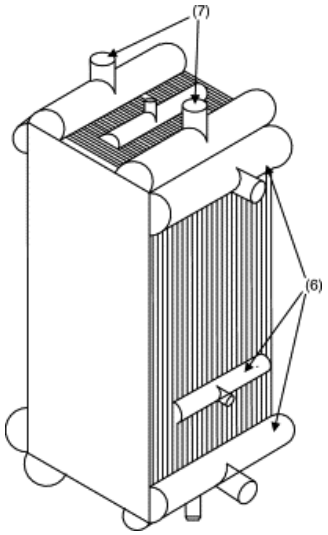

Figure 2.4: Schematic View of Cryogenic Heat Exchanger Showing the Manifolds (6) and nozzles (7) [18]

Amalgamation

In this process, mercury can form liquid solutions with various metals such Al, Au, Ag and Zn. As regards Al, the amalgam reaction starts when mercury wets the aluminium metal surface, but this is generally prevented by an Al_2O_3 protective surface oxide, which is placed on the aluminium metal surface. Mercury can migrate through this surface oxide if existing defects of this surface are increased, which could be a result of thermal or mechanical stresses. Additionally, abrasion and some chemical environments can destroy the protective oxide layer.

It should be noted, that for aluminium, the concentration of aluminium in the amalgam is low, further limiting the depth of the attack. [18]

Amalgam reaction:

$$Hg + Al \rightarrow Hg(Al)$$

Amalgam Corrosion

Amalgam corrosion is a process that takes place with moisture and minimum amounts of mercury. Small amounts of aluminium dissolve in liquid mercury and diffuse to the mercury-moist air surface and finally oxidize. In this process, aluminum is removed from the mercury and more mercury can dissolve and this process can continue until the aluminium is completely converted to oxide.

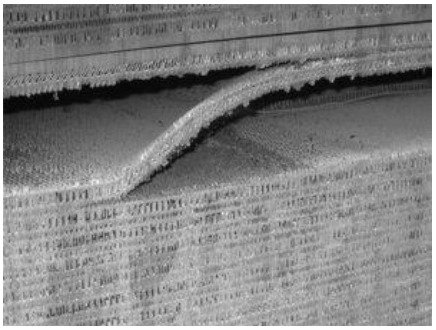

Figure 2.5: Core Separation Due to Amalgam Corrosion. [20]

The reaction stages can be seen below:

$$Hg + Al \rightarrow Hg(Al)$$

$$Hg(Al) + 6H_2O \rightarrow Al_2O_3\ 3H_2O + 3H_2 + Hg$$

Once amalgam is created small amounts of aluminium can dissolve in liquid mercury and diffuse to the mercury-moist air interface and then rapidly oxidize to free mercury which further dissolves and the process continues until the aluminum is completely converted to oxide.

Liquid metal Embrittlement (LME)

Liquid metal embrittlement (LME) is a complex metal fracture mechanism that occurs rapidly and can be triggered by the presence of liquid mercury. Mercury's accumulations in parts of natural gas plants has led to failures, since LME occurs rapidly and no adequate testing techniques exist to safely monitor the plant [18].

For the LME to take place three conditions must occur:

1. Presence of an embrittling liquid metal – mercury being a severe embrittling agent for aluminium alloys
2. The presence of a stress above a threshold value
3. "Wetting" of the substrate by the liquid metal – for aluminium alloys rupture of the oxide protective film between the substrate and liquid metal

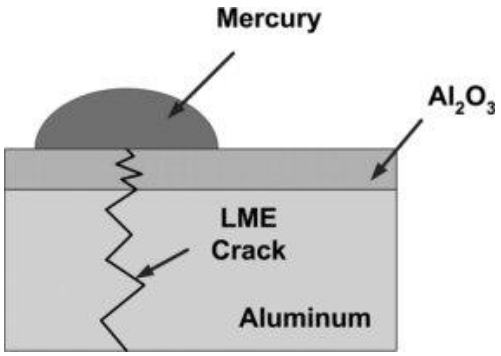

Figure 2.6: Liquid metal embrittlement of aluminium. [20]

Many metals are embrittled by certain liquid metals. Mercury embrittles liquid Al, Cu, Ti, Ni, Fe, Zn alloys. Al alloys are also embrittled by liquid Ga, In, Pb, Sn, Cd, and Na. Most cases of LME involve only adsorption of embrittling atoms at stressed surfaces and crack tips, no diffusion of embrittling atoms into the material or ahead of crack tips is involved. LME is generally much more severe than other embrittling processes, such as hydrogen embrittlement or stress-corrosion cracking, and once cracks have initiated, very rapid sub-critical cracking can occur even at low stresses.

Liquid metals are drawn into growing cracks so that the crack tip is always in contact with embrittling metal atoms. As with amalgamation, for LME cracks to initiate there must be intimate contact between liquid metals (in liquid phase) and solid metals. However, the intervening oxide films, used to protect the aluminum alloy, prevent wetting and adsorption. These films can be broken by mechanical processes, like abrasion on the surface by hard particles in natural gas or liquid systems, or by chemical processes like corrosion. Another factor could be the differential thermal expansion between aluminium substrate and the alumina oxide being a factor of around 3 could cause the oxide to crack when the heat exchanger is warmed. [18]

Mercury can accumulate in the aluminum equipment as liquid or solid deposits. In cold liquid streams, solid mercury particles can carry long distances and thus mercury deposits are often found in areas of limited flow far from the point of actual condensation or precipitation. In most cases, the LME failure mode is a leak in proximity to a weld but occasionally LME cracks propagate to greater distances to produce a rupture that allow sudden discharge of large quantities of gas or liquids. [20]

2.3.4.2 Health Effects on Humans

Mercury is toxic and raises health concerns for humans. An exposure to the various forms of mercury will harm a person's health depending on a number of factors, such as the following:

- The chemical form of mercury
- The dose
- The age of the person exposed
- The duration of exposure
- The route of exposure (inhalation, ingestion, dermal contact, etc.)
- The health of the person exposed

In general, according to [21], no human data indicate that exposure to any form of mercury causes cancer, since the available human data are very limited. Regarding the natural gas

industry, the main concern is elemental mercury. Elemental mercury primarily caused health effects when it is breathed as a vapor where it can be absorbed through the lungs. These exposures occur when elemental mercury is spilled and exposed to the air, particularly in warm or poorly ventilated indoor spaces. As regards other mercury compounds (inorganic and organic), they can be absorbed through the gastrointestinal tract and affect other systems via this route, such as the nervous system or the kidneys. Consequently, suitable personal protective equipment is required during maintenance work for the field personnel. [17, 22]

2.3.4.3 Environmental Effects

Human activity has significantly increased mercury levels over the past several centuries. Mercury emitted to the air can then build up in water and soils and can transform into methylmercury which accumulates in the tissues of wildlife and people.

Mercury follows continuously a biogeochemical cycle in the environment. The cycle is completed in six major steps [23] that are given below:

1. Degassing of mercury from rock, soils, and surface waters, or emissions from volcanoes and from human activities.
2. Movement in gaseous form through the atmosphere
3. Deposition of mercury on land and surface waters
4. Conversion of the element into insoluble mercury sulfide
5. Precipitation or bioconversion into more volatile or soluble forms such as methylmercury
6. Reentry into the atmosphere or bioaccumulation in food chains

Mercury in produced hydrocarbons may escape to the environment by several avenues of egress. These avenues may be generally categorized as wastewater, solid waste streams and air emissions. Wastewaters originate in production operations in the form of produced water and in refining and gas processing as wastewater. Solid waste streams are generated in production, transportation and in refining, while air emissions originate from fugitive emissions from process equipment and from combustion. [2]

3. Mercury Modelling

3.1 Thermodynamic Modelling

In this work, only purely thermodynamic models were tested. A thermodynamic model is an equilibrium model that assumes vapor-liquid equilibrium at each stage. Additionally rate-based models exist. Rate-based models assume that vapor-liquid equilibrium occurs only at the interface and use the Maxwell-Stefan equation to describe the mass transfer between the vapor phase and the liquid phase. It is also important to note that for all the tested models no reaction or species transformation was taken into consideration. Gas and liquid processing can transform one chemical form of mercury to another. A common reaction is that of elemental mercury with sulfur compounds that could be caused by the mixing of gas and condensate from sour and sweet wells. Also high temperature processes could convert diakylmercury and complexed mercury to the elemental form. [24]

An isolated system consisting of liquid and vapor phases in intimate contact eventually reaches a final state wherein no tendency exists for change to occur within the system. The temperature, pressure, and phase compositions reach final values which thereafter remain fixed. The system now is in equilibrium. When thermodynamics is applied to vapor liquid equilibrium, the goal is to find by calculation the temperatures, pressures, and compositions of the phases in equilibrium. These calculations are performed through thermodynamic models such as cubic equations of state the most popular of them being the PR and the SRK equations of state.

3.2 Models Considered for Evaluation

Very limited data are available on mercury modelling. It is clear that companies have developed their own models but these data remain classified and cannot be publicly accessed. A model developed by Statoil [25] was available and some mercury models were also found in the literature[26, 27]. Mercury models were also provided by the PRO/II software package. Finally, other classic models, such as Peng Robinson and Soave Redlich Kwong were evaluated and are all described at the following section.

3.2.1 Soave Redlich Kwong (SRK)

This equation of state originates from the original Redlich-Kwong equation of state. Soave altered the RK equation by including the effect of temperature in the attractive term in the *a* parameter. He also took into account the shape of each chemical compound using the acentric factor ω. The equation of state is given below. No binary interaction parameters for mercury were used in this model.

The model:

$$P = \frac{RT}{V-b} - \frac{\mathrm{a(T)}}{V(V+b)}$$

Where:

$$b = \sum_{i=1}^{N} x_i b_i$$

$$b_i = 0.08664 \frac{RT_{ci}}{P_{ci}}$$

=0 for mercury
≠0 for other

$$\mathrm{a}(T) = \sum_i \sum_j x_i x_j (\mathrm{a}_i \mathrm{a}_j)^{\frac{1}{2}} (1 - k_{ij})$$

$$\mathrm{a}_i = \mathrm{a}_{ci} \alpha_i$$

$$\mathrm{a}_{ci} = 0.42747 \frac{(RT_{ci})^2}{P_{ci}}$$

$$\alpha_i = \left(1 + m_i (1 - T_{ci}^{0.5})\right)^2$$

$$m_i = 0.48 + 1.574\omega_i - 0.176\omega_i^2$$

T_{ci}, P_{ci} = critical temperature and pressure of component i
ω_i = acentric factor for component i
k_{ij}= binary interaction parameter for components i and j

3.2.2 Peng Robinson (PR)

Peng and Robinson researchers kept the temperature dependence at the attractive term. However, they altered the denominator of the attractive term and changed the fitted parameters. Peng-Robinson was created in 1970 focusing on natural gas systems. No binary interaction parameters for mercury were used in this model.

The model:

$$P = \frac{RT}{V-b} - \frac{\mathrm{a}}{V(V+b) + b(V-b)}$$

Where:

$$b = \sum_{i=1}^{N} x_i b_i$$

$$b_i = 0.07780 \frac{RT_{ci}}{P_{ci}}$$

=0 for mercury
≠0 for other

$$\mathrm{a}(T) = \sum_i \sum_j x_i x_j (\mathrm{a}_i \mathrm{a}_j)^{\frac{1}{2}} (1 - k_{ij})$$

$$\mathrm{a}_i = \mathrm{a}_{ci} \alpha_i$$

$$\mathrm{a}_{ci} = 0.45724 \frac{(RT_{ci})^2}{P_{ci}}$$

$$\alpha_i = \left(1 + m_i(1 - T_{ci}^{0.5})\right)^2$$

$$m_i = 0.37464 + 1.54226\omega_i - 0.26992\omega_i^2$$

3.2.3 SRK PRO/II default

This model is the same as the SRK model described above, the only difference being that in this model, binary interaction parameters for mercury are used. Specifically the binary interaction parameters used for mercury are those provided in the PRO/II software package. Binary interaction parameters are used in the equations of state to help calibrate the extent of non-ideality of a given binary mixture. High non-idealities are expected in the liquid phase, thus the use of these parameters is expected to improve more the predictions for the liquid phase and less for the vapor phase.

The model:

$$P = \frac{RT}{V - b} - \frac{\mathrm{a(T)}}{V(V + b)}$$

Where:

$$b = \sum_{i=1}^{N} x_i b_i$$

$$b_i = 0.08664 \frac{RT_{ci}}{P_{ci}}$$

Default values from PRO/II package

$$\mathrm{a}(T) = \sum_i \sum_j x_i x_j \left(\mathrm{a}_i \mathrm{a}_j\right)^{\frac{1}{2}} \left(1 - k_{ij}\right)$$

$$\mathrm{a}_i = \mathrm{a}_{ci}\alpha_i$$

$$\mathrm{a}_{ci} = 0.42747 \frac{(RT_{ci})^2}{P_{ci}}$$

$$\alpha_i = \left(1 + m_i(1 - T_{ci}^{0.5})\right)^2$$

$$m_i = 0.48 + 1.574\omega_i - 0.176\omega_i^2$$

Binary interaction parameters for mercury:

The k_{ij}s provided by PRO/II are temperature dependent and are given below:

Table 3.1: Binary Interaction Parameters for Mercury Provided by PRO/II for the SRK EoS

$$k_{ij} = k_{ija} + \frac{k_{ijb}}{T}$$

System	k_{ija}	k_{ijb}
Mercury-Methane	-0.0081000	-18.039
Mercury-Ethane	-0.033000	-16.632
Mercury-Propane	-0.058000	-15.226
Mercury-n-butane	-0.082900	-13.820
Mercury-ibutane	-	-
Mercury-Pentane	-0.11830	-9.7036
Mercury-Hexane	-0.12870	-11.927
Mercury-CO_2	-	-
Mercury-N_2	-	-

3.2.4 PR PRO/II default

Again, this model is the same as the PR model described above, but instead of using zero k_{ij}s, here the binary interaction parameters used, between mercury and other components, are those of PRO/II software package. As for the SRK PRO/II default model, the use of k_{ij}s mainly improves the predictions for the liquid phase.

The model:

$$P = \frac{RT}{V-b} - \frac{\mathrm{a}}{V(V+b)+b(V-b)}$$

Where:

$$b = \sum_{i=1}^{N} x_i b_i$$

$$b_i = 0.07780\frac{RT_{ci}}{P_{ci}}$$

$$\mathrm{a}(T) = \sum_i \sum_j x_i x_j (\mathrm{a}_i \mathrm{a}_j)^{\frac{1}{2}} (1 - k_{ij})$$

Default values from PRO/II package

$$\mathrm{a}_i = \mathrm{a}_{ci}\alpha_i$$

$$\mathrm{a}_{ci} = 0.45724\frac{(RT_{ci})^2}{P_{ci}}$$

$$\alpha_i = \left(1 + m_i(1 - T_{ci}^{0.5})\right)^2$$

$$m_i = 0.37464 + 1.54226\omega_i - 0.26992\omega_i^2$$

Binary interaction parameters for mercury:

The k_{ij}s provided by PRO/II are temperature dependent and are given below:

Table 3.2: Binary Interaction Parameters for Mercury Provided by PRO/II for the PR EoS

$$k_{ij} = k_{ija} + \frac{k_{ijb}}{T}$$

System	k_{ija}	k_{ijb}
Mercury-Methane	0.20096	-33.895
Mercury-Ethane	0.16461	-29.915
Mercury-Propane	0.12827	-25.935
Mercury-n-butane	0.091921	-21.954
Mercury-ibutane	-	-
Mercury-Pentane	0.054602	-17.436
Mercury-Hexane	0.018124	-13.588
Mercury-CO_2	-	-
Mercury-N_2	-	-

3.2.5 SRK-Twu(Hg) – no k_{ij}

This equation of state is the same as the SRK described above, except for the alpha function used for mercury, which is now described by Twu's expression [28]. The introduction of this new alpha term is an effort to improve the vapor pressure prediction. SRK-Twu is an extended version of the Soave-Redlich-Kwong (SRK) cubic equation of state where the alpha function proposed by Twu et al are used. The temperature-dependent alpha function is able to predict vapor pressure and liquid heat capacity from the triple point to the critical point accurately for a large number of components, including both low and extremely high boiling point components. The alpha function has three parameters, L, M, and N, which are unique to each component and are determined from the regression of pure-component vapor pressure data. The introduction of this advanced expression of the alpha function results in accurate vapor pressure prediction and thus in accurate predictions for the vapor phase. No binary interaction parameters for mercury were used in this model. The improvement of the prediction of the vapor pressures when using an advanced expression of the alpha function can be seen below:

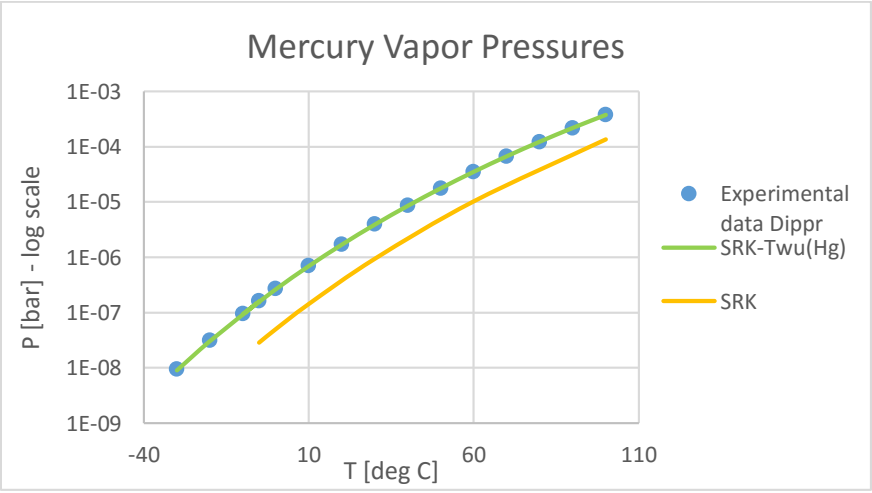

Figure 3.1: Mercury's Vapor Pressures Predicted by SRK and SRK-Twu(Hg)

The model:

$$P = \frac{RT}{V-b} - \frac{\mathrm{a(T)}}{V(V+b)}$$

Where:

$$b = \sum_{i=1}^{N} x_i b_i$$

$$b_i = 0.08664 \frac{RT_{ci}}{P_{ci}}$$

$$\mathrm{a}(T) = \sum_i \sum_j x_i x_j (\mathrm{a}_i \mathrm{a}_j)^{\frac{1}{2}} (1 - k_{ij})$$

k_{ij}: =0 for mercury, ≠0 for other

$$\mathrm{a}_i = \mathrm{a}_{ci} \alpha_i$$

$$\mathrm{a}_{ci} = 0.42747 \frac{(RT_{ci})^2}{P_{ci}}$$

Alpha function used for all components except for mercury:

$$\alpha_i = \left(1 + m_i(1 - T_{ci}^{0.5})\right)^2$$

$$m_i = 0.48 + 1.574\omega_i - 0.176\omega_i^2$$

Alpha function used for mercury:

$$\alpha_i = T_r^{N(M-1)} exp[L(1 - T_r^{MN})]$$

Twu's parameters are given at the following table:

Table 3.3: Twu's Parameters for Mercury by Mentzelos [12]

Parameter	For T=[-35^{0}C - 1235^{0}C]
L	0.09245
M	0.9784
N	2.244

Where:
L, M, N: parameters fitted to vapor pressure experimental data

3.2.6 PRMC(Hg) – no k_{ij}

This equation of state is the same as the PR described above, except for the alpha function used for mercury which is now described by Mathias Copeman expression [29]. The introduction of this new alpha term is an effort to improve the vapor pressure prediction. The temperature dependent alpha function has three parameters, m_1, m_2 and m_3, which are unique to each component and are determined from the regression of pure-component vapor pressure data, just like with Twu's expression. Again, the introduction of this advanced expression of the alpha function results in accurate vapor pressure prediction and thus in accurate predictions for the vapor phase. No binary interaction parameters for mercury were used in this model.

The model:

$$P = \frac{RT}{V-b} - \frac{\mathrm{a}}{V(V+b)+b(V-b)}$$

Where:

$$b = \sum_{i=1}^{N} x_i b_i$$

$$b_i = 0.07780\frac{RT_{ci}}{P_{ci}}$$

$$\mathrm{a}(T) = \sum_i \sum_j x_i x_j (\mathrm{a}_i \mathrm{a}_j)^{\frac{1}{2}} (1 - k_{ij})$$

=0 for mercury
≠0 for other

$$\mathrm{a}_i = \mathrm{a}_{ci}\alpha_i$$

$$\mathrm{a}_{ci} = 0.45724\frac{(RT_{ci})^2}{P_{ci}}$$

Alpha function used for all components except for mercury:

$$\alpha_i = \left(1 + m_i(1 - T_{ci}^{0.5})\right)^2$$

$$m_i = 0.37464 + 1.54226\omega_i - 0.26992\omega_i^2$$

Alpha function used for mercury:

$$\alpha_i = \left(1 + m_{1i}\left(1 - T_{ci}^{0.5}\right) + 1 + m_{2i}\left(1 - T_{ci}^{0.5}\right)^2 + 1 + m_{3i}(1 - T_{ci}^{0.5})^3\right)^2$$

Mathias-Copeman's parameters are given below:

Table 3.4: Mathias-Copeman Parameters for Mercury by Mentzelos [12]

Parameter	For T=[-35^{0}C - 1235^{0}C]
m_1	0.1491
m_1	-0.1652
m_1	0.1447

Where:
m_1, m_2, m_3: parameters fitted with vapor pressure experimental data

3.2.7 SRK-Twu(Hg) - Statoil 2011

Statoil in 2011, after a literature review used SRK-Twu (described above) to model mercury. The L, M, N parameters required for the alpha function were determined from the regression of pure component vapor pressure data which were taken from NIST. The simulator NeqSim was used to perform the fitting of the alpha function parameters. [30]

The model:

$$P = \frac{RT}{V-b} - \frac{\mathrm{a(T)}}{V(V+b)}$$

Where:

$$b = \sum_{i=1}^{N} x_i b_i$$

$$b_i = 0.08664 \frac{RT_{ci}}{P_{ci}}$$

$$\mathrm{a}(T) = \sum_i \sum_j x_i x_j (\mathrm{a}_i \mathrm{a}_j)^{\frac{1}{2}} (1 - k_{ij})$$

≠0 for all components

$$\mathrm{a}_i = \mathrm{a}_{ci} \alpha_i$$

$$\mathrm{a}_{ci} = 0.42747 \frac{(RT_{ci})^2}{P_{ci}}$$

Alpha function used for all components except for mercury:

$$\alpha_i = \left(1 + m_i(1 - T_{ci}^{0.5})\right)^2$$

$$m_i = 0.48 + 1.574\omega_i - 0.176\omega_i^2$$

Alpha function used for mercury:

$$\alpha_i = T_r^{N(M-1)} exp[L(1 - T_r^{MN})]$$

The critical parameters T_c, P_c, ω, taken from Aspen HYSYS version 7.1, and the L, M, N parameters obtained are shown below.

Table 3.5: Critical Parameters for Mercury by Aspen HYSYS 7.1

Critical Properties for Mercury	Value
T_c [K]	1735.15
P_c [31]	1608
ω	-0.16445

Table 3.6: Twu's Parameters for Mercury Proposed by Statoil in 2011 [30]

Twu's Parameters for Mercury	For T=[20^0C - 430^0C]
L	0.068584
M	0.985182
N	4.239459

Binary interaction parameters for mercury:

The solubility data reported by Okouchi et al, were used to generate binary interaction parameters of the SRK-Twu EOS for mercury. However, the solubility data reported include only the solubility of mercury in pentane, hexane, heptane and octane. After fitting the solubility data to the SRK-Twu, using the simulator NeqSim, binary interaction parameters were obtained for C_5-C_8. In order to obtain binary interaction parameters from C_1 to C_{10} a linear correlation

was made. Thus, using the correlation below, binary interaction parameters were generated and are given at Table 3.7.

Correlation: Not given because it is classified

Where:
CN: is carbon number
k_{ij}: is the interaction parameter between mercury and C_5-C_8

Table 3.7: Binary Interaction Parameters for the SRK-Twu(Hg) – Statoil 2011 model [30]

Carbon Number	Binary Interaction Parameter[k_{ij}]
1	classified
2	//
3	//
4	//
5	//
6	//
7	//
8	//
9	//
10	//

The main concerns about this model is about the binary interaction parameters. No data were found in the literature for mercury's solubility in C_1-C_4, which consist the largest part of natural gas. The binary interaction parameters used in this model were extrapolated from the fitted parameters, which only included data for mercury solubility in C_5-C_8. Finally, the developed correlation for the binary interaction parameters cannot distinguish isomers, as it only takes into account the carbon number and not the structure of the molecule.

3.2.8 PRMC - Mentzelos

This equation of state is the same as the *PRMC – no k_{ij}* described earlier, but now binary interaction parameters for mercury are porposed. Mentzelos calculated constant and temperature depended binary interaction parameters for mercury, where solubility data were available. For mercury systems, for which no solubility data were found in the literature (such as methane and ethane), generalized correlations were developed based on the existing data. [12]

It should be noticed that some generalized correlations take the form of a quadratic function, which could result in inaccurate results due to its parabolic form.

The model:

$$P = \frac{RT}{V-b} - \frac{\mathrm{a}}{V(V+b)+b(V-b)}$$

Where:

$$b = \sum_{i=1}^{N} x_i b_i$$

$$b_i = 0.07780 \frac{RT_{ci}}{P_{ci}}$$

$$\mathrm{a}(T) = \sum_i \sum_j x_i x_j (\mathrm{a}_i \mathrm{a}_j)^{\frac{1}{2}} (1 - k_{ij})$$

$\neq 0$ for all components

$$\mathrm{a}_i = \mathrm{a}_{ci} \alpha_i$$

$$\mathrm{a}_{ci} = 0.45724 \frac{(RT_{ci})^2}{P_{ci}}$$

$$\alpha_i = \left(1 + m_{1i}(1 - T_{ci}^{0.5}) + 1 + m_{2i}(1 - T_{ci}^{0.5})^2 + 1 + m_{3i}(1 - T_{ci}^{0.5})^3\right)^2$$

Mathias-Copeman's parameters for mercury for this model are given at Table 3.4.

Binary interaction parameters for mercury:

The binary interaction parameters developed along with generalized correlations for the k_{ij} parameters are given below. These correlations take into account both the normal boiling point and the structure of each component, thus differentiating isomers.

Table 3.8: Binary Interaction Parameters for the PRMC- Mentzelos Model [12]

System	K_{ij}			
	Constant	***K_{ij}=a+bT [K]***	***K_{ij}=a+b/T [K]***	***Based on generalized correlations***
Hg-methane	-	-	-	6.14E-01
Hg-ethane	-	-	-	3.57E-01
Hg-propane	2.27E-01	-	-	2.27E-01
Hg-ibutane	-	-	-	1.56E-01
Hg-n-butane	1.29E-01	-	-	1.32E-01
Hg-iC5	-	-	-	7.96E-02
Hg-nC5	3.99E-02	-0.0004T + 0.16	34.62/T - 0.078	6.61E-02
Hg-nC6	1.13E-02	-	-6.6/T + 0.033	2.05E-02
Hg-nC7	-1.12E-02	-	10.39/T - 0.047	-9.76E-03
Hg-nC8	-3.42E-02	0.0004T - 0.14	-30.35/T + 0.07	-2.82E-02
Hg-nC9	-	-	-	-3.73E-02
Hg-nC10	-7.32E-02	0.0015T - 0.53	-133.51/T + 0.38	-3.90E-02
Hg-2,2dmC4	2.97E-02	0.0016T - 0.44	-134.14/T + 0.49	4.54E-02
Hg-2,3-dm-C4	-	-	-	3.40E-02
2-m-C5	-	-	-	3.11E-02

System	K_{ij}			
	Constant	***K_{ij}=a+bT [K]***	***K_{ij}=a+b/T [K]***	***Based on generalized correlations***
3-mC5	-	-	-	2.73E-02
Hg-2,2,4tmC5	1.41E-02	0.0008T - 0.22	-68.37/T + 0.25	-
Hg-cyC6	3.69E-02	0.0013T - 0.35	-116.62/T + 0.43	2.46E-02
Hg-cyC7	-	-	-	-3.20E-02
Hg-cyC8	-	-	-	-7.76E-02
Hg-toluene	5.86E-02	0.0002T + 0.01	-15.22/T + 0.11	5.86E-02
Hg-mcyC6	1.65E-02	0.0004T - 0.10	-31.72/T + 0.13	-
Hg-benzene	1.08E-01	-0.0005T + 0.25	41.42/T - 0.03	1.08E-01
Hg-oxylene	4.43E-02	-0.0004T + 0.17	35.12/T - 0.076	4.43E-02
Hg-cis1,2dmcyC6	-3.18E-02	0.0010T - 0.33	-88.35/T + 0.26	-
Hg-cis1,4dmcyC6	-3.77E-02	-	-	-
Hg-trans1,4dmcyC6	-2.72E-02	0.0009T - 0.25	-74.05/T + 0.25	-
Hg-trans1,2dmcyC6	-2.23E-03	0.0009T - 0.31	-82.67/T + 0.25	-

Correlations:

Paraffinic HC: $k_{ij} = 6 \cdot 10^{-6} T_b^2 - 0.0053 T_b + 1.1312$
Naphthenic HC: $k_{ij} = -0.0015 T_b + 0.5554$
Aromatic HC: $k_{ij} = 2 \cdot 10^{-5} T_b^2 - 0.0149 T_b + 3.2052$

The critical properties used by Mentzelos are given at the following table:

Table 3.9: Critical Parameters Used in Mentzelos' Models [12]

Critical Properties for Mercury Used	DIPPR's Set
T_c [K]	1735.15
P_c [31]	1608
ω	-0.1645

3.2.9 SRK-Twu (All) – Mentzelos

In this model SRK equation of state is used along with Twu's expression for the alpha function for all components and not only for mercury. Mentzelos calculated constant and temperature depended binary interaction parameters for mercury, where solubility data were available. For mercury systems, for which no solubility data were found in the literature (such as methane and ethane), generalized correlations were developed based on the existing data. [12]

It should be noticed that some generalized correlations take the form of a quadratic function, which could result in inaccurate results due to its parabolic form.

The model [12]:

$$P = \frac{RT}{V-b} - \frac{\mathrm{a(T)}}{V(V+b)}$$

Where:

$$b = \sum_{i=1}^{N} x_i b_i$$

$$b_i = 0.08664 \frac{RT_{ci}}{P_{ci}}$$

$$\mathrm{a}(T) = \sum_i \sum_j x_i x_j (\mathrm{a}_i \mathrm{a}_j)^{\frac{1}{2}} (1 - k_{ij})$$

$k_{ij} \neq 0$ for all components

$$\mathrm{a}_i = \mathrm{a}_{ci} \alpha_i$$

$$\mathrm{a}_{ci} = 0.42747 \frac{(RT_{ci})^2}{P_{ci}}$$

$$\alpha_i = T_r^{N(M-1)} exp[L(1 - T_r^{MN})]$$

Twu's parameters for mercury used in this model are given at Table 3.3.

Binary interaction parameters for mercury:

The binary interaction parameters developed along with generalized correlations for the k_{ij} parameters are given below.

Table 3.10: Binary Interaction Parameters for the SRK-Twu(All) - Mentzelos Model [12]

System	K_{ij}			
	Constant	***K_{ij}=a+bT [K]***	***K_{ij}=a+b/T [K]***	***Based on generalized correlations***
Hg-methane	-	-	-	6.54E-01
Hg-ethane	-	-	-	3.82E-01
Hg-propane	2.45E-01	-	-	2.42E-01
Hg-ibutane	-	-	-	1.65E-01
Hg-n-butane	1.54E-01	-	-	1.39E-01
Hg-iC5	-	-	-	8.09E-02
Hg-nC5	5.21E-02	-0.0003T + 0.15	29.47/T - 0.049	6.57E-02
Hg-nC6	2.49E-02	-	-15.24/T +0.076	1.36E-02
Hg-nC7	3.38E-03	-	4.36/T - 0.012	-2.26E-02
Hg-nC8	-1.86E-02	0.0005T - 0.15	-39.23/T + 0.12	-4.65E-02
Hg-nC9	-	-	-	-6.06E-02
Hg-nC10	-5.44E-02	0.0016T - 0.53	-138.92/T + 0.41	-6.70E-02

System	K_{ij}			
	Constant	***K_{ij}=a+bT [K]***	***K_{ij}=a+b/T [K]***	***Based on generalized correlations***
Hg-2,2dmC4	4.34E-02	0.0017T - 0.46	- 143.76/T + 0.53	4.23E-02
Hg-2,3-dm-C4	-	-	-	2.93E-02
2-m-C5	-	-	-	2.59E-02
3-mC5	-	-	-	2.15E-02
Hg-2,2,4tmC5	3.11E-02	0.0009T - 0.23	- 75.30/T + 0.29	-
Hg-cyC6	4.83E-02	0.0014T - 0.36	-123.56/T + 0.46	4.74E-02
Hg-cyC7	-	-	-	-5.34E-03
Hg-cyC8	-	-	-	-4.79E-02
Hg-toluene	7.05E-02	0.0003T - 0.005	-21.75/T + 0.14	7.05E-02
Hg-mcyC6	2.91E-02	0.0005T - 0.10	-37.61/T + 0.16	-
Hg-benzene	1.18E-01	-0.0004T + 0.24	37.21/T - 0.008	1.18E-01
Hg-oxylene	5.64E-02	-0.0003T + 0.16	28.69/T - 0.042	5.64E-02
Hg-cis1,2dmcyC6	-1.68E-02	0.0010T - 0.33	-92.27/T + 0.29	-
Hg-cis1,4dmcyC6	-1.42E-02	-	-	-
Hg-trans1,4dmcyC6	-5.61E-03	0.0010T - 0.29	-83.63/T + 0.28	-
Hg-trans1,2dmcyC6	-3.02E-03	0.0009T - 0.28	-80.36/T + 0.26	-

Correlations:

Paraffinic HC: $k_{ij} = 6 \cdot 10^{-6}\, T_b^2 - 0.0055 T_b + 1.1927$
Naphthenic HC: $k_{ij} = -0.0014\, T_b + 0.5429$
Aromatic HC: $k_{ij} = 2 \cdot 10^{-5}\, T_b^2 - 0.0149 T_b + 3.1296$

The critical properties used by Mentzelos in this model are given in Table 3.9

3.2.10 SRK-Twu(Hg) - Mentzelos

In this model, SRK is used along with Twu's alpha expression for mercury only, while for all other components Soave's alpha expression is used. Again, Mentzelos calculated constant and temperature depended binary interaction parameters for mercury, where solubility data were available. For mercury systems, for which no solubility data were found in the literature (such as methane and ethane), generalized correlations were developed based on the existing data. [12]

It should be noticed that some generalized correlations take the form of a quadratic function, which could result in inaccurate results due to its parabolic form.

The model [12]:

$$P = \frac{RT}{V-b} - \frac{\mathrm{a(T)}}{V(V+b)}$$

Where:

$$b = \sum_{i=1}^{N} x_i b_i$$

$$b_i = 0.08664 \frac{RT_{ci}}{P_{ci}}$$

$$\mathrm{a}(T) = \sum_i \sum_j x_i x_j (\mathrm{a}_i \mathrm{a}_j)^{\frac{1}{2}} (1 - k_{ij})$$

≠0 for all components

$$\mathrm{a}_i = \mathrm{a}_{ci} \alpha_i$$

$$\mathrm{a}_{ci} = 0.42747 \frac{(RT_{ci})^2}{P_{ci}}$$

Alpha function used for all components except for mercury:

$$\alpha_i = \left(1 + m_i(1 - T_{ci}^{0.5})\right)^2$$

$$m_i = 0.48 + 1.574\omega_i - 0.176\omega_i^2$$

Alpha function used for mercury:

$$\alpha_i = T_r^{N(M-1)} exp[L(1 - T_r^{MN})]$$

Twu's parameters for mercury used in this model are given at Table 3.3.

Binary interaction parameters for mercury:

The binary interaction parameters developed along with generalized correlations for the k_{ij} parameters are given below.

Table 3.11: Binary Interaction Parameters for the SRK-Twu(Hg) - Mentzelos Model [12]

System	K_{ij}			
	Constant	***K_{ij}=a+bT [K]***	***K_{ij}=a+b/T [K]***	***Based on generalized correlations***
Hg-methane	-	-	-	6.31E-01
Hg-ethane	-	-	-	3.66E-01
Hg-propane	2.41E-01	-	-	2.31E-01
Hg-ibutane	-	-	-	1.57E-01
Hg-n-butane	1.488E-01	-	-	1.32E-01

System	K_{ij}			
	Constant	***K_{ij}=a+bT [K]***	***K_{ij}=a+b/T [K]***	***Based on generalized correlations***
Hg-nC5	5.24E-02	-0.0004T + 0.16	30.76/T - 0.053	6.27E-02
Hg-iC5	-	-	-13.600/T + 0.072	7.71E-02
Hg-nC6	2.64E-02	-	3.560/T - 0.008	1.39E-02
Hg-nC7	4.46E-03	-	-	-1.93E-02
Hg-nC8	-1.76E-02	0.0005T - 0.16	-40.82/T + 0.12	-4.05E-02
Hg-nC9	-	-	-	-5.21E-02
Hg-nC10	-5.34E-02	0.0017T - 0.55	-145.12/T + 0.44	-5.62E-02
Hg-2,2dmC4	4.41E-02	0.0017T - 0.45	-141.70/T + 0.53	4.07E-02
Hg-2,3-dm-C4	-	-	-	2.85E-02
2-m-C5	-	-	-	2.54E-02
3-mC5	-	-	-	2.12E-02
Hg-2,2,4tmC5	3.23E-02	0.0009T - 0.23	-74.52/T + 0.29	-
Hg-cyC6	4.83E-02	0.0014T - 0.37	-126.63/T + 0.47	4.84E-02
Hg-cyC7	-	-	-	-4.34E-03
Hg-cyC8	-	-	-	-4.69E-02
Hg-toluene	7.04E-02	0.0003T - 0.01	-22.27/T + 0.15	7.04E-02
Hg-mcyC6	2.92E-02	0.0005T - 0.11	-40.02/T + 0.17	-
Hg-benzene	1.177E-01	-0.0004T + 0.23	34.26/T + 0.002	1.18E-01
Hg-oxylene	5.83E-02	-0.0003T + 0.16	28.03/T - 0.038	5.83E-02
Hg-cis1,2dmcyC6	-2.29E-02	0.0012T - 0.37	-102.84/T + 0.32	-
Hg-cis1,4dmcyC6	-2.01E-02	-	-	-
Hg-trans1,4dmcyC6	-9.70E-03	0.0009T - 0.25	-79.38/T + 0.28	-
Hg-trans1,2dmcyC6	1.56E-02	0.0010T - 0.31	- 88.05/T + 0.29	-

Correlations:

Paraffinic HC: $k_{ij} = 6 \cdot 10^{-6}\, T_b^2 - 0.0054 T_b + 1.1588$
Naphthenic HC: $k_{ij} = -0.0014\, T_b + 0.5439$
Aromatic HC: $k_{ij} = 2 \cdot 10^{-5}\, T_b^2 - 0.0157 T_b + 3.2640$

The critical properties used by Mentzelos in this model are given in Table 3.9

3.2.11 SRK-Twu(Hg) – Statoil 2014

This equation of state is the same as the SRK-Twu(Hg)-no k_{ij} described earlier, but now binary interaction parameters for mercury are used. The introduction of the binary interaction parameters was made to improve the prediction for mercury in binary or multicomponent systems, especially for the liquid phase. This model is a continuation of the work done by Statoil in 2011, which takes into consideration three new literature references. These references are the master thesis of Mentzelos, Wiltec and GPA reports [32], with new experimental solubility data for mercury-hydrocarbon systems. The availability of new solubility data made it possible to generate new binary interaction parameters, not available before.

The model:

$$P = \frac{RT}{V-b} - \frac{\mathrm{a(T)}}{V(V+b)}$$

Where:

$$b = \sum_{i=1}^{N} x_i b_i$$

$$b_i = 0.08664 \frac{RT_{ci}}{P_{ci}}$$

$$\mathrm{a}(T) = \sum_i \sum_j x_i x_j (\mathrm{a}_i \mathrm{a}_j)^{\frac{1}{2}} (1 - k_{ij})$$

$k_{ij} \neq 0$ for all components

$$\mathrm{a}_i = \mathrm{a}_{ci} \alpha_i$$

$$\mathrm{a}_{ci} = 0.42747 \frac{(RT_{ci})^2}{P_{ci}}$$

Alpha function used for all components except for mercury:

$$\alpha_i = \left(1 + m_i(1 - T_{ci}^{0.5})\right)^2$$

$$m_i = 0.48 + 1.574\omega_i - 0.176\omega_i^2$$

Alpha function used for mercury:

$$\alpha_i = T_r^{N(M-1)} exp[L(1 - T_r^{MN})]$$

The critical parameters T_c, P_c, ω, and the L, M, N parameters used for this models are given at the Table 3.5 and Table 3.3 respectively.

Binary interaction parameters for mercury:

Based on the new solubility data provided by Wiltec and GPA reports binary interaction parameters for mercury were generated. For those components for which no experimental data were available, k_{ij} correlations were developed based on the available data. With these correlations one can calculate k_{ij}s, based on the component's carbon number and on whether they are paraffinic, naphthenic or aromatic hydrocarbons. These correlations, are significantly improved comparing with the SRK-Twu(Hg) – Statoil 2011 model, since they take into account

except for the carbon number also the structure of each molecule, thus differentiating isomers. The k_{ij}s and the correlations are given below.

Table 3.12: Binary Interaction Parameters for the SRK-Twu(Hg) Model [25]

System	K_{ij}
C_1 – Hg	classified
C_2 – Hg	//
C_3 – Hg	//
iC_4 – Hg	//
nC_4 – Hg	//
nC_5 – Hg	//
nC_6 – Hg	//
nC_7 – Hg	//
CyC6 – Hg	//
Benzene – Hg	//
nC_8 – Hg	//
MCyC6 – Hg	//
Toluene – Hg	//
o-Xylene – Hg	//
nC_{10} – Hg	//
N_2 – Hg	//
CO_2 – Hg	//

Comments

The binary interaction parameter for the n-butane-mercury system, provided by Statoil was fitted to solubility data for high temperatures ($T>184^0C$), which is not of interest for the natural gas processes. Therefore, a predicted k_{ij} was generated instead, using the correlation for the paraffinic hydrocarbons given below.

Correlations:

Paraffinic HC classified
Naphthenic HC //
Aromatic HC //

3.2.12 UMR-PRMC

UMR-PRMC is a predictive model belonging to the category of the EOS/G^E models. This model uses, instead of the classical mixing rules that use binary interaction parameters, a Unifac-type G^E model via the universal mixing rules develop by Voutsas et al [26] in combination with the PRMC model. The result is that this model considers that all components are comprised of the Unifac groups thus describing them as a combination of these groups. The main advantage of that, is that no experimental solubility data are needed for the model to make predictions. This is the reason why the UMR-PRMC model can be characterized as a predictive model.

The mixing rules used in the UMR-PRMC are given below:

The model

$$\frac{a}{bRT} = \frac{1}{A}\frac{G_{AC}^{E,SG} + G_{AC}^{E,res}}{RT} + \sum_i x_i \frac{a_i}{b_i RT}$$

$$b = \sum_i \sum_j x_i x_j b_{ij}$$

$$b_{ij} = \left(\frac{b_i^{\frac{1}{2}} + b_j^{\frac{1}{2}}}{2}\right)^2$$

$$\frac{G_{AC}^{E,SG}}{RT} = 5\sum_i x_i q_i ln\left(\frac{\theta_\iota}{\varphi_\iota}\right)$$

$$\frac{G_{AC}^{E,res}}{RT} = \sum_i x_i v_k^i ln\left(\frac{\Gamma_k}{\Gamma_k^i}\right)$$

$$\ln(\Gamma_k) = Q_k\left[1 - ln\left(\sum_m \theta_m \Psi_{\mu\kappa}\right) - \sum_m \frac{\theta_m \Psi_{mk}}{\sum_n \theta_n \Psi_{nm}}\right]$$

For component i:

$$\varphi_i = \frac{x_i r_i}{\sum_j x_j r_j}$$

$$\theta_i = \frac{x_i q_i}{\sum_j x_j q_j}$$

For Unifac group m:

$$\theta_m = \frac{Q_m X_m}{\sum_n Q_n X_n}$$

$$X_m = \frac{\sum_j v_m^{(i)} x_j}{\sum_j \sum_n v_n^{(j)} x_j}$$

$$\Psi_{nm} = e^{-\frac{A_{nm} + B_{nm}(T-298.15) + C_{nm}(T-298.15)^2}{T}}$$

Where:

- A_{nm}, B_{nm}, C_{nm} are the Unifac interaction parameters between groups n and m
- b is the co-volume parameter of an EOS
- ν is the molar volume
- ri is the relative Van der Waals volume of compound "i"
- qi is the relative Van der Waals surface area of compound "i"
- Q_k is the relative Van der Waals surface area of sub-group "k"

- x is the mole fraction
- X_m is the group mole fraction of group "m"
- Ψ is the Unifac parameter
- $G_{AC}^{E,SG}$ is the Staverman-Guggenheim term of the combinatorial part of the excess Gibbs energy
- $G_{AC}^{E,res}$ is the Staverman-Guggenheim term of the residual part of the excess Gibbs energy
- R is the global constant for gasses
- Γ_k is the residual activity coefficient of group "k" in a solution
- θ_i is the surface area fraction of component "i"
- φ_i is the segment fraction of component "i"
- T is the absolute temperature [K]
- The parameter "A" is equal to -0.53

For the development of this model for mercury, mercury was considered to be a separate Unifac group and based on its solubility data with other hydrocarbons, the group interaction parameters for the Unifac model were calculated. The model developed and proposed by Mentzelos [27] is the following.

Unifac's group interaction parameters for mercury are given at the following table.

Table 3.13: Unifac's Group Interaction Parameters for Mercury [27]

i	j	A_{ij} [K]	B_{ij} [-]	C_{ij} [K^{-1}]	A_{ji} [K]	B_{ji} [-]	C_{ji} [K^{-1}]
ACH	Hg	classified	classified	classified	classified	classified	classified
$ACCH_3$	Hg	//	//	//	//	//	//
CH_2	Hg	//	//	//	//	//	//
cy-CH_2	Hg	//	//	//	//	//	//
CH_4	Hg	//	//	//	//	//	//
C_2H_6	Hg	//	//	//	//	//	//
CO_2	Hg	//	//	//	//	//	//
N_2	Hg	//	//	//	//	//	//
H_2O	Hg	//	//	//	//	//	//

The two following parameters are also necessary for the UMR-PRMC model.

- Relative Van der Waals volume parameter (r)=10.598
- Relative Van der Waals surface area parameter (q) = 8.739

3.3 Models Selected for Evaluation

In this work, eight models were tested. The first two models are the most popular equations of state used today, meaning SRK and PR. The purpose for testing this model is to test how these really popular models behave regarding mercury. Then the default SRK, referred to as SRK PRO/II default, and PR, referred to as PR PRO/II default, found in the PRO/II software package were evaluated. These models have k_{ij}s for mercury systems, thus improving mainly the predictive ability for the liquid phase. Thus, these two models are the "liquid correction" models. Then the SRK-Twu(Hg) - no k_{ij} and then PRMC(Hg) - no k_{ij} were evaluated. These

two models use advanced expressions for the alpha function of the equations of state. These expressions include parameters which are fitted to experimental vapor pressure data, which results in improved predictive ability for the vapor phase. These two models are the "vapor phase correction" models. Finally, the model developed by Statoil in 2014, which from now on it will be referred to as SRK-Twu(Hg), was evaluated. This model is an improvement of Statoil's model in 2011, which now takes into account new solubility data from new sources. This model includes binary interaction parameters for mercury, while it also uses Twu's advanced expression for the alpha function. These two facts result in an improvement for both the liquid and the vapor phase. The model provided by Statoil in 2011 and Mentzelos models were not selected for further evaluation since they were taken into account for the creation of Statoil model in 2014 (SRK-Twu(Hg)). Finally, the UMR-PRMC model will only be evaluated at the case studies presented at Chapter 5 and not for the binary and multicomponent mixtures, like all the other models, as this evaluation was made by Metzelos [27].

Concluding the models selected for evaluation are the following:

1. SRK
2. PR

Most Popular Models Used

3. SRK PRO/II default
4. PR PRO/II default

"Liquid Phase Correction"

5. SRK-Twu(Hg) - no k_{ij}
6. PRMC(Hg) - no k_{ij}

"Vapor Phase Correction"

7. SRK-Twu(Hg) → Statoil's Model
8. MRU-PRMC

3.4 Additional Work on Mercury Modelling

As mentioned before, very limited data are available on mercury modelling, since companies keep their models classified. One model is provided in the Multiflash product from Infochem Computer Services, which was acquired by KBC.

The Infochem mercury model is stated to be able to handle simultaneously any number of phases on any type including vapor, hydrocarbon liquid, aqueous, liquid mercury and solid mercury or other solids. The model can use three different equations of state, RKSA (Redlich Kwong-Soave Advanced), PRA (Peng-Robinson Advanced) and CPA-Infochem (Cubic Plus Association). These models are in-house optimized models of the standard RKS, PR and CPA models. In a study for a Middle East natural gas processing plant, conducted by KBC, Multiflash was used to simulate mercury's distribution and it was stated by the author that the model accurately described mercury's distribution in the plant. The Infochem mercury models were not available for evaluation. [31]

This model was also used by ConocoPhillips in 2012 [16]. However at this work additional work was done. An HgS equilibrium model was developed. The conversion of Hg^0 to HgS was modelled based on a series of curves for the amount of THg present as HgS. The proportion of total mercury (THg) present as HgS, was characterized using a K value, which is a function of Hg^0 concentration in a phase:

$$K(Hg^0) = \frac{HgS_{eq}}{THg}$$

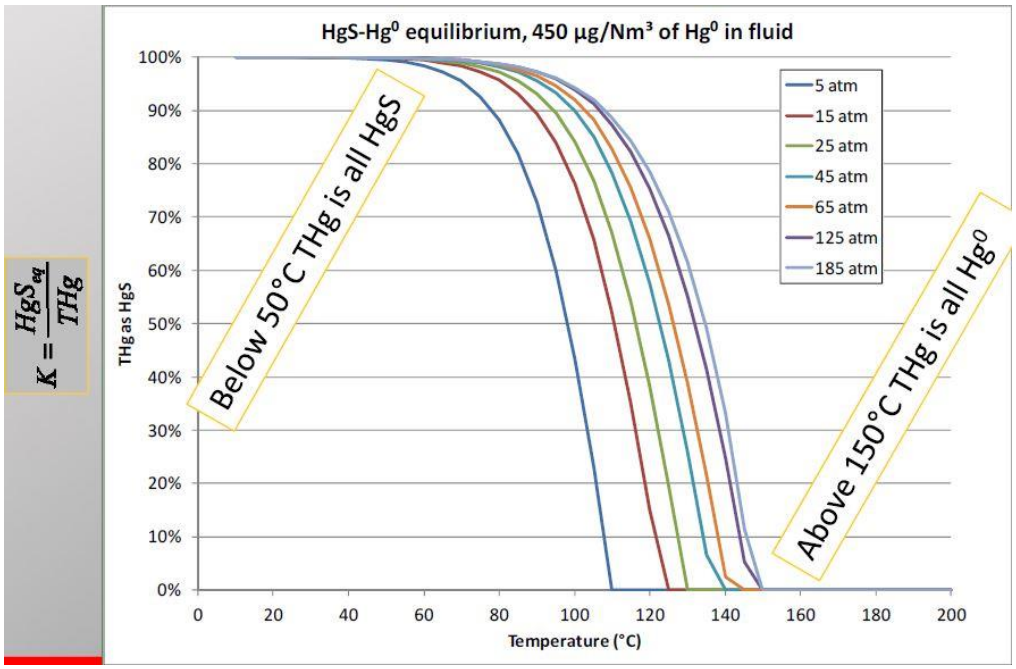

Figure 3.2: HgS-HgO equilibrium Characterization [16]

The developed model by ConocoPhillips [16] works as follows:

Soluble Hg^0 in each phase is converted to HgS, using the K value, and remains in that phase. HgS precipitating from a solid Hg^0 phase is partitioned between hydrocarbon liquid and aqueous phases as per the solubility of Hg^0 in those phases. Thus, HgS partitioning model depends on accurate prediction of Hg^0 distribution between aqueous and hydrocarbon phases. Multiflash software from Infochem Computer Services Ltd. was used for that cause. The model developed was designed to predict:

- a separate Hg^0 solid phase
- HgS precipitation as a solid non-thermodynamic component of vapor, hydrocarbon liquid and aqueous phases
- Conversion of Hg^0 to HgS and HgS to Hg^0

4. Evaluation of Models

In this part an evaluation of the selected models was made. The evaluation of the models is based on two main parts.

At the first part, the models were tested against binary and multicomponent experimental solubility data for mercury provided by Wiltec [32]. The available experimental solubility data for binary mixtures of mercury with other components were compared to the results given by the selected models. The available binary experimental data were for mixtures of mercury with the following components:

- Methane (C_1)
- Ethane (C_2)
- Propane (C_3)
- iButane (iC_4)
- nPentane (nC_5)
- Carbon dioxide (CO_2)
- Nitrogen (N_2)

Regarding the SRK PRO/II default and PR PRO/II default models, they were not used for the iC_4-Hg, CO_2-Hg and N_2-Hg systems, since no binary interaction parameters for mercury are provided for these systems by PRO/II.

The available multicomponent mixtures for which an evaluation was made are the following:

- Natural Gas
- $nC_4 + nC_5 + nC_6$ (liquid)
- $iC_4 + C_3$ (liquid)

It should be noted that the binary interaction parameters for the SRK-Twu(Hg) model were fitted to the same experimental data (Wiltec data), thus the results given by this model are not pure predictions for the binary mixtures. On the other hand, for the multicomponent mixtures the results given by all models are pure predictions. The exact compositions of the multicomponent mixtures are given later.

At the second part, a k-values analysis was made. This analysis is necessary to better understand how the models tend to distribute mercury between the vapor and the liquid phase. The K values can be calculated by the following formula where y and x is mercury's composition in the vapor and liquid phase respectively.

$$k = \frac{y}{x}$$

Finally, especially for the SRK-Twu(Hg) model, the prediction ability of the model's k_{ij}-correlations was tested. As stated before, the model provides three correlations for the components for which no solubility data were available and thus no binary interaction parameters could be calculated. These correlations can generate binary interaction parameters for a hydrocarbon component based on whether it is paraffinic, naphthenic or aromatic and based on its carbon number. To make the evaluation of the correlations, a k_{ij} was generated by the correlation for the paraffinic components and tested against new solubility data that were found for the nC_{12}-Hg system. [33]

4.1 Evaluation of the Models for Binary Mixtures

Experimental data were available for multiple binary hydrocarbon systems at different pressures and temperatures from Wiltec's report [32]. The results and the deviations from the experimental data of all models except for the UMR-PRMC model are given below. The evaluation of the UMR-PRMC model was made by Mentzelos [27] .

It must be noted that the binary interaction parameters for mercury for the SRK-Twu(Hg) model were fitted to the same experimental data that are being compared to. That means, that the SRK-Twu(Hg) model provides pure predictions only for the multicomponent mixtures.

Mercury in Methane

Figure 4.1: Hg's Solubility in C_1 (P=27.58 bara) – Vapor Phase

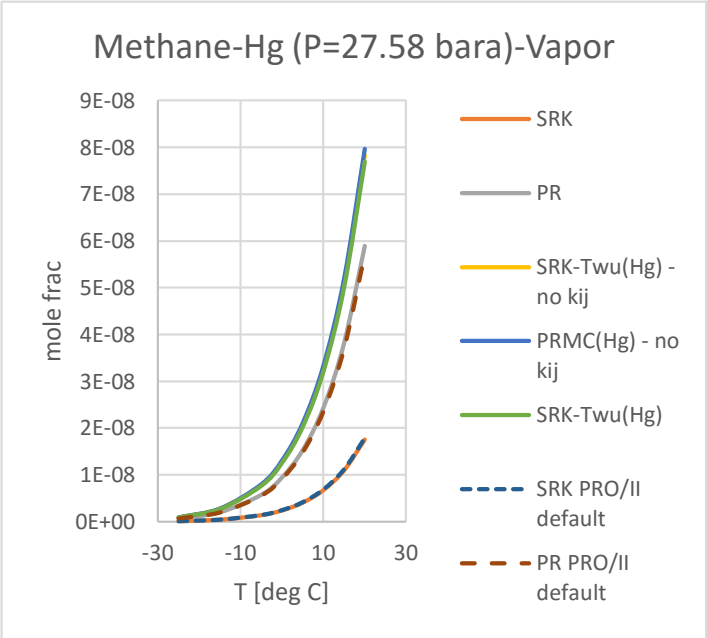

Figure 4.2: Hg's Solubility in C_1 (P=34.47 bara) – Vapor Phase

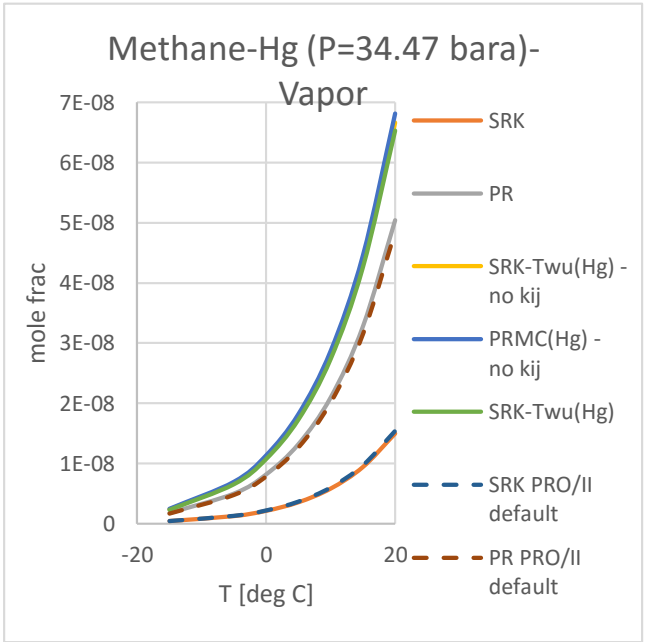

Figure 4.3: Hg's Solubility in C_1 (P=68.95 bara) – Vapor Phase

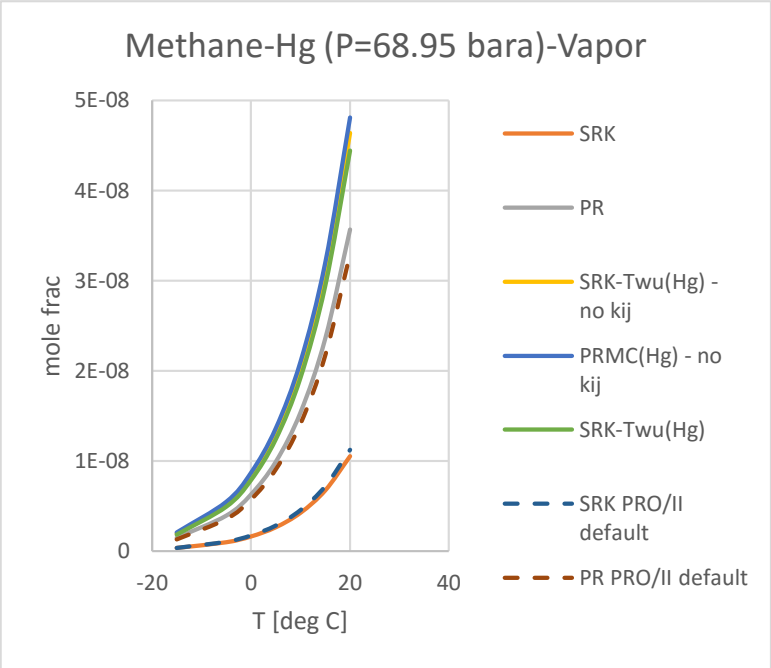

Comments:

- In general, the most important factor for this system, which is in the vapor phase, is the prediction of the vapor pressures. The vapor pressures are accurately predicted by the SRK-Twu(Hg)-no k_{jj}, PRMC-no k_{ij} and SRK-Twu(Hg) models and thus they accurately predict the solubility of mercury. For higher pressures the SRK-Twu(Hg) model provides results that are slightly more accurate.

- It can also be seen that the PR model, which, in general, predicts more accurately the vapor pressures than the SRK model, also predicts better the solubility of mercury in methane than the SRK model. It can also be seen that the PR and SRK models systematically under-predict the solubility of mercury in methane.

- The SRK and PR models and the SRK PRO/II default and PR PRO/II default models have almost identical behavior describing the methane-mercury system. This was expected as the only thing that is different between these models, is that the PRO/II models use k_{ij} parameters, which have major effect on the liquid phase and minor effect on the vapor phase.

Table 4.1: Deviations of the Models for the Methane-Mercury System

Error %	SRK	PR	SRK PRO/II default	PR PRO/II default	SRK-Twu(Hg)– no k_{ij}	PRMC(Hg)– no k_{ij}	SRK-Twu(Hg)
P=27.58 bara (vapor)	80,97%	25,78%	80,38%	28,16%	2,05%	3,45%	1,70%
P=34.37 bara (vapor)	79,90%	23,81%	79,14%	26,85%	3,14%	5,50%	1,72%
P=68.95 bara (vapor)	78,73%	19,37%	77,01%	25,98%	6,51%	11,17%	3,87%
Total	79,97%	23,29%	78,93%	27,06%	3,69%	6,34%	2,33%

Figure 4.4: Hg's Solubility in C_2 (P=54-67 bara) – Liquid Phase

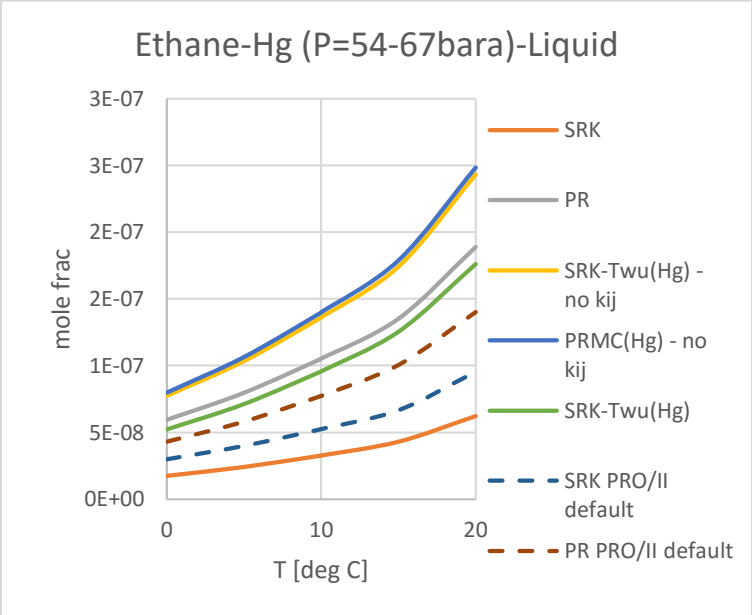

Figure 4.5: Hg's Solubility in C_2 (P=82 bara) – Liquid Phase

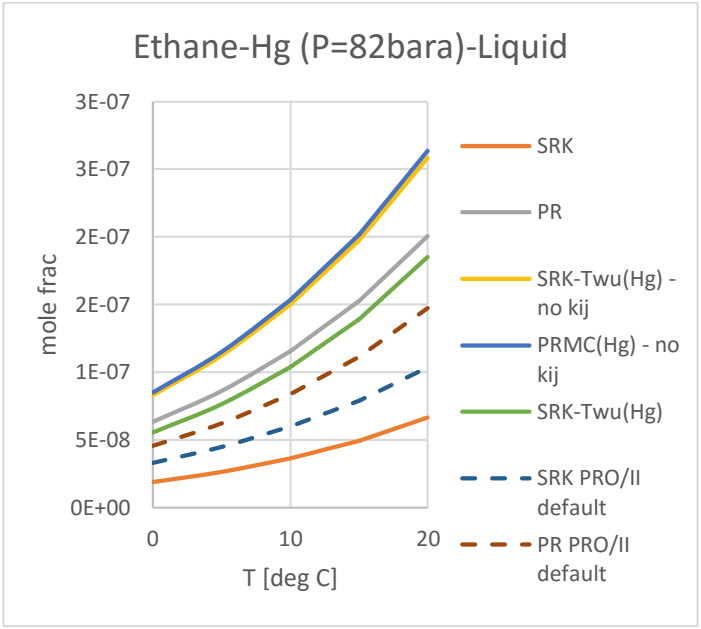

Figure 4.6: Hg's Solubility in C_2 (P=23-37 bara) – Vapor Phase

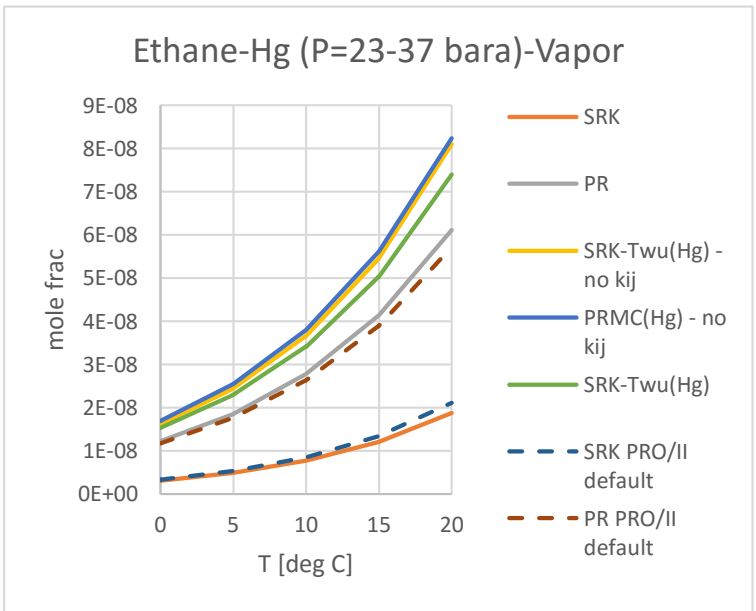

Comments:

- The results presented above indicate that the liquid phase is accurately described by the *SRK-Twu(Hg)* and PR models. Between those two models, the *SRK-Twu(Hg)* model gives better predictions especially at high pressures. The *PRMC(Hg) - no* k_{ij} and *SRK-Twu(Hg)-no* k_{ij} models over predict mercury's solubility in the liquid phase, while the SRK model under-predicts mercury's solubility.

- For the vapor phase, the best models are again SRK-Twu(Hg) – no k_{ij} and PRMC(Hg)- no k_{ij}, while SRK-Twu(Hg) has a higher deviation. The PR and SRK models under-predict the solubility of mercury in ethane.

- As regards the SRK and PR default PRO/II models, it can be seen that when using the k_{ij} parameters, then the prediction for the liquid phase is more accurate, while the prediction for the vapor phase remains almost the same. However, PR's behavior should be discussed. For PR it seems that when using no k_{ij} the prediction is better. This is due to cancelation of error, since PR inaccurately predicts y_i, γ_i and P_i^s which cancel each other's error. This leads to a good prediction of the liquid phase, x_i, when solving the equilibrium.

$$x_i = \frac{y_i P}{\gamma_i P_i^s}$$

Where:
x_i : composition of the component i in the liquid phase
y_i : composition of the component i in the vapor phase
P : pressure of the system
γ_i : activity coefficient of the component i
P_i^s : vapor pressure of component I at the temperature of the system

If this effect did not take place then it would be expected that the liquid phase would be better described when binary interaction parameters were used.

Table 4.2: Deviations of the Models for the Ethane-Mercury System

Error %	SRK	PR	SRK PRO/II default	PR PRO/II default	SRK-Twu(Hg)– no k_{ij}	PRMC(Hg)– no k_{ij}	SRK-Twu(Hg)
P=54-67 bara (liquid)	67,29%	5,46%	47,53%	22,76%	35,87%	39,38%	4,58%
P=82 bara (liquid)	64,26%	13,42%	41,33%	17,65%	47,33%	50,49%	2,16%
P=23-37 bara (vapor)	81,77%	34,04%	79,91%	37,50%	12,75%	9,68%	18,75%
Total	72,03%	19,07%	58,32%	26,97%	30,31%	31,14%	9,39%

Mercury in Propane

Figure 4.7: Hg's Solubility in C_3 (P=48.26 bara) – Liquid Phase

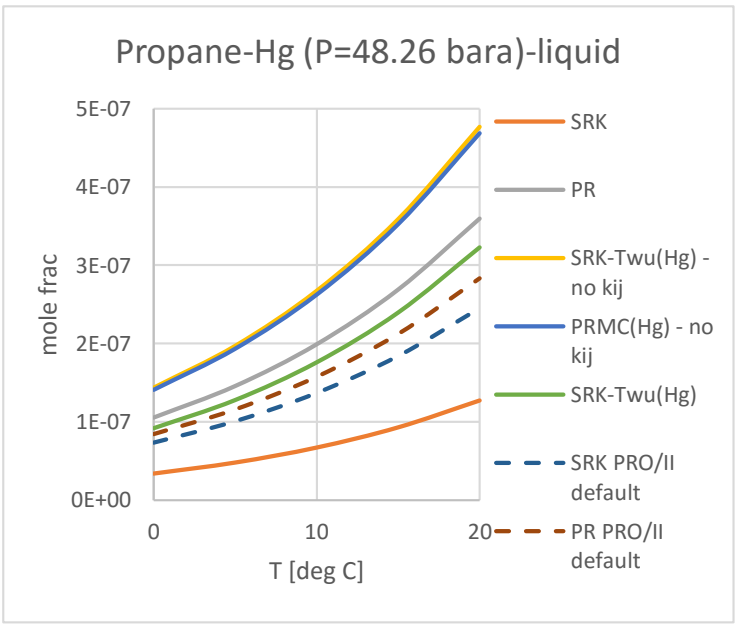

Figure 4.8: Hg's Solubility in C_3 (P=68.95 bara) – Liquid Phase

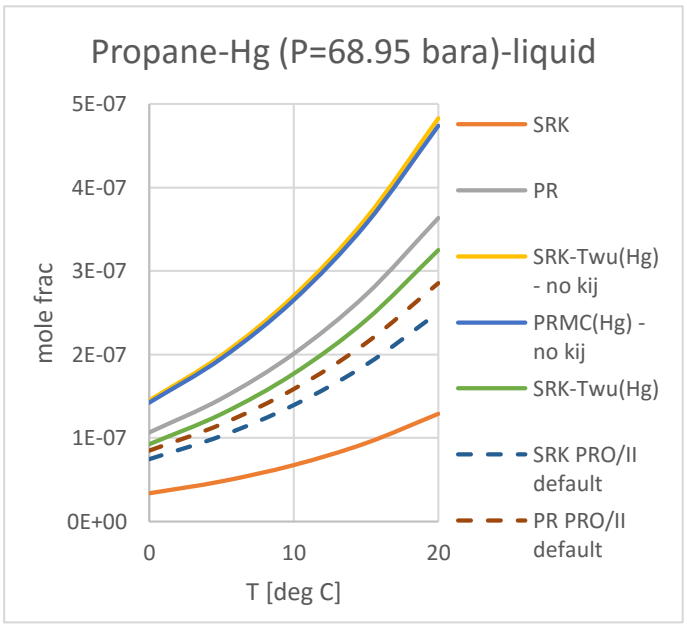

Figure 4.9: Hg's Solubility in C_3 (P=4-8 bara) – Vapor Phase

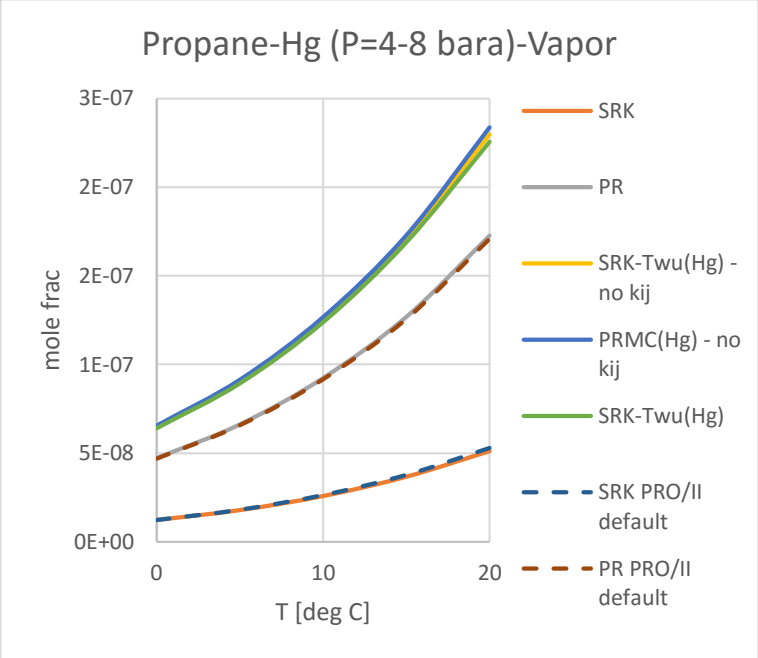

Comments:

- For the liquid phase the only accurate prediction is made by the SRK-Twu(Hg) model while all other models fail. Additionally, it should be noted that PR, SRK-Twu(Hg)-no k_{ij} and PRMC(Hg)-no k_{ij} systematically over-predict the solubility of mercury in propane, while SRK continues to systematically under-predict mercury's solubility.

- For the vapor phase, as already mentioned, the most important factor is the accurate prediction of the vapor pressures and not the binary interaction parameters. Thus, SRK-Twu(Hg)- no k_{ij}, PRMC(Hg)-no k_{ij} and SRK-Twu(Hg) models have the smallest and similar deviations. On the other hand, PR and SRK models deviate far more from the experimental data, under-predicting mercury's solubility.

- Regarding the SRK and PR default PRO/II models, it can be seen, when comparing with SRK and PR, that the use of k_{ij} parameters enhances the prediction for the liquid phase, while the vapor phase remains intact. The behavior of PR model is the same as in the ethane-mercury system and was explaned above.

Table 4.3: Deviations of the Models for the Propane-Mercury System

Error %	SRK	PR	SRK PRO/II default	PR PRO/II default	SRK-Twu(Hg)– no k_{ij}	PRMC(Hg)– no k_{ij}	SRK-Twu(Hg)
P=48.26 bara (liquid)	62,44%	12,09%	22,98%	11,29%	50,66%	47,90%	1,04%
P=68.95 bara (liquid)	61,51%	14,57%	20,53%	9,52%	54,11%	51,11%	1,23%
P=4-8 bara (vapor)	81,66%	34,29%	81,21%	34,81%	10,77%	9,75%	12,01%
Total	68,53%	20,31%	41,57%	18,54%	38,51%	36,25%	4,76%

Figure 4.10: Hg's Solubility in iC_4 (P=4-8 bara) – Liquid Phase

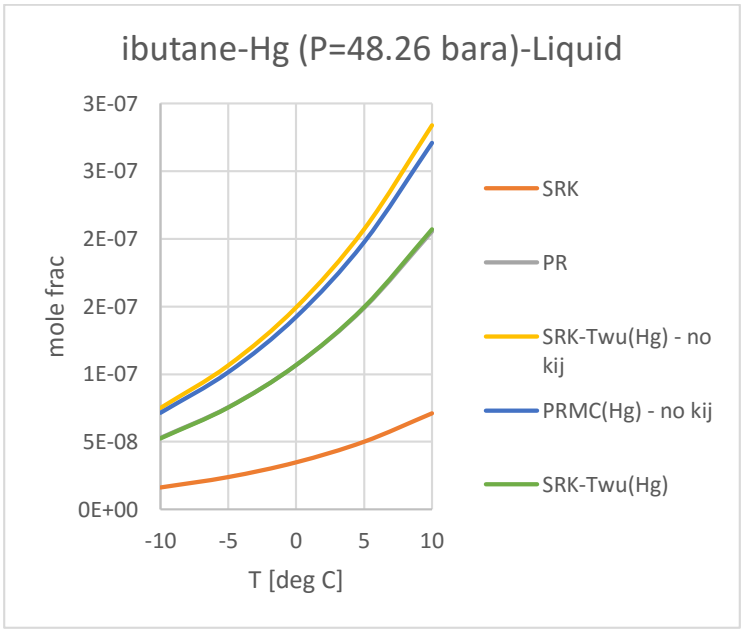

Figure 4.11: Hg's Solubility in iC_4 (P=4-8 bara) – Liquid Phase

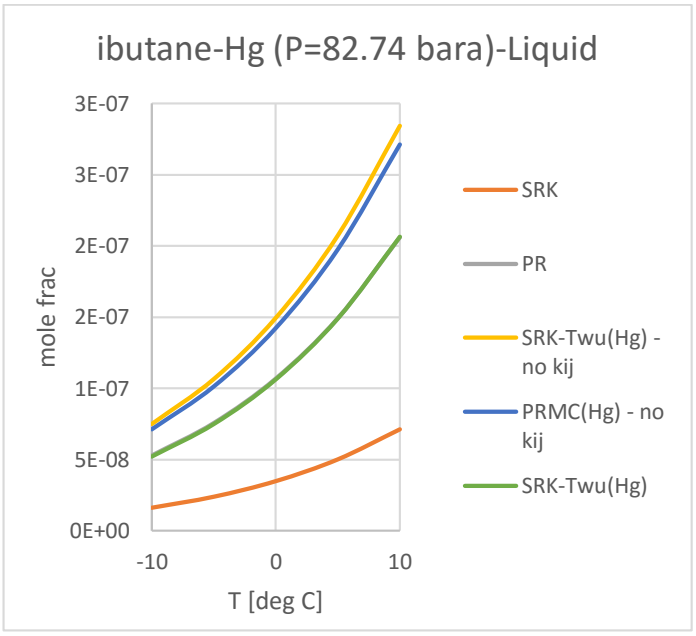

Figure 4.12: Hg's Solubility in iC_4 (P=0.9-1.9 bara) – Vapor Phase

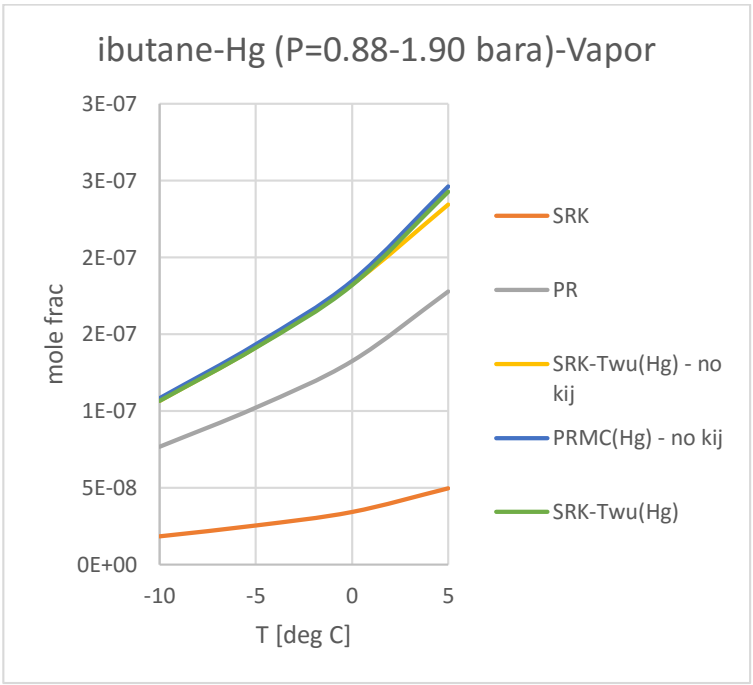

Comments:

- As it can be seen in the diagrams above, the SRK-Twu(Hg) and PR model accurately describe the liquid phase, while the SRK-Twu(Hg)-no k_{ij} and PRMC(Hg)-no k_{ij} over-predict mercury's solubility. On the other hand, the SRK model under predicts the solubility of mercury in ibutane.

- In the vapor phase, SRK-Twu(Hg)- no k_{ij}, PRMC(Hg)- no k_{ij} and SRK-Twu(Hg), that accurately predict the vapor pressures, can accurately predict the solubility of mercury in ibutane. Both the SRK and PR models under-predict mercury's solubility.

Table 4.4: Deviations of the Models for the iButane-Mercury System

Error%	SRK	PR	SRK-Twu(Hg)-no k_{ij}	PRMC(Hg)-no k_{ij}	SRK-Twu(Hg)
P=48.26 bara (liquid)	67,59%	1,17%	39,11%	32,62%	0,81%
P=82.74 bara (liquid)	66,61%	2,20%	43,03%	36,33%	1,82%
P=0.88-1.90 bara (vapor)	84,13%	36,93%	13,23%	11,45%	12,90%
Total	73,49%	14,90%	30,63%	25,84%	5,66%

Mercury in n-Pentane

Figure 4.13: Hg's Solubility in nC_5 (P=17.9-20.7 bara) – Liquid Phase

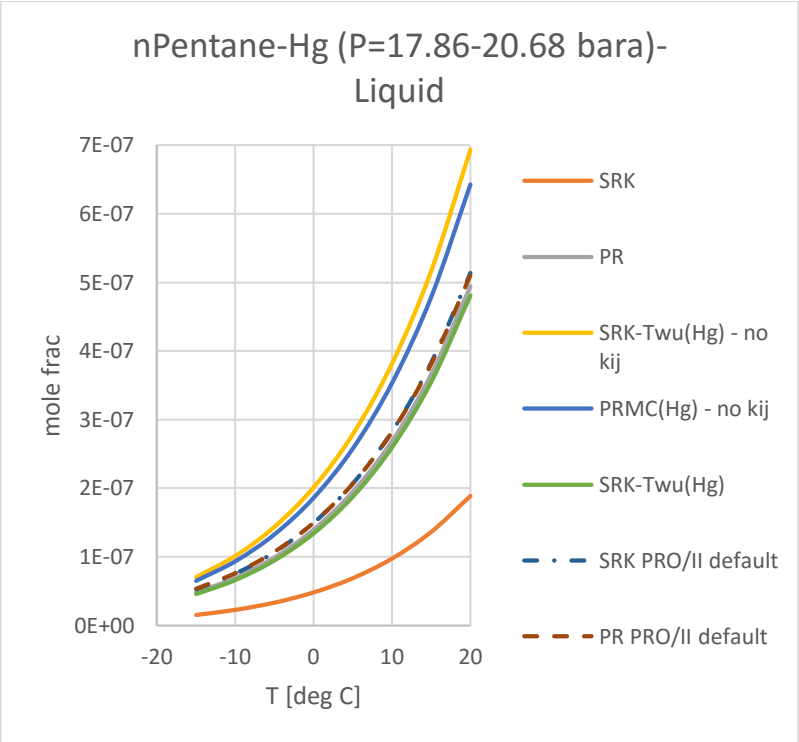

Comments:

- The SRK-Twu(Hg) and PR models can accurately predict the solubility of mercury in n-Pentane. Both the SRK-Twu(Hg)-no k_{ij} and PRMC(Hg)-no k_{ij} models make over-prediction, while the SRK makes an under-prediction of mercury's solubility

- As explained before, PR can accurately predict mercury's solubility for the liquid phase due to cancelation of error. On the other hand, the use of k_{ij} parameters in the SRK PRO/II default and PR PRO/II default models improve, as expected the prediction for the liquid phase, comparing with the SRK and PR models respectively.

Table 4.5: Deviations of the Models for the Pentane-Mercury System

Error %	SRK	PR	SRK PRO/II default	PR PRO/II default	SRK-Twu(Hg)–no k_{ij}	PRMC(Hg)–no k_{ij}	SRK-Twu(Hg)
P=17.86-20.68 bara (liquid)	62,65%	7,81%	15,07%	15,03%	54,90%	43,02%	4,20%

Mercury in CO_2

Figure 4.14: Hg's Solubility in CO_2 (P=82.7 bara) – Liquid Phase

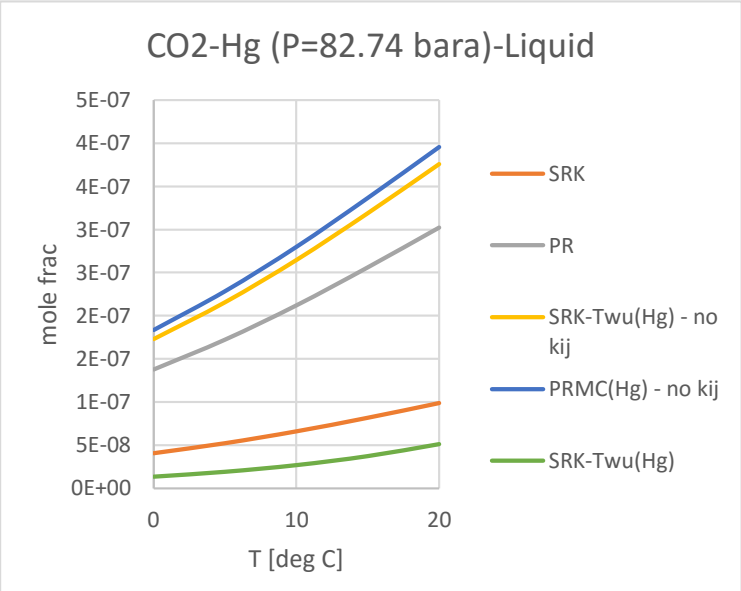

Figure 4.15: Hg's Solubility in CO_2 (P=103.4 bara) – Liquid Phase

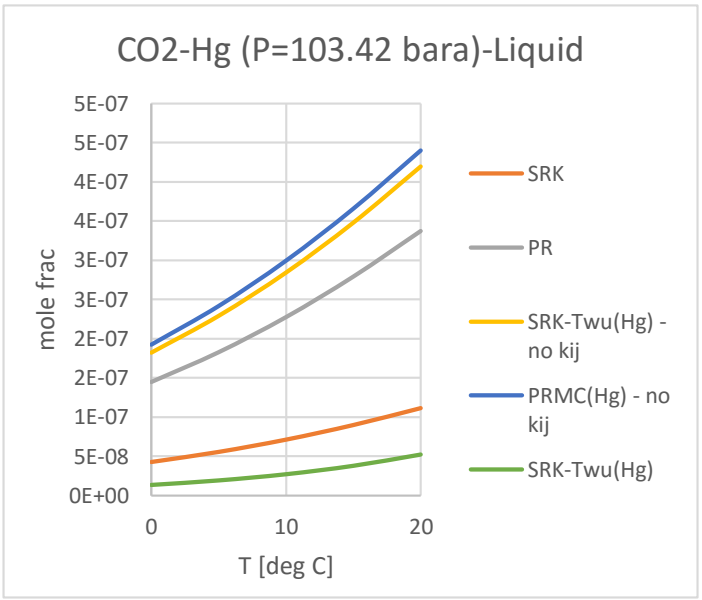

Figure 4.16: Hg's Solubility in CO_2 (P=34-57 bara) – Vapor Phase

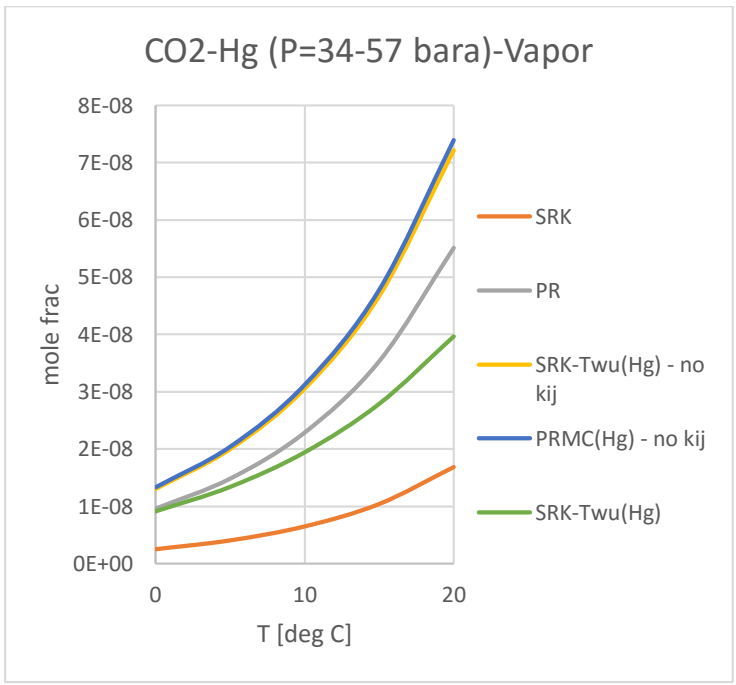

Comments:

- In the CO_2-mercury system, the most accurate model is SRK-Twu(Hg) model. Equations of state are not applicable for polar compounds. The carbon dioxide may not have dipole moment, but it has quadrupole moment. Thus, equations of state are not expected to give accurate predictions without the use of binary interaction parameters. Given the results presented above, it can be seen that the liquid phase is accurately predicted only by the SRK-Twu(Hg) model, while all other models fail to make an accurate prediction.

- For the vapor phase though, SRK-Twu(Hg) and PR models seem to give the best results. The SRK-Twu(Hg) model has a deviation of 16%, which is similar to the deviations seen for all binary hydrocarbon mixtures. On the other hand, the PR model, seems to have less deviation from the experimental data comparing with the binary hydrocarbon vapor systems tested above.

Table 4.6: Deviations of the Models for the CO_2-Mercury System

Error%	SRK	PR	SRK-Twu(Hg)-no k_{ij}	PRMC(Hg)-no k_{ij}	SRK-Twu(Hg)
P=82.74 bara (liquid)	145,03%	693,76%	892,09%	948,44%	6,70%
P=103.42 bara (liquid)	171,12%	770,84%	991,05%	1048,90%	5,60%
P=34-57 bara (vapor)	71,57%	7,02%	33,12%	36,11%	16,30%
Total	129,24%	490,54%	638,76%	677,81%	9,53%

Mercury in Nitrogen

Figure 4.17: Hg's Solubility in N_2 (T=0 ^{O}C) – Vapor Phase

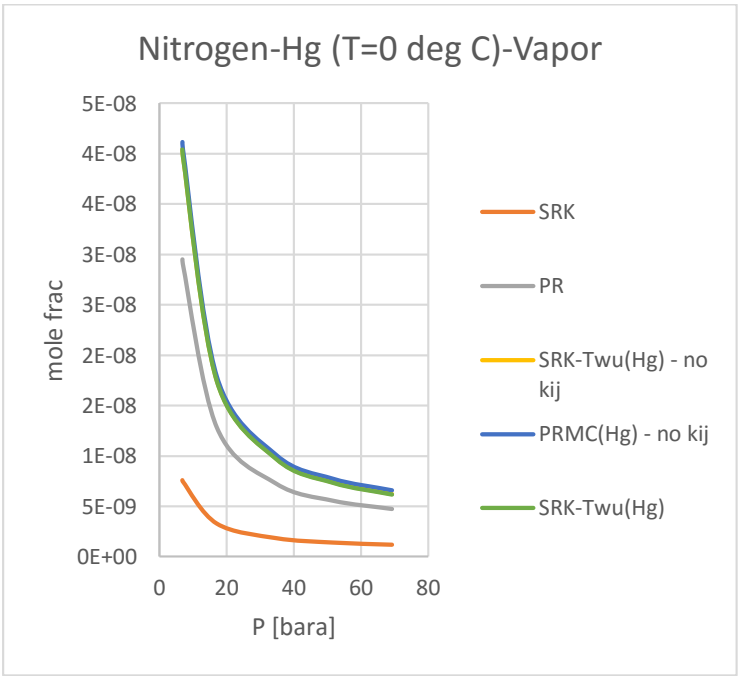

Comments:

The prediction of the nitrogen-mercury system in vapor phase is accurately predicted, due to the use of the advanced expression for the alpha function, by SRK-Twu(Hg), SRK-Twu(Hg)-no k_{ij} and PRMC(Hg)-no k_{ij} model while the PR and SRK models make under-predictions.

Table 4.7: Deviations of the Models for the Nitrogen-Mercury System

Error%	SRK	PR	SRK-Twu(Hg)-no k_{ij}	PRMC(Hg)-no k_{ij}	SRK-Twu(Hg)
T=0 ^{0}C (Vapor)	79,86%	20,85%	7,18%	10,25%	6,75%

4.2 Evaluation of the Models for Multicomponent Mixtures

Experimental data are available for three hydrocarbon mixtures. The composition of these mixtures are shown below along with the results and the deviations calculated.

Natural Gas Mixture

Component	Molar Composition
Methane:	0.881
Ethane:	0.062
Propane:	0.0251
Nitrogen:	0.0103
Carbon Dioxide:	0.0216

Figure 4.18: Hg's Solubility in NG (P=27.6 bara) – Vapor Phase

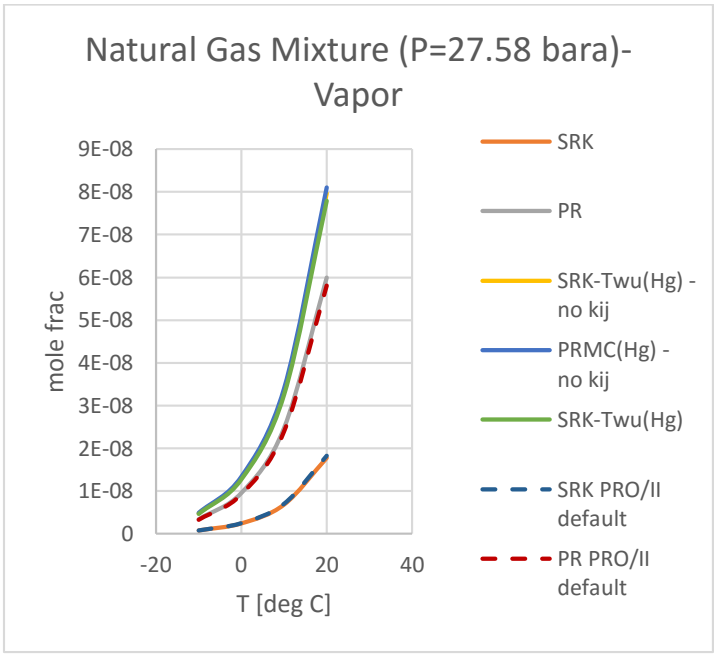

Figure 4.19: Hg's Solubility in NG (P=69 bara) – Vapor Phase

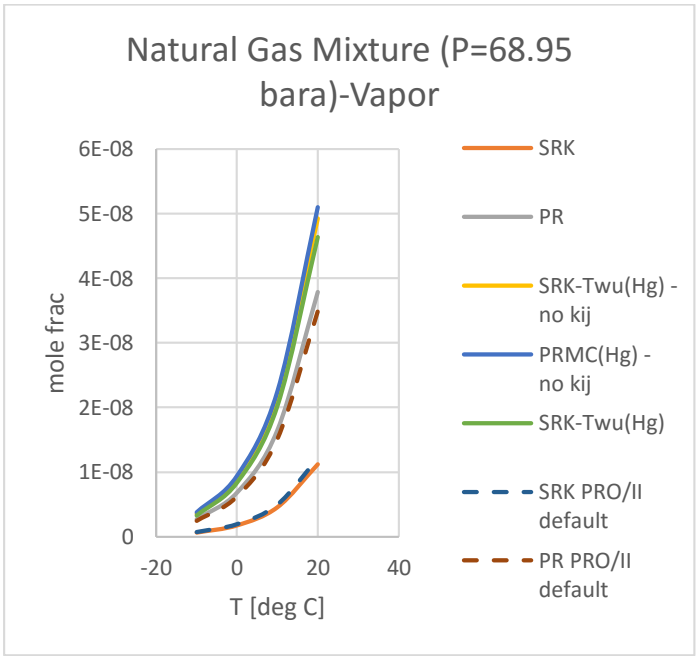

Comments:

As with the binary mixtures, the best prediction for a vapor phase is given by the SRK-Twu(Hg), SRK-Twu(Hg)-no k_{ij} and PRMC(Hg)-no k_{ij} models. Between these three models, SRK-Twu(Hg) model is better when it comes to higher pressures. The PR and SRK models under-predict the solubility of mercury in this vapor phase mixture.

As this system is in the vapor phase, no big deviations between the SRK and PR and SRK PRO/II default and PR PRO/II default models were expected. It should be noted that this mixture includes CO_2 and N_2 for which PRO/II has no interaction parameters for mercury. These components are in small quantities and thus they have no major effect in the prediction of mercury's solubility.

Table 4.8: Deviations of the Models for the NG-Mercury System

Error %	SRK	PR	SRK PRO/II default	PR PRO/II default	SRK-Twu(Hg)– no k_{ij}	PRMC(Hg)– no k_{ij}	SRK-Twu(Hg)
P=27.58 bara	81,61%	31,16%	81,00%	33,34%	7,40%	7,10%	9,38%
P=68.95 bara	79,40%	22,97%	77,47%	29,43%	8,06%	10,85%	6,85%
Total	80,50%	27,07%	79,24%	31,39%	7,73%	8,97%	8,11%

Isobutane + Propane Mixtures (liquid)

Component	Molar Composition
Propane:	0.594
Isobutane:	0.406

Figure 4.20: Hg's Solubility in iC_4+C_3 (P=35-48 bara) – Liquid Phase

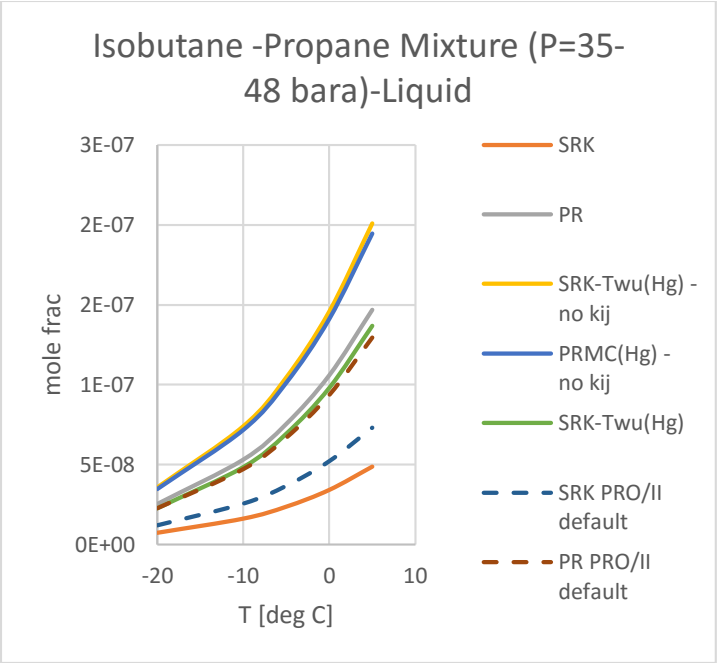

Figure 4.21: Hg's Solubility in NG (P=69 bara) – Liquid Phase

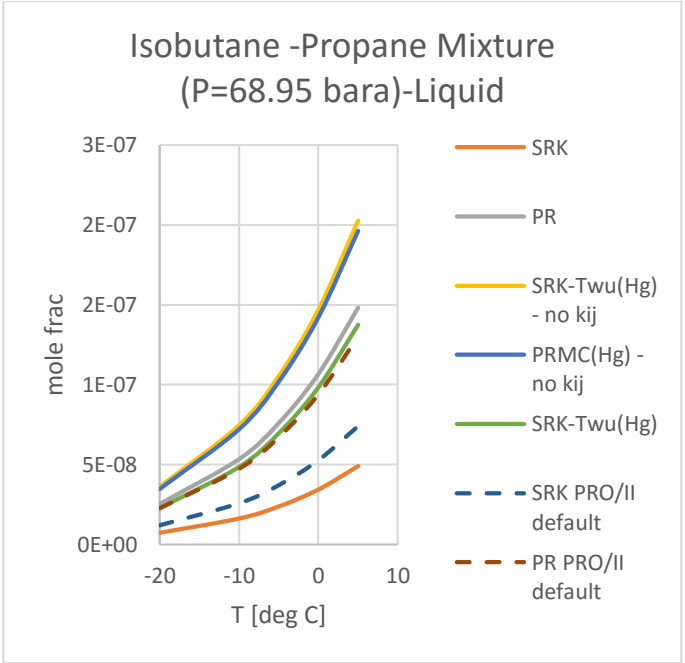

Comments:

For this mixture, as with the binary mixtures for the liquid phase, the most accurate predictions are made by SRK-Twu(Hg) and PR. The SRK-Twu(Hg)-no k_{ij} and PRMC(Hg)-no k_{ij} models, are over-predicting while the SRK model continues to under-predict mercury's solubility. The good prediction by PR was expected, as explained above, due to cancelation of error. Considering the default PRO/II models, the use of binary interaction parameters improve the solubility prediction for the liquid phase. It should be noted, that there is no k_{ij} for the ibutane in the PRO/II database and the improvement of the prediction is only due to the propane-mercury k_{ij}. Again, the behavior of the models is qualitative the same comparing to the binary mixtures presented above.

Table 4.9: Deviations of the Models for the iC_4+C_3 - Mercury System

Error %	SRK	PR	SRK PRO/II default	PR PRO/II default	SRK-Twu(Hg)– no k_{ij}	PRMC(Hg)– no k_{ij}	SRK-Twu(Hg)
P=35-48 bara	69,37%	4,44%	52,13%	12,34%	37,24%	32,84%	9,12%
P=68.95 bara	67,35%	6,19%	48,71%	6,75%	46,24%	41,43%	4,19%
Total	68,36%	5,31%	50,42%	9,55%	41,74%	37,14%	6,65%

n-Butane + n-Pentane + n-Hexane Mixture (liquid)

Component	Molar Composition
nButane:	0.324
nPentane:	0.335
nHexane:	0.341

Figure 4.22: Hg's Solubility in $nC_4+nC_5+nC_6$ (P=69 bara) – Liquid Phase

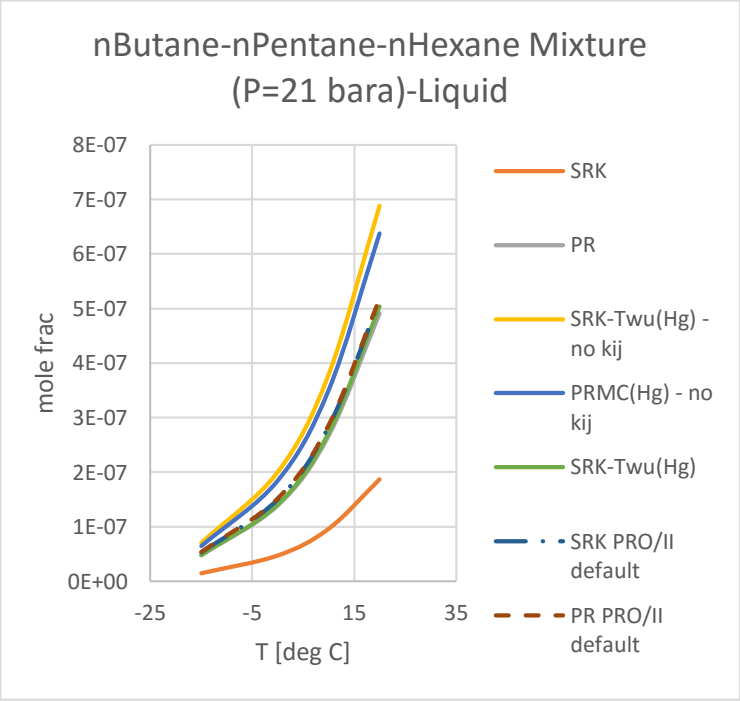

Comments:

Again, for this mixture in the liquid phase, the SRK-Twu(Hg) and PR models are the most accurate ones, while the PRMC(Hg)-no k_{ij} and SRK-Twu(Hg)-no k_{ij} over-predict mercury's solubility. On the other hand, the SRK model under-predicts mercury's solubility. The use of k_{ij}s by the default PRO/II models improve the prediction for the liquid phase, like in all the other cases.

Table 4.10: Deviations of the Models for the nC4+C5+nC6 - Mercury System

Error %	SRK	PR	SRK PRO/II default	PR PRO/II default	SRK-Twu(Hg)– no k_{ij}	PRMC(Hg)– no k_{ij}	SRK-Twu(Hg)
P=21 bara	63,39%	6,28%	15,20%	16,65%	53,04%	41,19%	7,91%

Comments

After the comparison of the models against binary and multicomponent mixtures it was found that the SRK-Twu(Hg) model can more accurately predict both for the vapor and the liquid phase. This is expected, as comparing to the other models this one is the only one that accurately describe the vapor phase, due to Twu's expression for the alpha function, and the liquid phase, due to the use of binary interaction parameters.

SRK-Twu(Hg) model, is a fitted model when comparing to the binary experimental data as already mentioned. However, for the multicomponent hydrocarbon mixtures this model as all the others give pure predictions. As the behavior of all models is qualitative the same, for both the binary and multicomponent mixtures, then one can safely say that the SRK-Twu(Hg) model is the best model between the models tested.

The liquid phase is accurately described when binary interaction parameters are used

- It was noted that for the liquid phase the only accurate model was the SRK-Twu(Hg), as it uses binary interaction parameters, which are necessary for a liquid phase considering its non-ideality. It was also noted that the PRMC(Hg)-no k_{ij} and the SRK-Twu(Hg)- no k_{ij} models systematically over-predict the solubility of mercury in the liquid phase, while the SRK model systematically makes under-predictions of mercury's solubility for the liquid phase. The SRK PRO/II default and PR PRO/II default models improve the predictions for the liquid phase, when comparing to the SRK and PR models, but still the predictions provided by these models are not very accurate.
- The PR model, was also found to be good for the prediction of the liquid phase, but this is due to cancelation of error. PR inaccurately predicts both y_i, γ_i and P_i^s which cancel each other's error. This leads to a good prediction of the liquid phase, x_i, when solving the equilibrium. [34]

$$x_i = \frac{y_i P}{\gamma_i P_i^s}$$

Where:
x_i : composition of the component i in the liquid phase
y_i : composition of the component i in the vapor phase
P : pressure of the system
γ_i : activity coefficient of the component i
P_i^s : vapor pressure of component i at the temperature of the system

The vapor phase is accurately described when the vapor pressures are accurately described

For the vapor phase prediction, it seems that the most important factor is the correct prediction of the vapor pressures. This is achieved mainly by the SRK-Twu(Hg), PRMC(Hg)-no k_{ij} and SRK-Twu(Hg)- no k_{ij} models, thus these models have all similar results. The PR and SRK models systematically make under-predictions for the vapor phase with the PR model being the most accurate between these two. The default SRK and PR PRO/II models were also found to under-predict mercury's solubility for the vapor phase.
For all mixtures in vapor phase, except for the methane-mercury system, while the SRK-Twu(Hg), SRK-Twu(Hg)-no k_{ij} and PRMC(Hg)- no k_{ij} models give the best results, the

deviation is still around 12%. This behavior is expected for systems being at high pressures since then the systems become non-ideal. However, for the propane-mercury and ibutane-mercury systems, the results presented above were not expected as both of these systems are at low pressures. The deviations between these models and the experimental data could be attributed to the uncertainty of the experimental data.
On the other hand, for the methane-mercury system, these models give accurate predictions except for PRMC(Hg)- no k_{ij} at high pressures.

4.3 Evaluation of the Models Based on K values for Binary Systems

In addition to the analysis made above, the K values were calculated for the components that experimental data were available for both the liquid and the vapor phase. This analysis is necessary to better understand how the models tend to distribute mercury between the vapor and the liquid phase. Below, the K values expression can be found along with the results of the analysis.

$$k = \frac{y}{x}$$

Where:

y = mercury composition in vapor phase
x = mercury composition in liquid phase

Figure 4.23: K values for the C_2-Hg System (P=23-54 bara)

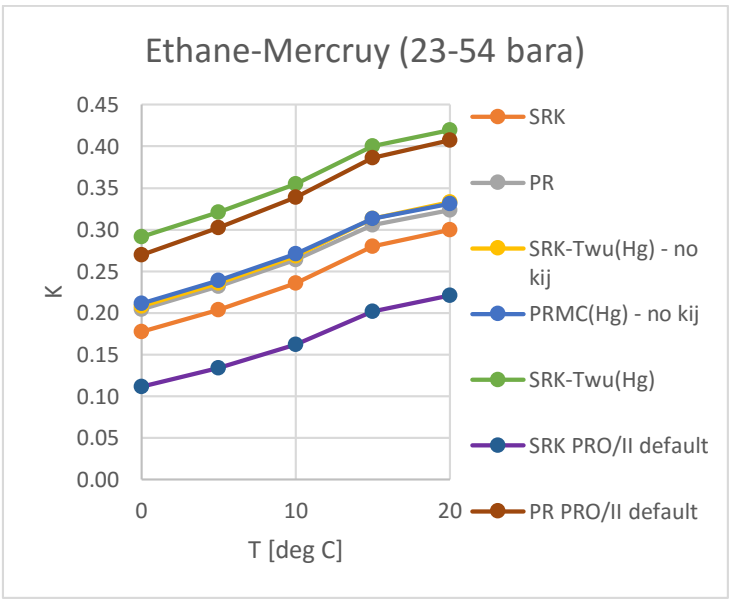

Figure 4.24: K values for the C_3-Hg System (P=4-48 bara)

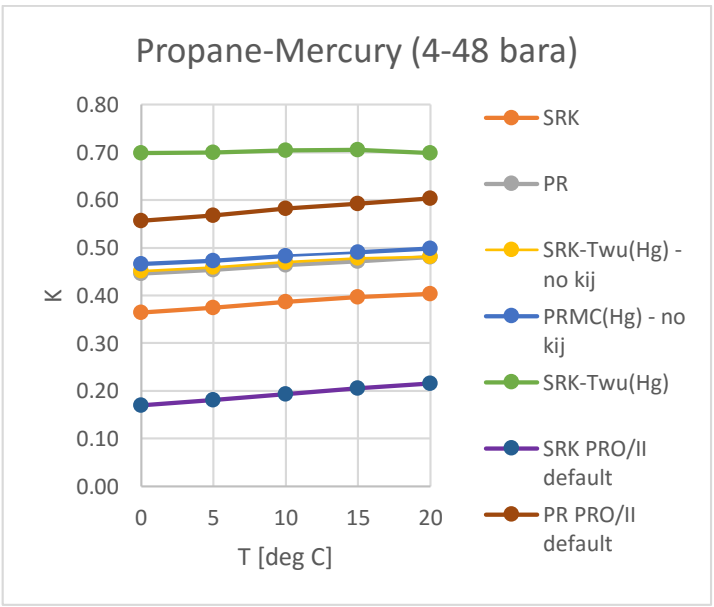

Figure 4.25: K values for the iC_4-Hg System (P=1-48 bara)

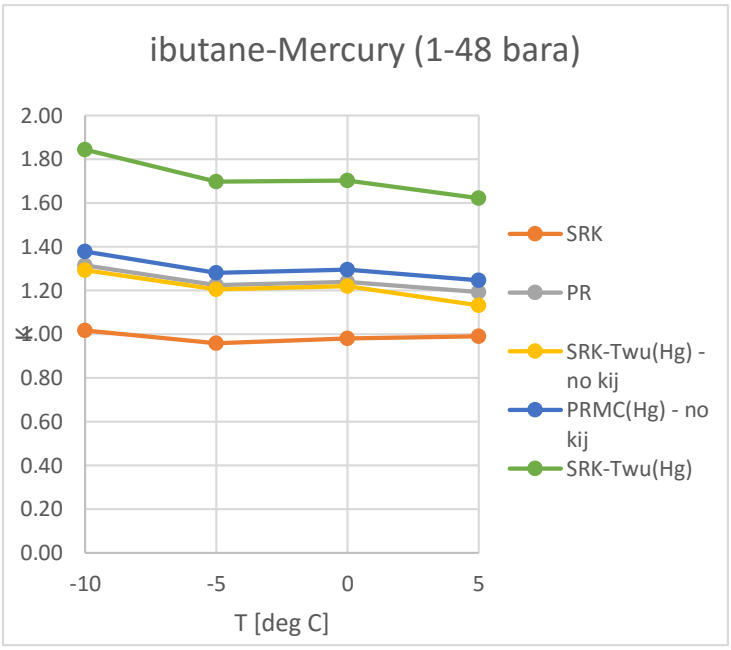

Figure 4.26: K values for the CO_2-Hg System (P=34-82 bara)

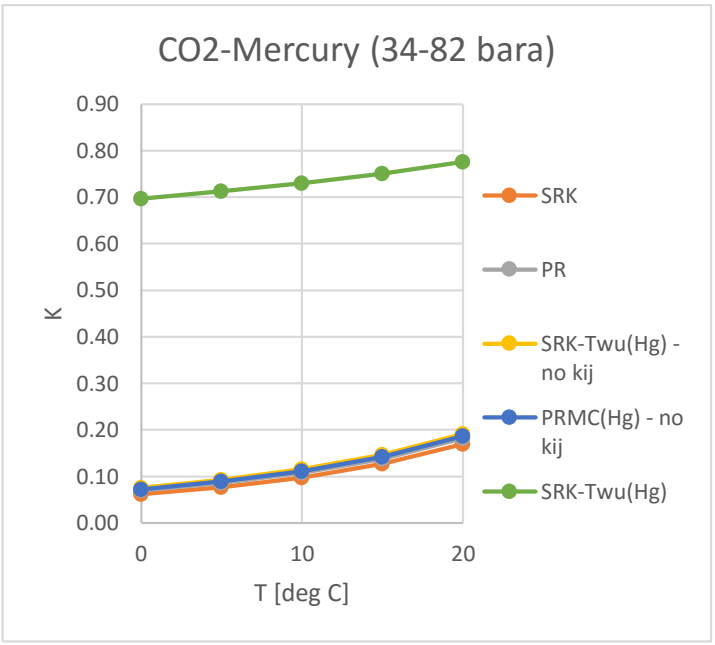

Table 4.11: K-Values Deviations

Error %	SRK	PR	SRK PRO/II default	PR PRO/II default	SRK-Twu(Hg)– no k_{ij}	PRMC(Hg)– no k_{ij}	SRK-Twu(Hg)
Ethane	43,35%	36,89%	60,97%	18,89%	35,58%	35,11%	14,82%
Propane	51,23%	41,35%	75,56%	26,47%	40,73%	38,94%	11,17%
ibutane	49,15%	36,09%	-	-	37,73%	33,12%	11,76%
CO_2	87,33%	86,15%	-	-	85,24%	85,70%	13,27%
Total	57,77%	50,12%	68,27%	22,68%	49,82%	48,22%	12,76%

Comments

The most accurate prediction, for the K values, is made by the SRK-Twu(Hg) model, but still with a deviation around 13%. For all systems, all models make under-prediction of the K values. This means, that all models predict that mercury partitions more to the liquid phase than what the experimental data indicate.

The systematic under-prediction of the K values for all models can be explained as follows having in mind Figures **Error! Reference source not found.**-Figure 4.17: Hg's Solubility in N_2 (T=0 ^{O}C) – Vapor Phase:

- SRK-Twu(Hg) model accurately predicts the liquid phase but under-predicts the vapor phase with a deviation around 10%.

$$k = \frac{0.9}{1} = 0.90$$

Thus, the calculated K value is expected to be lower than the experimental value with a deviation around 10%.

- The PRMC(Hg)-no k_{ij} and SRK-Twu(Hg)-no k_{ij} models over-predict by 50% mercury's solubility in the liquid phase but they under predict mercury's solubility in the vapor phase by 10% deviation.

$$k = \frac{0.9}{1.5} = 0.60$$

  Thus, the calculated K value is expected to be lower than the experimental value with a deviation around 40%.

- The PR model tends to under-predict by 30% mercury's solubility in the vapor phase, but it slightly over-predicts the liquid phase by 10%

$$k = \frac{0.7}{1.1} = 0.64$$

  Thus, the calculated K value is expected to be lower than the experimental value with a deviation around 40%.

- The SRK model tends to under-predict by 80% mercury's solubility in the vapor phase and the liquid phase by 60%

$$k = \frac{0.2}{0.4} = 0.5$$

  Thus, the calculated K value is expected to be lower than the experimental value with a deviation around 50%.

- The SRK PRO/II default model tends to under-predict by 80% mercury's solubility in the vapor phase and the liquid phase by 30%

$$k = \frac{0.2}{0.7} = 0.28$$

  Thus, the calculated K value is expected to be lower than the experimental value with a deviation around 70%.

- The PR PRO/II default model tends to under-predict by 30% mercury's solubility in the vapor phase and the liquid phase by 10%

$$k = \frac{0.7}{0.9} = 0.77$$

  Thus, the calculated K value is expected to be lower than the experimental value with a deviation around 23%.

- Regarding the CO_2 – Mercury system
  1. The SRK model under-predicts the vapor phase by 70% and over-predicts the liquid phase by 150%.

$$k = \frac{0.3}{2.5} = 0.12$$

     Thus, the calculated K value is expected to be lower than the experimental value with a deviation around 90%.

  2. The PR model over-predicts the vapor phase by 7% and over-predicts the liquid phase by 750%.

$$k = \frac{1.07}{8.5} = 0.13$$

Thus, the calculated K value is expected to be lower than the experimental value with a deviation around 85%.

3. The SRK-Twu(Hg)-no k_{ij} and PRMC(Hg)-no k_{ij} models over-predict the vapor phase by 35% and over-predicts the liquid phase by 950%.

$$k = \frac{1.35}{10.5} = 0.13$$

Thus, the calculated K value is expected to be lower than the experimental value with a deviation around 85%.

It is interesting to find, that the PR PRO/II default model predicts more accurately the K-values than the PR while the case is exactly the opposite for SRK PRO/II default and SRK models.

The predicted K-values from the PR PRO/II default increased comparing to the PR model, and this is because the predicted mercury's solubility decreased. PR predicted higher mercury's solubility, due to cancelation of error as was already explained. As regards the SRK PRO/II default and SRK models, SRK under-predicts mercury's solubility both for the vapor phase and for the liquid phase. The SRK PRO/II default uses k_{ij} parameters, thus describing better the liquid phase but still under-predicting for the vapor phase and therefore under-predicting also the K values. This resulted in even lower K-values comparing to the ones predicted by SRK, which already under-predicted them.

4.4 Evaluation of the Prediction Ability of the SRK-Twu(Hg) Model's Correlations

In this part, an evaluation of the SRK-Twu(Hg) model's correlations was made. This was made possible since new solubility data were found. These data were published by AICHE [33].

Specifically, AICHE provides temperature depended correlations for mercury's solubility in different hydrocarbon components. The applicability range for temperatures for these correlations is -65^{0}C-65^{0}C. These correlations by AICHE are given at the following table:

Table 4.12: AICHE's Correlations for Mercury's Solubility [33]

Hg^0 [ng/g] at 25^{0}C	**Solvent**	**Hg^0 Solubility (T: [^{0}C])**	**N**	**R^2**
2206	n-pentane	396 $e^{0,0687T}$	14	0,997
2139	n-hexane	433 $e^{0,0639T}$	10	0,999
1988	n-octane	437 $e^{0,0606T}$	18	0,988
1884	n-dodecane	404 $e^{0,0616T}$	44	0,985
1313	Iso-octane	251 $e^{0,0662T}$	18	0,992
1840	All alkanes	357 $e^{0,0656T}$	221	0,964
2718	benzene	684 $e^{0,0552T}$	12	0,964
2762	toluene	640 $e^{0,0585T}$	23	0,987
2778	ethylbenzene	722 $e^{0,0539T}$	8	0,993
2640	o-xylene	598 $e^{0,0594T}$	12	0,989
2708	All aromatics	673 $e^{0,0557T}$	65	0,960

Hg^0 [ng/g] at 25^0C	Solvent	Hg^0 Solubility (T: [^0C])	N	R^2
1417	Methylene chloride	$406\ e^{0,0500T}$	14	0,996
640	Methanol	$156\ e^{0,0565T}$	14	0,979
52,1	water	$17\ e^{0,0448T}$	13	0,979

These data were compared to the ones found in Mentzelos work [12]. The compounds that exist in both databases are the following: n-pentane, n-hexane, n- octane, benzene, toluene and o- xylene.

It was found that the new data are in very good agreement with the old data for o-xylene, toluene and benzene. For n-pentane, n-hexane and n-octane data from both sources are in good agreement in general, with the greatest deviations existing at high temperatures. The average deviation between the two sources is 17% and thus it is regarded that the new data are reliable. The results of this comparison are given below:

Figure 4.27: Evaluation of AICHE data - Hg's Solubility in nC_5

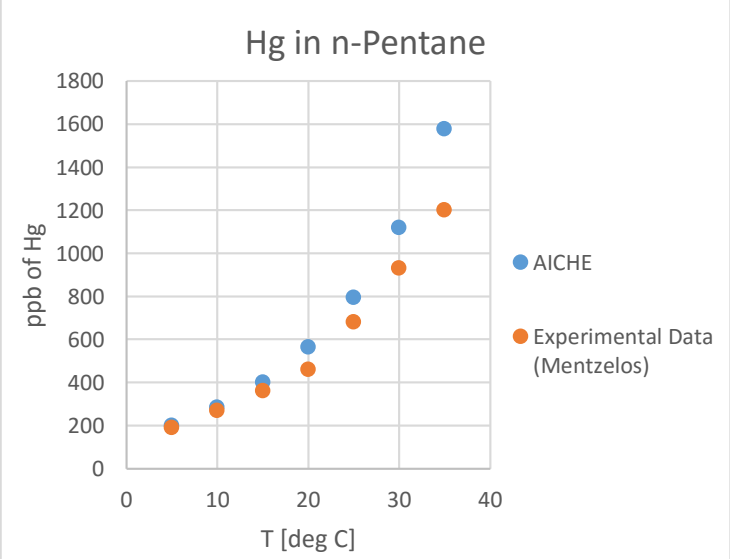

Figure 4.28: Evaluation of AICHE data - Hg's Solubility in nC_6

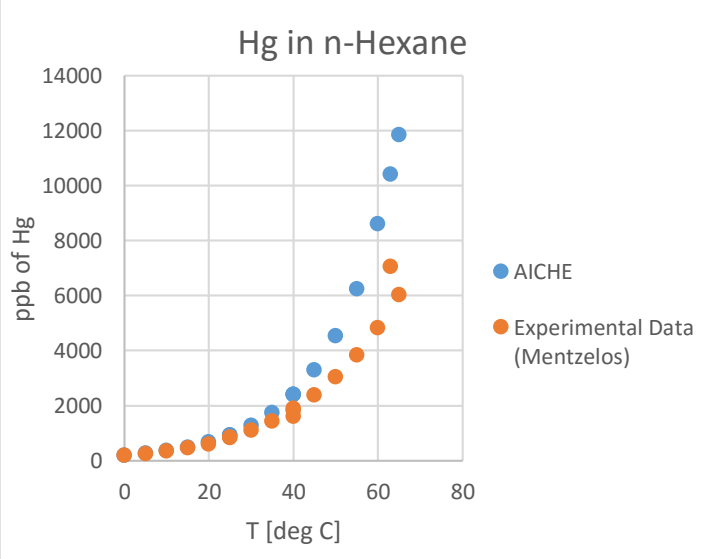

Figure 4.29: Evaluation of AICHE data - Hg's Solubility in nC_8

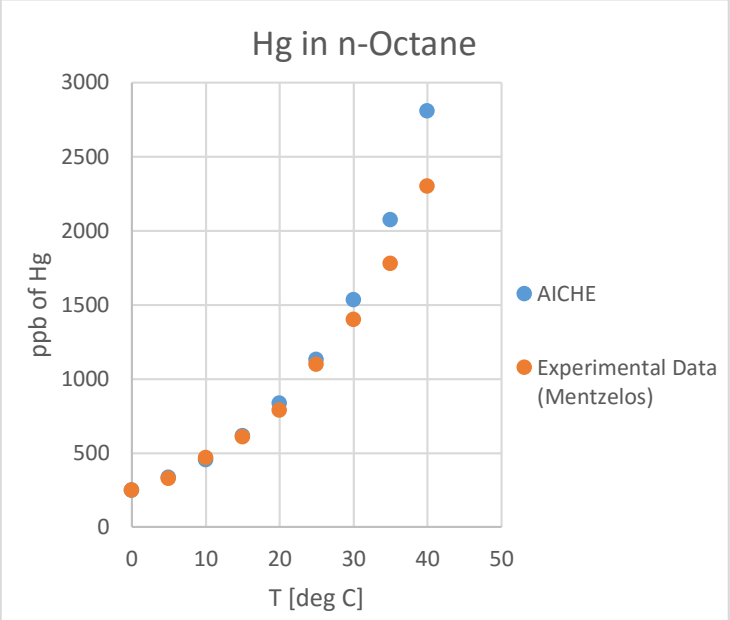

Figure 4.30: Evaluation of AICHE data - Hg's Solubility in Benzene

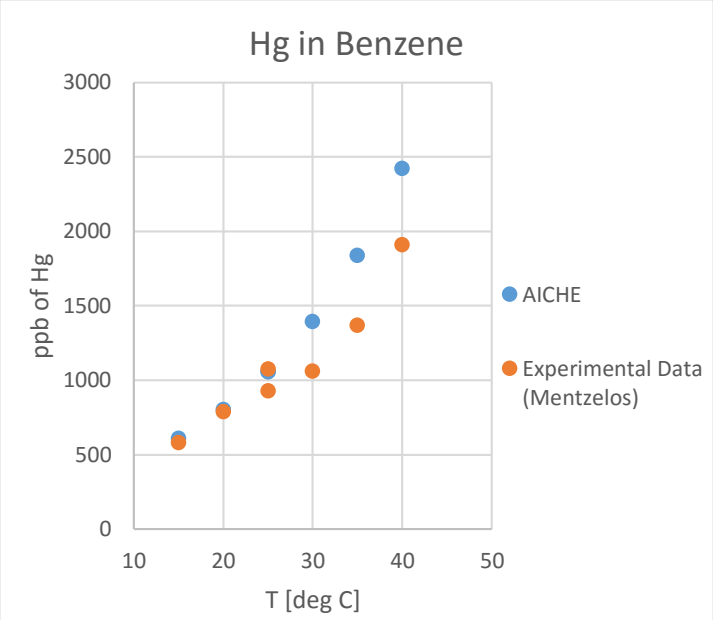

Figure 4.31: Evaluation of AICHE data - Hg's Solubility in Toluene

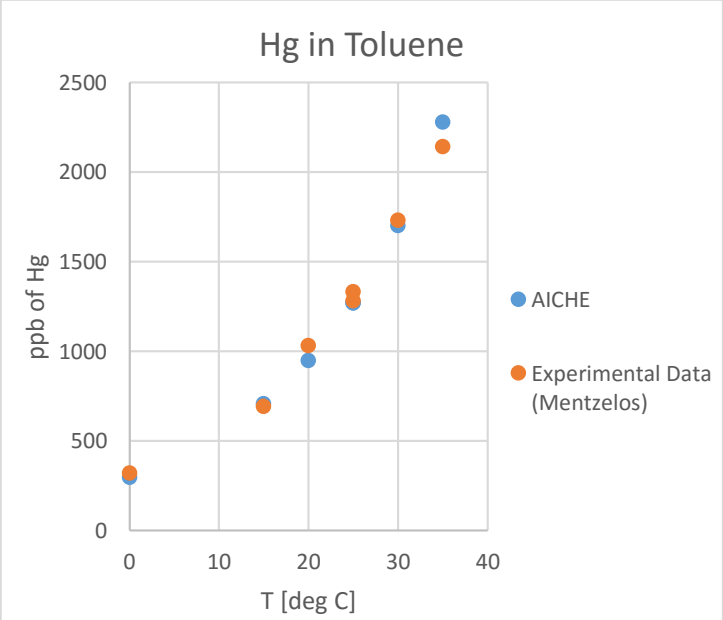

Figure 4.32: Evaluation of AICHE data - Hg's Solubility in O-xylene

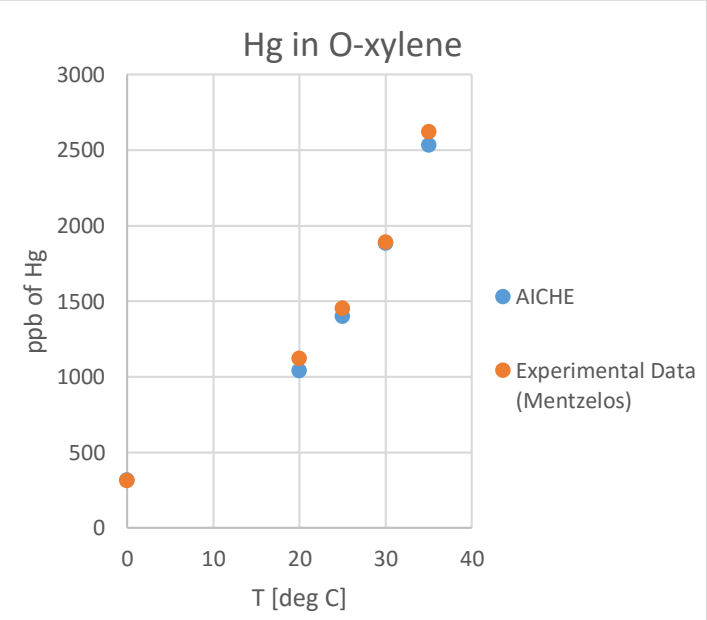

Since the new data are considered reliable, they were used to evaluate the correlations made by Statoil in 2014. Unfortunately, experimental data for only one system were provided by AICHE, for which a k_{ij} can be predicted by Statoil's correlation for the SRK-Twu(Hg) model. That system is the ndodecane-mercury system and thus the evaluation made here is based only on the evaluation of this system.

The correlation for paraffinic hydrocarbons for the SRK-Twu(Hg) was used to generate a k_{ij} for the ndodecane-mercury system. This k_{ij} was used along with the SRK-Twu(Hg) model. Then, the correlation for ndodecane by AICHE was used to generate pseudo-experimental solubility data for the nC_{12}-Hg system. The results are presented below:

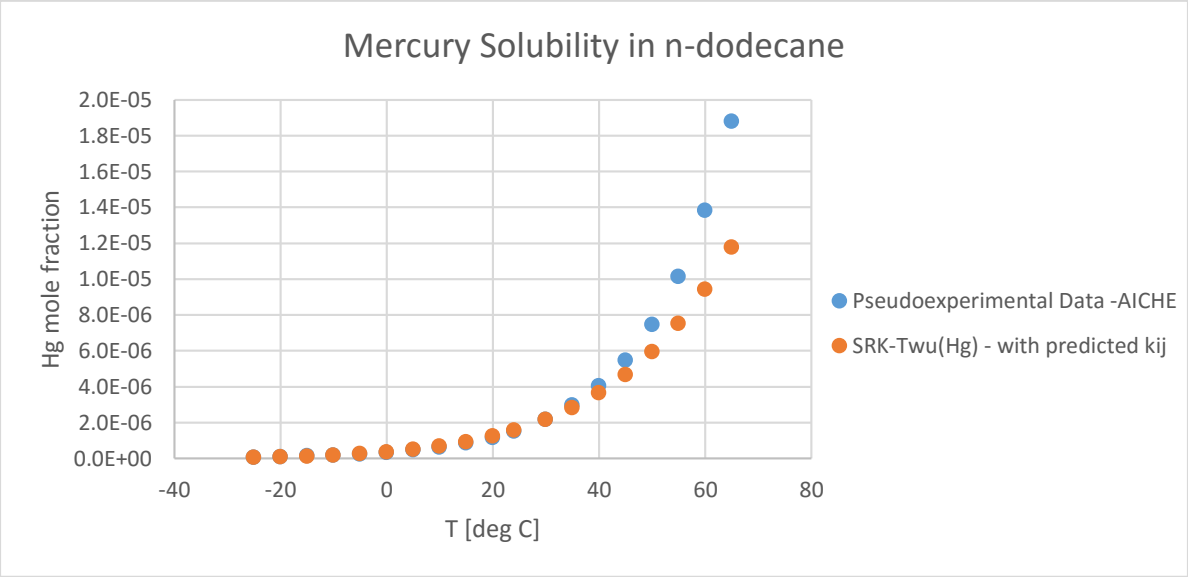

Figure 4.33: Evaluation of AICHE data - Hg's Solubility in nC_{12}

Comments

As it can be seen, the results given by the use of the predicted k_{ij} with the SRK-Twu(Hg) model are in good agreement with the AICHE data up to the temperature of 40^0C. For higher temperatures the deviation becomes higher. It should be noted, though, that when comparing the two data sets, AICHE's data were also found to have positive deviations for all the other systems as shows at Figures Figure 4.27: Evaluation of AICHE data - Hg's Solubility in nC_5-Figure 4.32: Evaluation of AICHE data - Hg's Solubility in O-xylene. For that reason, the positive deviations found for higher temperatures could be attributed to the fact that only pseudo data are available which are generated by a correlation, which was created based on experimental data. Thus, the deviation experienced here is regarded to be because of the fact that a correlation of experimental data is used and not real experimental data.
In conclusion, the correlations provided by Statoil for the SRK-Twu(Hg) model are considered to be reliable and can be used for extrapolation in order to predict binary interaction parameters for hydrocarbon components for which no solubility data are available. Of course, this conclusion is based on an evaluation of only one system and therefore the use of these functions is recommended for hydrocarbons from C_5 to C_{12} only.

4.5 Discussion

The analysis of mercury's solubility in binary and multicomponent hydrocarbon mixtures indicated that the SRK-Twu(Hg) model is the most accurate and consistent, between the seven models tested, for both the liquid and the vapor phase. It is reported by Mentzelos [27], that the UMR-PRMC model can also accurately predict mercury's solubility for both the vapor and liquid phase and thus this model is also considered to be a reliable one.

The original SRK and PR models are not capable of accurately describing mercury's solubility neither for the liquid nor for the vapor phase. The SRK PRO/II default and PR PRO/II default models improved the predictions for the liquid phase, comparing with the SRK and PR respectively, but they did not improve the predictions for the vapor phase. The PRMC(Hg)-no k_{ij} and SRK-Twu(Hg)-no k_{ij} models can accurately describe the vapor phase but not the liquid phase of the systems tested.

- The most consistent model for both the liquid and vapor phase is the SRK-Twu(Hg) model. The liquid phase is very well predicted, but mercury's solubility in the vapor phase is under-predicted by 10%, which results in an under-prediction of the K values.

- From the analysis made above, it is clear that when one tries to better describe the vapor phase, that results in an over-prediction for the liquid phase by 50%, which in turn requires binary interaction parameters to get it fixed. Thus, PRMC(Hg)-no k_{ij} and SRK-Twu(Hg)-no k_{ij} models better describe the vapor phase but they over-predict mercury's solubility in the liquid phase. The vapor phase prediction although better is still and under prediction of around 10%. The over-prediction in the liquid phase and under-prediction of the vapor phase results in an under-prediction of the K values.

- The SRK model cannot accurately predict the vapor phase, neither the liquid phase, since it cannot accurately predict mercury's vapor pressures and no k_{ij} parameters are used for any mercury-HC system. SRK always under-predicts mercury's solubility in hydrocarbon systems, for the vapor phase by 80% and the liquid phase by 60%, which results also in an under-prediction of the K values.

- The PR model, in general, can predict with more accuracy mercury's vapor pressures than the SRK model. That results in better but still an under-prediction of mercury's solubility in the vapor phase by 30%. PR also under-predicts for the liquid phase having a small deviation of 10%, due to cancelation of error, as explained above. These facts, also result in an under-prediction of the K values.

- After analyzing the SRK and PR PRO/II default models, it was found that the binary interaction parameters improved the prediction in the liquid phase, comparing to the SRK and PR respectively, but left intact the vapor phase prediction. This could possibly lead to worse K value prediction (lower K values) and thus to worse prediction of mercury's distribution in a process. This is the case for the SRK PRO/II default model, which provides worse results than the SRK model. However, the case is not the same for the PR and PR PRO/II default models. The results acquired by the PR PRO/II default model were found to be better than the results by PR. This different behavior is believed to be due to the fact that in general PR provides better predictions for the vapor phase, that the SRK. Therefore, the prediction for the vapor phase is better and when using the k_{ij}s then the prediction for the liquid is also qualitatively better, since no cancellation of error takes place. All these suggest that PR PRO/II default provides better results than the SRK PRO/II default models.

- It should be noted that if one uses for their model only vapor phase correction, through an advanced expression for the alpha function such as Twu's or Mathias-Copeman expression, or only liquid phase correction, through the use of binary interaction parameters, they could

possibly get worse results for the K values. That could result to worse predictions of mercury's distribution in a process. It is recommended that both vapor phase and liquid phase correction should be applied at the same time

5. Case Studies – Comparison to Field Data

At the previous parts, an evaluation of the selected models found in the literature was made. The best and most accurate models were found to be the SRK-Twu(Hg) and the UMR-PRMC models, which can both accurately describe mercury's solubility in different hydrocarbon components for both the liquid and the vapor phase.

At this part, three case studies are examined in order to further evaluate the models. In these case studies, simulations of two plants (Plant A and Plant B) were performed and field data from a third plant (Plant C) were used for evaluation. Specifically, for Plant A, no field data were available, thus in this simulation all the eight models that were selected were used for the simulation to further understand the behavior of the models. For Plant B, field data were available. For this simulation, only the best of the models was tested, meaning the SRK-Twu(Hg) and the UMR-PRMC model. Finally, for Plant C, field data were available, however not enough data where provided by Statoil to make the simulations possible. Therefore, for Plant C a qualitative description of mercury's distribution is made.

For these simulations the PRO/II 9.3 software was used to perform the simulations for Plant A for all models except for the UMR-PRMC model. For the UMR-PRMC model, the simulations were made using the CAPE-OPEN platform in Aspen HYSYS 8.6. Finally, the simulations of Plant B were made in Aspen HYSYS 8.6.

5.1 Simulation of Plant A

Rich gas from the fields is transported to Plant A via pipelines. First of all, the pressure and temperature are adjusted. Then the water in the gas is removed so that it can be cooled down to a low temperature (-60°C) without causing ice accretion in pipes and other equipment. The gas is then sent to the separator plant where the wet gas (NGL) is separated out. The wet gas is then sent on to the fractionation plant where it is split into propane, normal butane, iso-butane and naphtha. Ethane is separated out in a special plant and is sold as a separate product. When all these elements have been separated from the gas, the remainings (sales gas or dry gas), which consists mainly of methane.

5.1.1 Simulation Results of Plant A

In this part, a part of the simulation of the Plant A will be presented. The part of the plant that is going to be presented is the fractionation part. This process, also presented below, is consisted of a series of distillation columns that partition the components of natural gas.

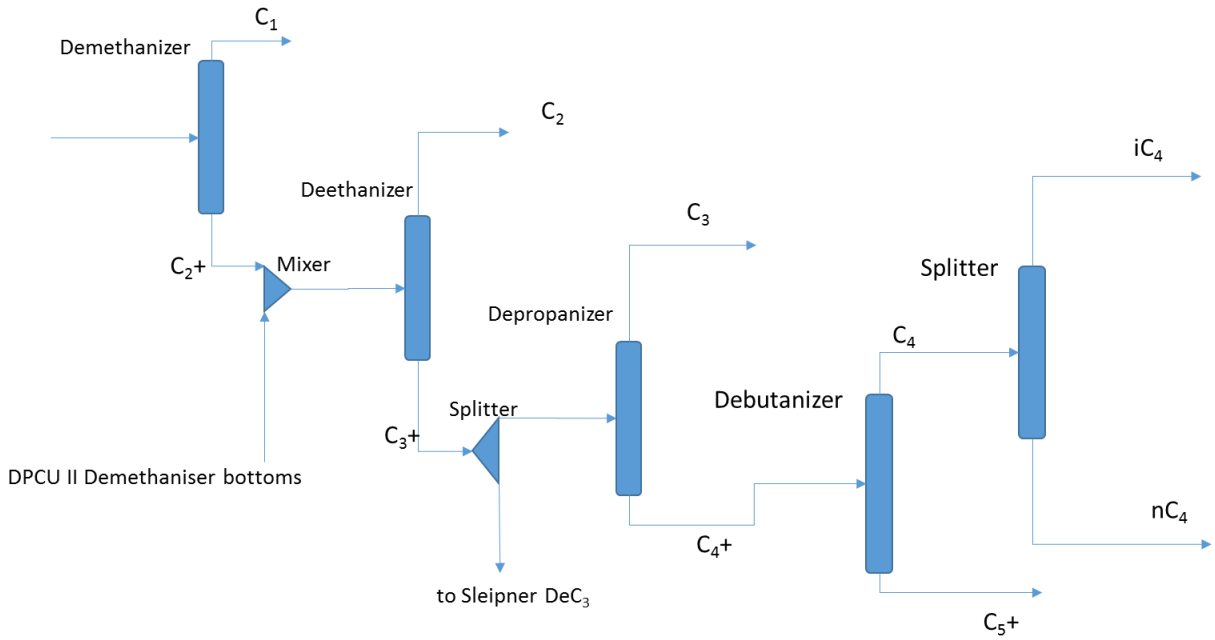

Figure 5.1: Fractionation Part of Plant A

The first column is called Demethanizer and partitions methane as a top product and C_2+ as a bottom product. The second column, called Deethanizer, takes as feed the C_2+ fraction and partitions ethane and the C_3+ fraction. The third column, called Depropanizer takes as feed the C_3+ fraction and partitions propane as a top product and C_4+ fraction as the bottom product. The C_4+ fraction is the feed for the next column called Debutanizer, where the top product consists of nC_4 and iC_4 and the bottom product is the C_5+ fraction. Then, the top product is headed to the splitter, where iC_4 is retrieved as a top product, while the nC_4 is retrieved at the bottom product of the column.

All eight models that were discussed previously, were used for the simulation of this process. The implementation of the all the models, expect for the UMR-PRMC model, in PRO/II, which was used for these simulations, is straightforward as the user can choose the desired equation of state and then the user can apply the desired expression for the alpha function separately for each component. Of course, the user is also able to apply their desired binary interaction parameters. The UMR-PRMC model was tested through the CAPE-OPEN platform in Aspen HYSYS 8.6 as stated earlier.

5.1.1.1 Demethanizer

This column partitions methane and the C_2+ fraction. The column operates at 34 bar and the temperature range is -60 ^{0}C, at the top of the column, and 50 ^{0}C, at the bottom of the column. The way mercury partitions in the column, according each model, is shown at the following table.

Table 5.1: Mercury's Partitioning at the Demethanizer at Plant A

Model	Percentage of mercury at the top	Percentage of mercury at the bottom
SRK	4,7%	95,3%
PR	6,0%	94,0%

Model	Percentage of mercury at the top	Percentage of mercury at the bottom
SRK PRO/II default	2,4%	97,6%
PR PRO/II default	6,4%	93,6%
SRK-Twu(Hg)-no k_{ij}	5,9%	94,1%
PRMC(Hg)-no k_{ij}	6,2%	93,8%
SRK-Twu(Hg)	9,6%	90,4%
UMR-PRMC	0.9%	99.1%

As it can be seen that all models, except for the SRK-Twu(Hg) model, predict that 1-6% percent of the mercury that enters the Demethanizer ends up at the top product. The SRK-Twu(Hg) model predicts a higher percentage of 10% at the top.

The explanation for this behavior can be given considering the K values, shown at the evaluation part in Figures Figure 4.23-Figure 4.26 and Figures Figure 5.2-Figure 5.3. The system becomes richer in ethane and propane from the top of the column to the bottom. As it can be seen in the Figure 4.23, Figure 4.24, Figure 5.2 and Figure 5.3 for the K values for both ethane and propane, the models tend to favor the partitioning of mercury in the liquid phase, since the K values are lower than 1. Thus, when going down the column this tendency becomes stronger and most of the mercury ends up at the bottom.

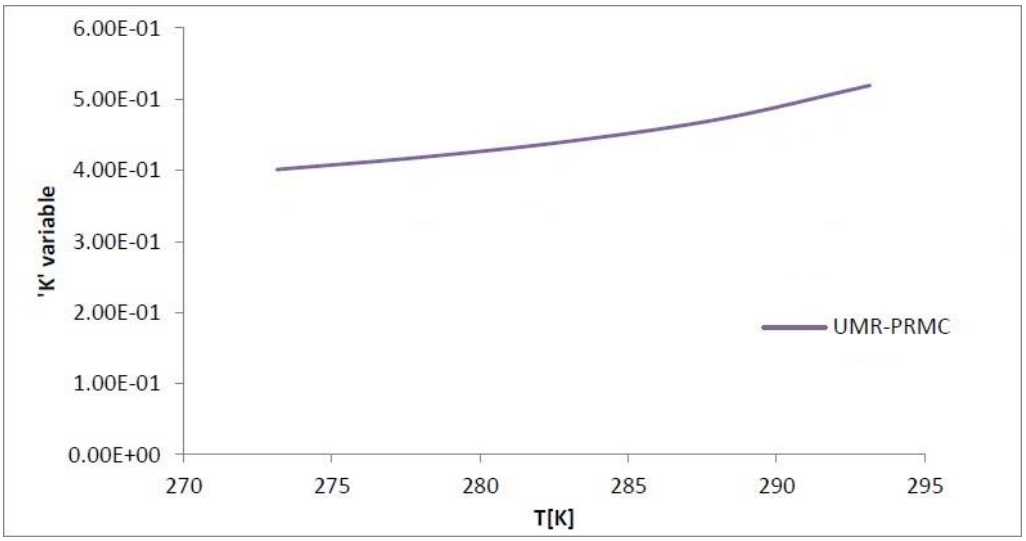

Figure 5.2: K values calculated by UMR-PRMC for the C_2-Hg System (P=23-54 bara) [27]

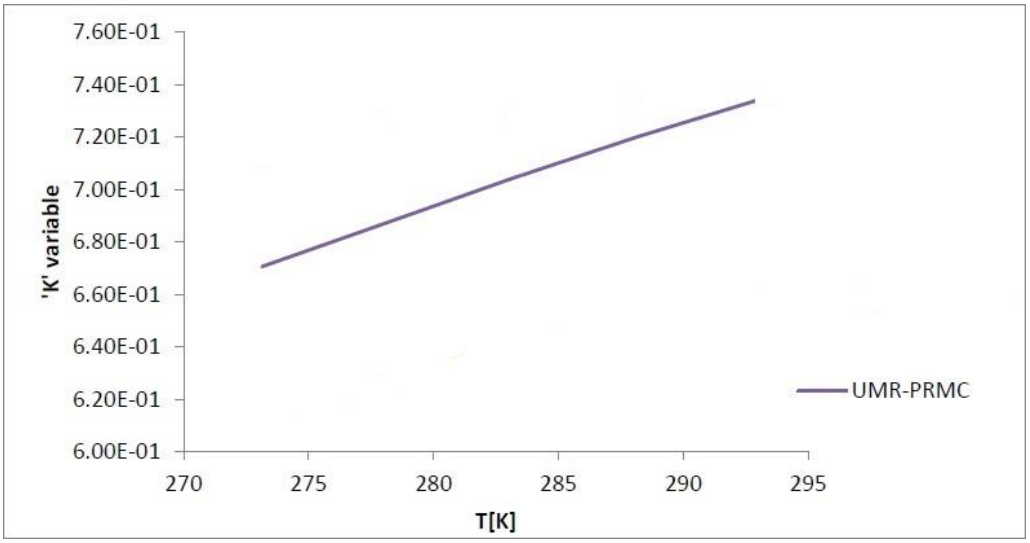

Figure 5.3: K values calculated by UMR-PRMC for the C_3-Hg System (P=4-48 bara) [27]

The percentage of mercury reaching the top of the column is very high, regarding how low the K-values are and that is because of the position of the feeds entering the column as explained below. In particular, the greatest effect is caused by the first feed, which enters the column at the first stage.

At the figure below, one can see the K values for mercury in the Demethanizer.

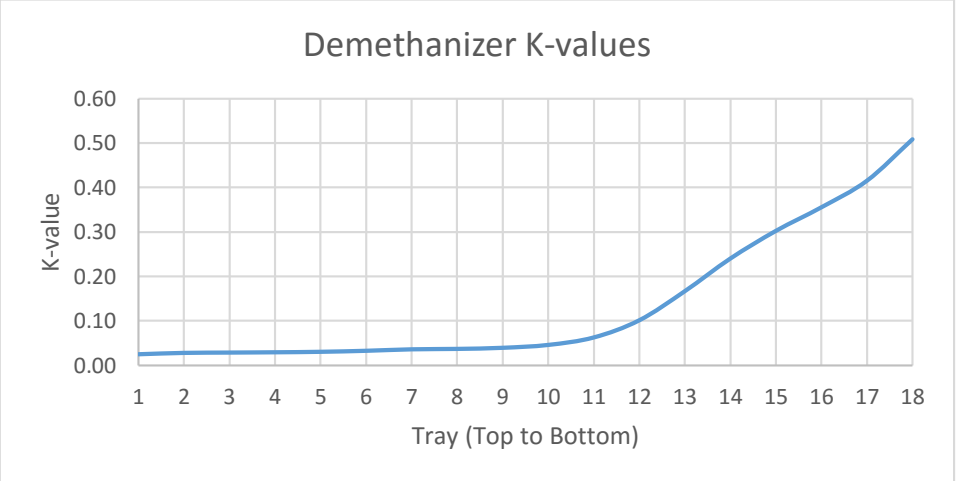

Figure 5.4: K values for Mercury in the Demethanizer at Plant A

The K-values are well below 1, which means that mercury is mostly concentrated at the liquid phase. However, SRK-Twu(Hg) model predicts that 10% of the mercury entering the column ends up at the top product, which is very high for the K-values presented above.

This is due to the position of the feed of the column. Specifically, this column has three feeds.

1. The first feed enters the column at the 1st stage and contains 20% of the mercury entering the column.
2. The second feed enters the column at the 2nd stage, containing 46% of the mercury entering the column.

3. The third feed enter the column at the 7th stage, containing 34% of the mercury entering the column.

The biggest amount of mercury entering the column via the third feed is headed at the bottom of the column, because mercury does not have the chance to move upwards due to the low K values. However, some small part of the mercury entering that stage reaches the stage above, but still the biggest part of this mercury ends up again at the stage below due to the low K values. The same thing happens with the mercury entering the column via the second feed. On the other hand, mercury entering via the first feed can go upwards and head directly to the top product as there is no stage above and thus all mercury that partitions to the vapor phase ends up at the methane product and thus to the sales gas.

To test it, a forth feed was created, that contained all the amount of mercury that previously existed in the first feed, all other components of the first feed remained intact. The forth feed was tested entering at the 2nd and 3rd stage of the column. The results are given below.

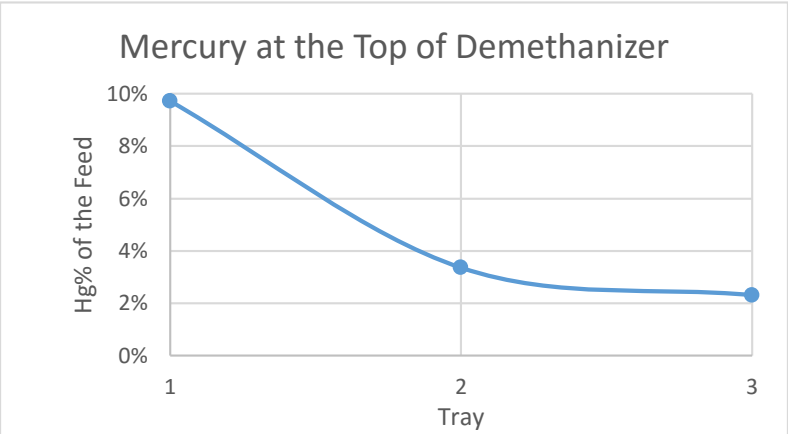

Figure 5.5: Percentage of Hg Reaching the Top of the Demethanizer with Respect to the Inlet Point

As it is clear from Figure 5.5, mercury entering the column at the first stage mainly affects the total amount of mercury that ends up at the methane product. Therefore, to control the amount of mercury reaching the sales gas, it is recommended to control the amount of mercury entering via the first feed of the column.

5.1.1.2 Deethanizer

This column partitions ethane and the C_3+ fraction. The column operates at 26.5 bar and the temperature range is 1 ^{0}C, at the top of the column, and 96 ^{0}C at the bottom of the column.

Table 5.2: Mercury's Partitioning at the Deethanizer at Plant A

Model	Percentage of mercury at the top	Percentage of mercury at the bottom
SRK	0,0%	100,0%
PR	0,0%	100,0%
SRK PRO/II default	0,0%	100,0%
PR PRO/II default	0,1%	99,9%

Model	Percentage of mercury at the top	Percentage of mercury at the bottom
SRK-Twu(Hg)-no k_{ij}	0,0%	100,0%
PRMC(Hg)-no k_{ij}	0,0%	100,0%
SRK-Twu(Hg)	0,3%	99,7%
UMR-PRMC	0.4%	99.6%

All models agree that almost 100% of the mercury ends up at the bottom product. This was expected, as the bottom product consists mostly of C_3 and C_4 products, and mercury is known to strongly follow them. The K values analysis, shown at Figures Figure 4.23-Figure 4.25, Figure 5.2, Figure 5.3 and Figure 5.7, can be used again to explain the behavior of mercury's partitioning. The top product is rich in ethane, for which the K-values are lower than 1. Which means that mercury prefers to follow the liquid phase down the column and not the top product. Moreover, the bottom products are propane, ibutane and nbutane. Propane also has low K values which further support that mercury should end at the bottom product. As regards ibutane, mercury's K values are well above 1 and this is also expected to be the case for nbutane. These K-values would lead mercury to the top product, but both ibutane and nbutane are in very small amounts at the stages between the feed stage and the top stage, as seen at Figure 5.6, and these quantities are not enough to get mercury to the top product.

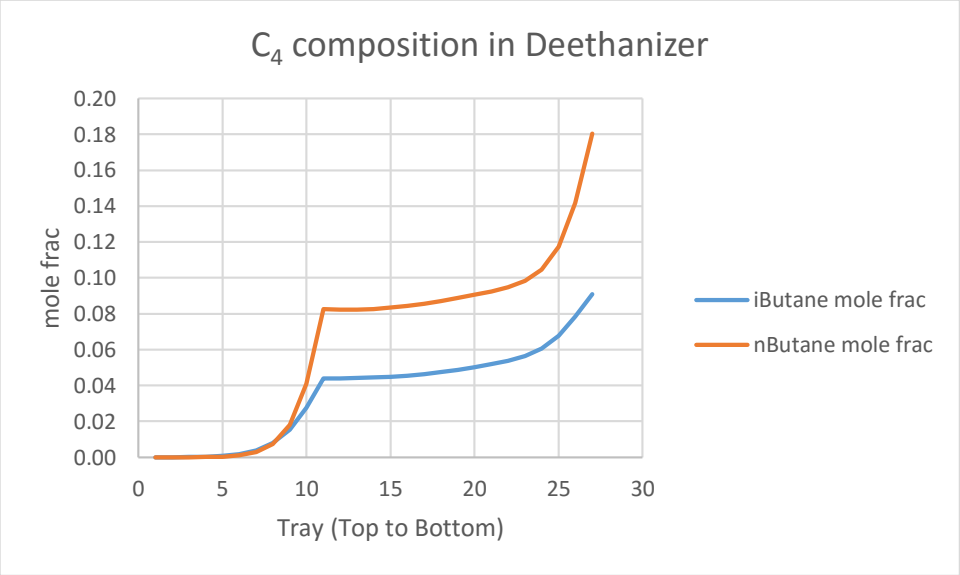

Figure 5.6: Composition of iC_4 and nC_4 in the Deethanizer at Plant A

Below, the K values for the ibutane calculated by the UMR-PRMC model are presented.

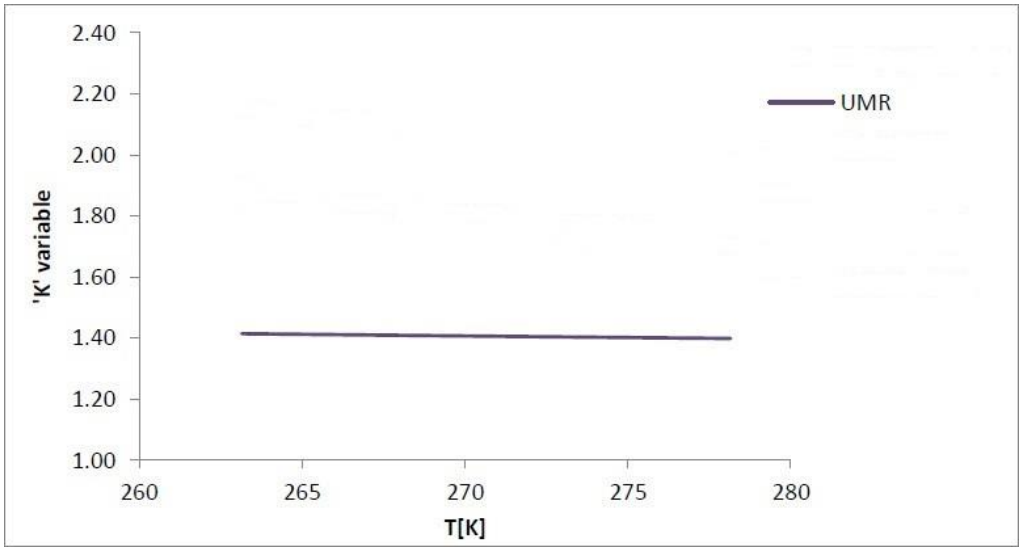

Figure 5.7: K values calculated for UMR-PRMC for the iC4-Hg System (P=1-48 bara)

5.1.1.3 Depropanizer

This column partitions propane and the C_4+ fraction. The column operates at 12 bar and the temperature range is 34 ^{0}C, at the top of the column, and 100 ^{0}C at the bottom of the column.

Table 5.3: Mercury's Partitioning at the Depropanizer at Plant A

Model	Percentage of mercury at the top	Percentage of mercury at the bottom
SRK	3,7%	96,3%
PR	18,7%	81,3%
SRK PRO/II default	0,0%	100,0%
PR PRO/II default	36,2%	63,8%
SRK-Twu(Hg)-no k_{ij}	18,6%	81,4%
PRMC(Hg)-no k_{ij}	22,5%	77,5%
SRK-Twu(Hg)	56,1%	43,9%
UMR-PRMC	62,5%	37,5%

At the two previous columns, mercury followed mostly the bottom product, which is not the case for the Depropanizer. The top product consists mostly of propane. Mercury's K values in propane are below 1, thus preventing mercury from reaching the top product. On the other hand, the top product consists mostly of nbutane and ibutane. Mercury in ibutane has K values well above 1, which prevents mercury from reaching the bottom product. The result is mercury's distribution almost 50-50 (according to the SRK-Twu(Hg) model) between the top and bottom product. This behavior was expected as mercury is known to follow both the C_3 and C_4 products.

The PR, SRK-Twu(Hg)-no k_{ij} and PRMC(Hg)-no k_{ij} models agree that almost 20% of mercury ends up at the top of the column, while SRK-Twu(Hg) predicts that around 56% of mercury ends up at the top of the column. If one sees the K values, for mercury in propane and ibutane, then it can be seen that the PR, SRK-Twu(Hg)-no k_{ij} and PRMC(Hg)-no k_{ij} models almost have the same K values, which means that they partition mercury the same way between the vapor

and liquid phase. On the other hand, SRK-Twu(Hg) model differs from the other models and is closer to the experimental data, having less tendency to send mercury to the liquid phase, in contrast to the others. This is why SRK-Twu(Hg) model predicts more mercury at the top product than the other models. The results provided by the UMR-PRMC model are similar to those of the SRK-Twu(Hg) model.

It is interesting to notice, that the SRK PRO/II default provides worse results than the SRK. As explained before, this behavior is due to the fact, that although binary interaction parameters are used, no vapor phase correction actions are done (for example the use of Twu's alpha function). The SRK under-predicts mercury's solubility in the liquid phase. But when using k_{ij}s this under-prediction is less, resulting in even lower K-values.

The PR PRO/II default model provides the closest results to the SRK-Twu(Hg) model. This was expected, as the K values calculated for the propane-mercury system by the PR PRO/II default model are also the closest results to the SRK-Twu(Hg) model.

5.1.1.4 Debutanizer

This column partitions C_4 and the C_5+ fraction. This column operates at 4 bars and the temperature range is 37 ^{0}C, at the top of the column, and 95 ^{0}C, at the bottom of the column.

Table 5.4: Mercury's Partitioning at the Debutanizer at Plant A

Model	Percentage of mercury at the top	Percentage of mercury at the bottom
SRK	99,7%	0,3%
PR	100,0%	0,0%
SRK PRO/II default	66,2%	33,8%
PR PRO/II default	100,0%	0,0%
SRK-Twu(Hg)-no k_{ij}	100,0%	0,0%
PRMC(Hg)-no k_{ij}	100,0%	0,0%
SRK-Twu(Hg)	100,0%	0,0%
UMR-PRMC	100,0%	00%

All models agree that almost 100% of the mercury entering the column ends up at the top product. This was expected as mercury strongly follows the C_4 compounds. This can further be supported by mercury's K values in ibutane being well above 1, which leads mercury to the vapor phase and to the top product. Furthermore, as seen at the figure below, mercury's concentration at the column follows the same trend as ibutane's concentration inside the column, which means that ibutane's concentration heavily affects mercury's distribution inside the debutanizer.

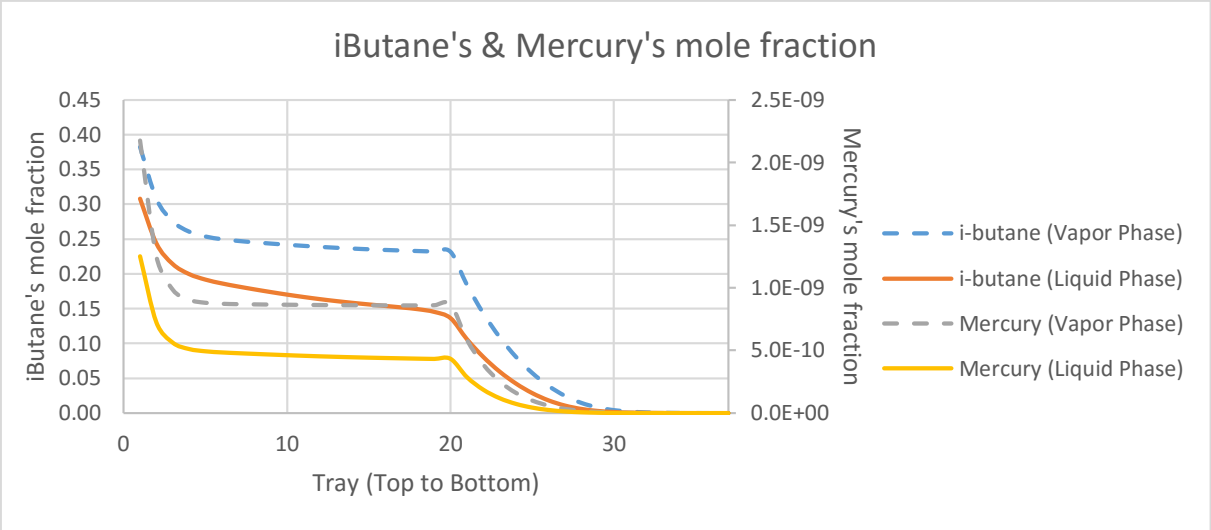

Figure 5.8: Mercury's and iButane's Mole Fraction at the Debutanizer at Plant A

5.1.1.5 Splitter

This column partitions ibutane as the top product and nbutane as the bottom product. This column operates at 5 bar and the temperature range is 35 ^{0}C to 53 ^{0}C.

Table 5.5: Mercury's Partitioning at the Splitter at Plant A

Model	Percentage of mercury at the top	Percentage of mercury at the bottom
SRK	28,5%	71,5%
PR	89,8%	10,2%
SRK PRO/II default	0,0%	100%
PR PRO/II default	99,6%	0,4%
SRK-Twu(Hg)-no k_{ij}	81,2%	18,8%
PRMC(Hg)-no k_{ij}	95,8%	4,2%
SRK-Twu(Hg)	100,0%	0,0%
UMR-PRMC	100,0%	0,0%

All models, expect from the SRK model, agree that the biggest part of mercury ends up at the ibutane product. Specifically, the SRK-Twu(Hg) and UMR-PRMC models predict that 100% of the mercury ends up at the ibutane product. All mercury is headed at the top product because of the high K values of mercury in ibutane as seen at Figure 4.25. Mercury in n-butane is expected to also have high K values, which further support the fact that mercury is headed to the ibutane product and not to the nbutane.

Here, it can be clearly seen that when only the liquid phase is corrected, worse results can be obtained. The SRK PRO/II default model predicts that all mercury follows the ibutane product, while SRK predicts that only 30% of mercury ends up at the ibutane product.

5.1.2 Discussion of the Results – Plant A

In the simulations made, deviations, between the models, existed mainly at the Depropanizer and at the Splitter, but this is due to the K values of the components as explained above. In the

simulations, it was clear that mercury follows strongly the propane and C_4 compounds. It was also noticed that for the Demethanizer the first feed is mainly responsible for the mercury reaching the methane product. Thus if one wanted to minimize mercury in sales gas, then they should minimize mercury in that stream.

The SRK-Twu(Hg) model suggests that 10% of the mercury entering the fractionation part ends up at the methane product, while the remaining mercury splits, almost 50-50 between propane and ibutane. The UMR-PRMC model suggests that 1% of the mercury entering the fractionation part ends up at the methane product, while the remaining mercury splits, almost 60-40 between propane and ibutane.

For the distribution results to be accurate, the models must be able to accurately predict the K values. The best models for doing so, was found to be the SRK-Twu(Hg) and the UMR-PRMC. The PR PRO/II default model, was found to give the second best results after the SRK-Twu(Hg) model for the K values. It was also found to give the closest results to the SRK-Twu(Hg) model in the simulations of Plant A. Therefore, PR PRO/II default model is regarded the best model after the SRK-Twu(Hg) and the UMR-PRMC models.

It is interesting to notice, that the SRK PRO/II default model provides worse results for the K values than the SRK. And this due to the fact, that although binary interaction parameters are used, no vapor phase correction actions are performed. Specifically, the SRK under-predicts mercury's solubility in the liquid phase, but when using k_{ij}s this under-prediction is less, resulting in even lower K-values. However, the case is not the same for the PR and PR PRO/II default models. The results acquired by the PR PRO/II default model were found to be better than the results by PR. This different behavior is believed to be due to the fact that in general PR provides better predictions for the vapor pressures, thus also for the vapor phase, that the SRK. Therefore, the prediction for the vapor phase is better and when using the k_{ij}s then the prediction for the liquid is also qualitatively better, since no cancellation of error takes place. All these suggest that PR PRO/II default provides better results than the SRK PRO/II default models.

5.2 Simulation of Plant B

At this part, an evaluation of the SRK-Twu(Hg) and UMR-PRMC models will be made, testing them against field data, since field data became available for Plant B. These models were selected since it was found, by the previous analysis, to be the best of all the models. The evaluation will be made using Aspen HYSYS 8.6 software package. For the implementation of the UMR-PRMC model in Aspen HYSYS the CAPE-OPEN platform was used.

In order to continue with the evaluation, the following topics should be addressed.

- Implementation of the SRK-Twu(Hg) model in Aspen HYSYS

  The SRK-Twu(Hg) model cannot be directly implemented in Aspen HYSYS, since the user cannot choose separately the expression for the alpha function for each component. The user can only choose a specific model, which applies the same alpha function to all components. Thus, now the SRK-Twu(Hg) model cannot be directly implemented, but the SRK-Twu(All) can. The difference between these two models is that Twu's expression for the alpha function is now used for all components and not only for mercury as happens with

the SRK-Twu(Hg) model. This new model, from now on, will be referred to as SRK-Twu(All).
As it will be shown later, it was found that both models provide almost identical results and thus SRK-Twu(All) can be safely used instead of SRK-Twu(Hg) for the implementation of the model in Aspen HYSYS. Another way to implement SRK-Twu(Hg) model is to implement it through the CAPE-OPEN platform. This kind of implementation was not done in this work.

- Binary interaction parameter for the mercury-water system

  The simulation file Plant B includes water as a component. However, no binary interaction parameter for the mercury-water system was available up to this point. The new solubility data found [33] were used to generate a new k_{ij} for the SRK-Twu(All) model.

5.2.1 Comparison between SRK-Twu(All) and SRK-Twu(Hg) Models

SRK-Twu(Hg) uses Twu's expression for the alpha function only for mercury while for all other components the Soave's expression is used. This model cannot be directly implemented in Aspen HYSYS since there is no option to select a particular alpha function for a specific component. However, one can select to implement SRK-Twu(All), which means that Twu's alpha function will be used for all components. The parameters required for the alpha function for all components, except for mercury, are provided by Aspen HYSYS software package. For mercury, the same parameters used in the SRK-Twu(Hg) model, given in Table 3.3 , are also used in SRK-Twu(All).

In this part, a comparison between these two models was made in order to verify the applicability of the SRK-Twu(Hg) model in Aspen HYSYS. It should be noted that for both models the binary interaction parameters used are those of SRK-Twu(Hg) model. The results are given at the table below.

Table 5.6: Comparison Between the SRK-Twu(Hg) and SRK-Twu(All) Models

Mixture of Mercury with:	Deviation Between SRK-Twu(Hg) and SRK-Twu(All)	SRK-Twu(Hg) deviation from experimental data	SRK-Twu(All) deviation from experimental data (Wiltec)
Methane	0,91%	2,39%	2,23%
Ethane	0,46%	9,39%	9,36%
Propane	0,04%	4,76%	4,76%
ibutane	0,17%	5,86%	5,88%
n-Pentane	0,48%	4,20%	3,86%
CO_2	0,13%	9,53%	9,54%
Nitrogen	1,57%	6,75%	5,22%
Natural Gas Mixture	1,74%	6,85%	7,61%
ibutane + Propane	0,10%	6,65%	6,58%
n-Butane + n-Pentane + n-Hexane	0,48%	7,91%	7,38%

Following the results, at Table 5.6, and the fact that the average deviation between the two models is 0.5%, it is clear that the two models provide almost identical results. Thus, it can be safely said that SRK-Twu(All) can be used instead of SRK-Twu(Hg), using parameters from the SRK-Twu(Hg) model in order to implement SRK-Twu(Hg) model in Aspen HYSYS.

5.2.2 Development of New Binary Interaction Parameter for the Mercury-Water System

Water is a component in the simulation file of Plant B. No binary interaction parameter exists for the water-mercury system since no solubility data were found up to this point. A correlation provided by AICHE was found, which provides solubility data for the mercury-water system. Based on this correlation a binary interaction parameter for this system was calculated.

The correlation provided by AICHE can be found at Table 4.12 and is given below:

$$S_{Hg^0} = 17\, e^{0{,}0448\,T}$$

Where:
S_{Hg}: Hg^0 solubility in water in ng/g
T: Temperature in ^0C

This correlation is stated to be valid between -65^{0}C and +65^{0}C and was used to generate pseudo-experimental data. These data, were then used to fit the binary interaction parameters for mercury-water system using the SRK-Twu(All) model.

Water it is a highly polar component and can develop hydrogen bonds. Equations of state like the SRK are known not to accurately predict these systems, thus a correction of the vapor pressure prediction using Twu's expression for the alpha function, as well as the use of binary interaction parameters are of high importance. It is recommended that for the water component Twu's or Mathias-Copeman's expressions along with binary interaction parameters should be used.

A dynamic process simulator, NeqSim**,** was used to calculate the new k_{ij} for the water-mercury system. The calculated k_{ij} is given below:

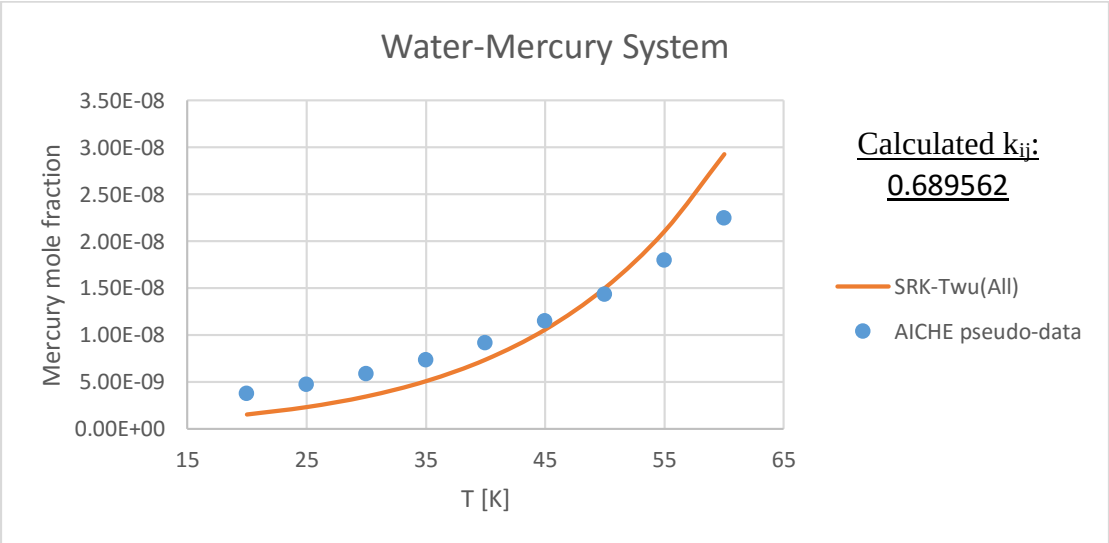

Figure 5.9: Mercury's Solubility in Water

The average deviation for the temperature range tested, which is between 20^0C and 60^0C is 29%. This temperature range was selected for fitting as these temperatures are mostly found in the simulation file were water separations take place.

5.2.3 Evaluation of SRK-Twu(All) Model Based on the Plant B Field Data

In this part, SRK-Twu(All) and the UMR-PRMC models were tested against field data from Plant B. The SRK-Twu(All) model was used instead of the SRK-Twu(Hg) model since the latter can only be implemented in Aspen HYSYS using CAPE-OPEN. The only way to implement the UMR-PRMC in Aspen HYSYS was through the CAPE-OPEN platform, thus this platform was used.

The SRK-Twu(All) model uses SRK EOS with Twu's alpha function for all components. The model is using the default Aspen HYSYS critical parameters (T_c, P_c, ω). The L, M, N parameters for Twu's alpha expression and the binary interaction parameters are the default Aspen HYSYS parameters for all components but for mercury. For mercury the k_{ij}s and the L, M, N parameters used are those of SRK-Twu(Hg) model, given at the Tables Table 3.12 and Table 3.3 respectively. The new binary interaction parameter for the water-mercury system calculated earlier (5.2.2) was implemented in the simulation file.

5.2.3.1 Process Description

The process is consisted of two parts. The first part is the one that leads to the natural gas product and the second one is the one that leads to the LPG and C_5+ products. The feed enters the plant and after some flash drums is split between those two parts.

The part of the feed that is leaded to the "natural gas product part" goes through some flash drums. Then it is leaded through a H_2S and Hg removal unit as well as a CO_2 removal unit. The stream is then leaded through some heat exchangers and flash drums to the dehydration unit and from there to the cold box. After the cold box, a flash drum leads its bottom product to the Demethanizer column. This stream is the lowest feed inlet of the column, as this column has three feed inlets. Part of the top product of the flash drum is leaded in cold box again for further cooling and then makes its way as the top feed inlet of the Demethanizer column. The remaining part of the top product of the flash drum enters the column as the middle feed inlet. The top product of the column is the natural gas product, while the bottom product is the C_3+ product and is headed to the "LPG and C_5+ product part" of the plant for further fractionation.

As regards the "LPG and C_5+ product part" of the plant, the feed stream is enriched by bottom products of flash drums of the "natural gas product part". Then, the stream is leaded through some flash drums to a stabilizer column. The light products are recycled and added to the feed of the "natural gas product part", while the heavy stabilized products are headed, along with the Demethanizer bottom product, to a new distillation column. This column fractionates LPG and C_5+ product. The process is shown at Figure 5.10.

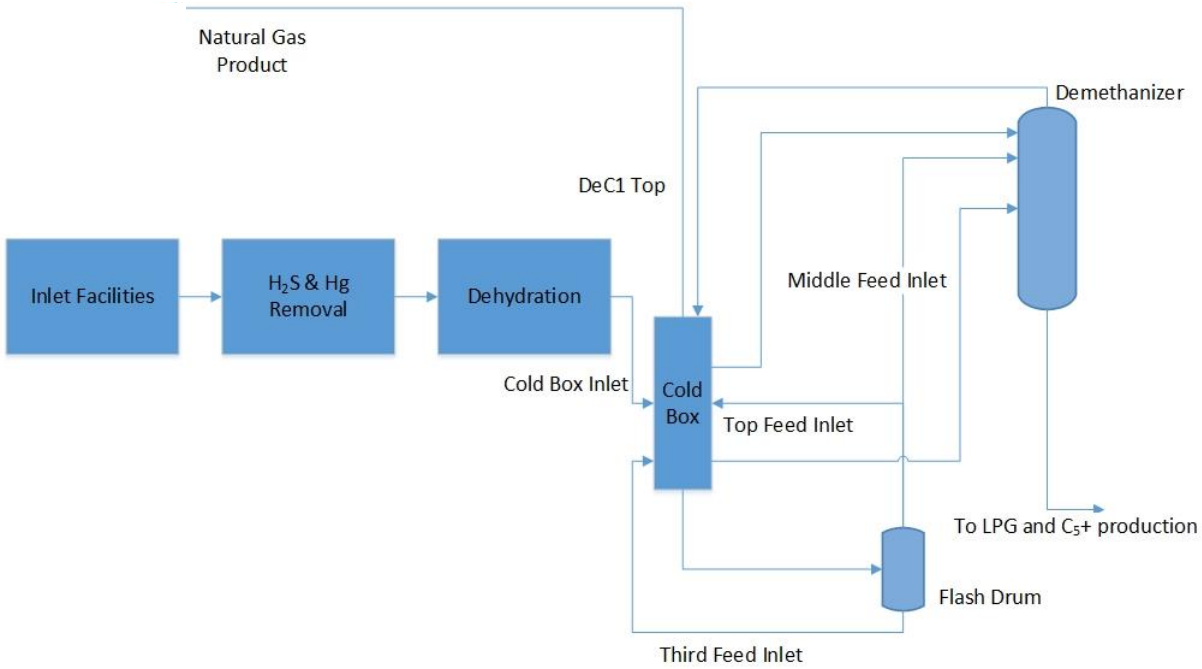

Figure 5.10: Plant B Process

5.2.3.2 Simulation Results

In the process described above, there are some points that should be noted. The Hg, H_2S and CO_2 removal units as well as the dehydration unit cannot be directly simulated in Aspen HYSYS. Instead, a component splitter operation is used. A component splitter is a pseudo process that splits a selected component.

The mercury concentration field data are available for two periods, September 2014 and November 2014. Data are available for Train 1 and Train 2 of the process. It should be noted that at the time of the sampling the mercury removal unit was not in service for Train 1. It should also be noted that in Train 2 the mercury adsorber was in operation but severely damaged.

The experimental data are available at the following locations and can be found at the process diagram above (Figure 5.10):

- Outlet of H_2S & Hg Removal Unit
- Outlet of CO_2 Removal Unit
- Cold Box Inlet
- Top Feed Inlet
- DeC1 Top Product
- Natural Gas Product

As already stated, since the removal units cannot be simulated it is important to know the experimental values at the outlet of these units. Thus, for the cases that these data were available, the experimental values where set as the set points in the Aspen HYSYS simulation. This is the case for the November 2014 Train 1 and the November 2014 Train 2 campaigns. For the other cases where the outlet mercury concentration of the removal units was not available, the Cold Box Inlet point was set as the set point in the Aspen HYSYS simulation.

The results of the simulations are given below. The * mark means that the designated point was used as the set point for the current simulation. In order to calculate mercury's flow, the total flow of each stream is necessary. The actual flows of the streams were not available, therefore, to calculate both the calculated and the experimental mercury flow, the total flow of each stream were taken from the Aspen HYSYS simulation files.

Cold Box Inlet is set as the Basis Point

Table 5.7: SRK-Twu(All) Model Evaluation from Plant B Field Data, September 2014 - Train 1

September 2014 - Train 1	Experimental		Calculated SRK-Twu(All)		Calculated UMR-PRMC	
	Mercury Concentrations [ng/Sm^3]	Mercury Flow [kmol/hr *10^8]	Mercury Concentrations [ng/Sm^3]	Mercury Flow [kmol/hr *10^8]	Mercury Concentrations [ng/Sm^3]	Mercury Flow [kmol/hr *10^8]
Cold Box Inlet*	Classified	Classified	Classified	Classified	Classified	Classified
Top Feed Inlet	//	//	101	5,5	101	5,5
DeC1 Top Product	//	//	13	2,4	8	1,4
Natural Gas Product	//	//	13	2,4	8	1,4

Table 5.8: SRK-Twu(All) Model Evaluation from Plant B Field Data, September 2014 - Train 2

September 2014 - Train 2	Experimental		Calculated SRK-Twu(All)		Calculated UMR-PRMC	
	Mercury Concentrations [ng/Sm^3]	Mercury Flow [kmol/hr *10^8]	Mercury Concentrations [ng/Sm^3]	Mercury Flow [kmol/hr *10^8]	Mercury Concentrations [ng/Sm^3]	Mercury Flow [kmol/hr *10^8]
Cold Box Inlet*	Classified	Classified	Classified	Classified	Classified	Classified
Top Feed Inlet	//	//	76	4,1	76	4,1
DeC1 Top Product	//	//	10	1,9	6	1,1
Natural Gas Product	-	-	10	1,9	6	1,1

Table 5.9: SRK-Twu(All) Model Evaluation from Plant B Field Data, November 2014 - Train 1 (Cold Box Inlet Being The Set Point)

November 2014 - Train 1	Experimental		Calculated SRK-Twu(All)		Calculated UMR-PRMC	
	Mercury Concentrations [ng/Sm^3]	Mercury Flow [kmol/hr *10^8]	Mercury Concentrations [ng/Sm^3]	Mercury Flow [kmol/hr *10^8]	Mercury Concentrations [ng/Sm^3]	Mercury Flow [kmol/hr *10^8]
Cold Box Inlet*	Classified	Classified	Classified	Classified	Classified	Classified
Top Feed Inlet	//	//	92	5,0	92	5.0
DeC1 Top Product	//	//	12	2,2	7	1.3
Natural Gas Product	//	//	12	2,2	7	1.3

Table 5.10: SRK-Twu(All) Model Evaluation from Plant B Field Data, November 2014 - Train 2 (Cold Box Inlet Being The Set Point)

November 2014 - Train 1	Experimental		Calculated SRK-Twu(All)		Calculated UMR-PRMC	
	Mercury Concentrations [ng/Sm^3]	Mercury Flow [kmol/hr *10^8]	Mercury Concentrations [ng/Sm^3]	Mercury Flow [kmol/hr *10^8]	Mercury Concentrations [ng/Sm^3]	Mercury Flow [kmol/hr *10^8]
Cold Box Inlet*	Classified	Classified	Classified	Classified	Classified	Classified
Top Feed Inlet	//	//	90	4,9	90	4.9
DeC1 Top Product	//	//	12	2,2	7	1.3
Natural Gas Product	-	-	12	2,2	7	1.3

In the cases above, it can be seen that the SRK-Twu(All) and the UMR-PRMC models provide almost identical results.

In these case, the Cold Box Inlet is set as the set point. Between the Cold Box Inlet Point and the Top Feed Inlet point there is one flash drum. Both models are in good agreement with the provided field data for the Top Feed Inlet. Thus, the distribution of mercury in the three feed inlets of the Demethanizer calculated by the two models is in good agreement with the field data.

As regards the distribution of mercury in the column the field data indicate that 95% of the mercury entering the column ends up at the top product, while the SRK-Twu(All) and the UMR-PRMC predict that only 11% and 6,5% respectively, of the mercury entering the column reaches the top product.

Along the way from DeC1 Top Product to the Natural Gas Product, the models calculate the same composition, since the stream is the same. The field data indicate a mercury reduction along the way. This could be an indication of mercury's absorption at the pipe walls.

The Outlets of the H_2S & Hg Removal Unit and CO_2 Removal Unit are set as the Base Point

Table 5.11: SRK-Twu(All) Model Evaluation from Plant B Field Data, November 2014 - Train 1 (Outlets of the H_2S, Hg and CO_2 Removal Units Being The Set Points)

November 2014 - Train 1	Experimental		Calculated SRK-Twu(All)	
	Mercury Concentrations [ng/Sm^3]	Mercury Flow [kmol/hr *10^8]	Mercury Concentrations [ng/Sm^3]	Mercury Flow [kmol/hr *10^8]
After H_2S & Hg Removal Unit*	Classified	Classified	Classified	Classified
After CO_2 Removal Unit*	//	//	//	//
Cold Box Inlet	//	//	102	20,0
Top Feed Inlet	//	//	100	5,4
DeC1 Top Product	//	//	116	21,7
Natural Gas Product	//	//	100	18,7

In this case the set points are the outlets of the H_2S & Hg Removal Unit and CO_2 Removal Unit. It should be noted that in this case the material balances are not valid, as at the top of the column (DeC1 Top Product) there is more mercury than at the feed of the column (Cold Box Inlet).

The field data indicate that the amount of mercury that reaches the column ends up at the top product and that some absorption takes place between the top of the column and the final natural gas product. The model, on the other hand, indicates that only 11% of the mercury reaching the column reaches the top product. In addition, the model accurately describes the concentration at the Cold Box Inlet and at the Top Feed Inlet.

The Outlet of the H_2S and Hg Removal Unit is set as the Base Point

Table 5.12: SRK-Twu(All) Model Evaluation from Plant B Field Data, November 2014 - Train 2 (Outlet of the H_2S and Hg removal Units Being The Set Point)

November 2014 - Train 2	Experimental		Calculated SRK-Twu(All)	
	Mercury Concentrations [ng/Sm^3]	Mercury Flow [kmol/hr *10^8]	Mercury Concentrations [ng/Sm^3]	Mercury Flow [kmol/hr *10^8]
After H_2S & Hg Removal Unit*	Classified	Classified	Classified	Classified
After CO_2 Removal Unit	-	-	973	103,3
Cold Box Inlet	Classified	Classified	929	182,2
Top Feed Inlet	//	//	835	45,3
DeC1 Top Product	//	//	109	20,3
Natural Gas Product	-	-	0	0,0

In this case, the mass balances based in the experimental data are not valid, since the DeC1 Top Product has more mercury than the mercury actually entering the column. In this case Cold Box Inlet mercury concentration in not in agreement with the field data. This could be because the CO_2 removal is neither simulated nor experimental data at the outlet of this unit exist.

The Top Feed Inlet is in worse agreement with the field data when comparing with the previous cases. The DeC1 Top Product is in better agreement with the field data when comparing with the previous cases, but this is due to the fact that the model always calculates one order of magnitude lower mercury concentration at the top of the column than the Cold Box Inlet. And since, the Cold Box inlet is calculated with one order of magnitude higher mercury's concentration, the cancellation of error leads to good results at the top of the column.

5.2.1 Discussion of the Results – Plant B

The experimental data indicate that 95% of the mercury entering the Demethanizer ends up at the top product of the column. On the other hand the SRK-Twu(All) model indicates that only around 11% of the mercury entering the column ends up at the top product, while the same percentage for the UMR-PRMC model is 6,5%. Regarding the SRK-Twu(All), this conclusion is in agreement with the study Plant A(5.1), where the mercury calculated reaching the top product, at the Demethanizer, was also around 10% of the mercury entering the column. Statoil in 2011, used the SRK-Twu(Hg)-Statoil 2011 model, to simulate the fractionation part of Plant A. Similar results were acquired then predicting that only 10% of the mercury entering the Demethanizer follows the sales gas [30]. UMR-PRMC indicates a lower percentage of mercury reaching the sales product.

It should be noted, that the two models are in good agreement with the field data in all cases at the Cold Box Inlet and the Top Feed Inlet points, which both are outlets of flash drums. This indicates that the models are accurate at flash calculations.

The mass balances using the experimental data were not always valid. This could be due to experimental error, mercury deposition or mercury absorption at the pipe walls. In general, the uncertainty of the field data was considered to be high. The deviations between the field data

and the models does not necessarily mean that the models used are not accurate, since the models were found to be able to handle flash calculations.

However, the models used are equilibrium models and do not take into account reactions, depositions and absorptions. Thus, the deviation between the experimental data and the calculated results at the DeC1 Top Product point, could be attributed to experimental error, but also to mercury depositions at the sample point. It must be noted, that the models used here are purely thermodynamic models and such models require corrections for non-equilibrium conditions. It is known that the rate of condensation and dissolution of Hg^0 are slow in liquid at low temperatures [4], such as at the top of the Demethanizer. Thus, it is possible that a correction should be applied for the model at these conditions to further improve the models.

The degree of saturation of mercury for all the streams around the cold box, the flash drum after the cold box and the Demethanizer was calculated using the SRK-Twu(All). It was found that none of the streams is close to saturation and therefore it is not probable that liquid condensation of mercury will occur in that streams under normal operating conditions.

Table 5.13: Degree of Saturation for Mercury for Plant B Using the SRK-Twu(All) model

Point of Calculation	Degree of Saturation for Mercury (SRK-Twu(All))
Cold Box Inlet	0.00%
DeC1 Top Product	0.00%
Top Feed Inlet (before valve)	0.00%
Top Feed Inlet (after valve)	0.00%
Middle Feed Inlet (after expander)	0.01%
Third Feed Inlet	0.01%
Top of the Demethanizer(right after the Demethanizer)	0.00%
Bottom of the Demethanizer(right after the Demethanizer)	0.00%

5.3 Plant C – Qualitative Evaluation based on Field Data

For Plant C, field data were available, however not enough data where provided by Statoil to make the simulations possible. Therefore, for Plant C a qualitative description of mercury's distribution is made.

5.3.1 Process Description

The gas that arrives onshore at Plant C is processed and liquefied. Processing involves removal of water/MEG (added initially to inhibit ice formation in the pipeline) and condensate, followed by CO_2 removal, water removal (from the wet gas) and mercury removal. The gas is then cooled and nitrogen is removed to produce LNG and LPG which are then exported along with the treated condensate via dedicated boats. A block diagram of the process is given below.

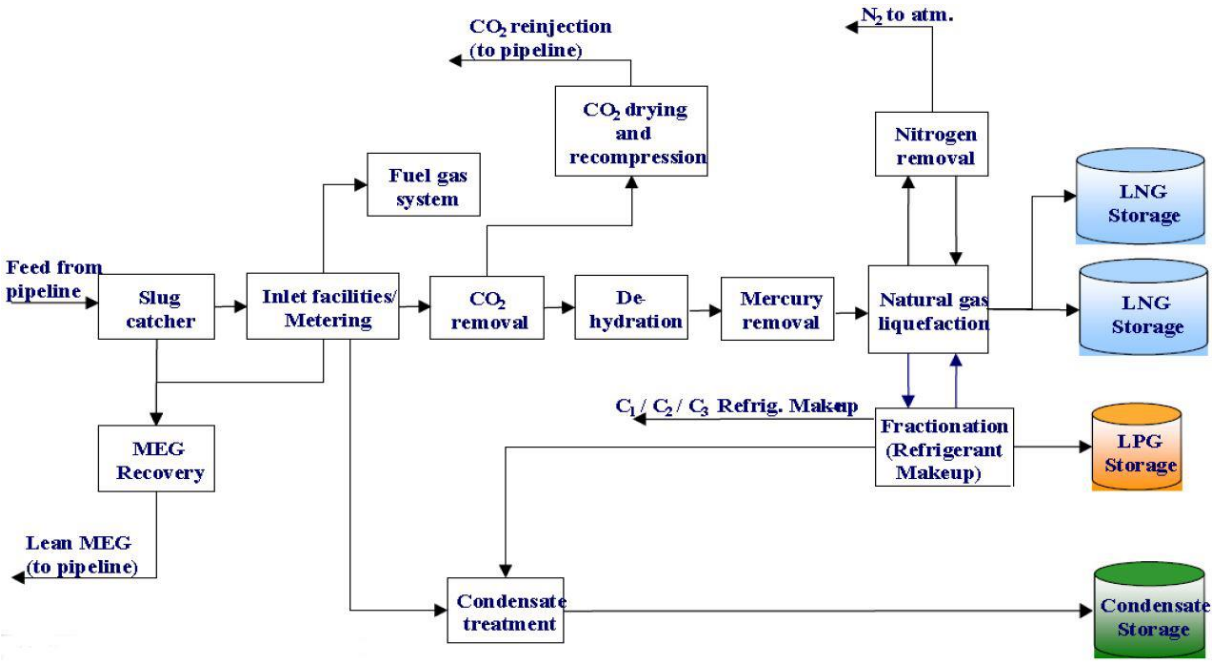

Figure 5.11: Block Diagram of the Processing Scheme in Plant C

5.3.2 Plant C Surveys Results

Two surveys [35, 36] were made at Plant C and they included several measurements at different parts of the process. The aim was to quantify mercury across the Plant C and to give an overview of mercury's distribution within the plant.

It was found that mercury is removed at MEG regeneration column, as the presence of common hydrate inhibitors increase the Hg content in the aqueous phase relative to "pure" water. It was also found that mercury is removed at the carbon dioxide removal unit due to amines. This was expected because, as stated earlier, mercury can react with the H_2S scavenged by the amine to transform into HgS, which could then be found in the amine filters. Mercury was also removed at the dehydration unit. This could be due to the presence of molecular sieves, because mercury is absorbed onto metals. It could also be due to the fact that elemental mercury in gas will dissolve in the liquid glycol dehydrators during treatment for contaminants. Mercury was also found to be removed from the process at the effluent treatment in sludge as HgS.

Mercury was found to reach the environment either directly or via different disposal routes.

- Mercury exists at the CO_2 stream for re-injection, but this stream is occasionally vented to the atmosphere
- Mercury can reach the atmosphere also when flaring the gas or after the combustion of fuel gas
- The sludge removed from the water in the effluent treatment, and solids from the MEG sedimentation tank contained mercury in non-volatile form

5.4 Discussion

The simulations made at the previous sections using the SRK-Twu(All) and UMR-PRMC models indicated that around 10% and 6,5% respectively, of the mercury entering the Demethanizer follows the sales gas, while the remaining mercury concentrates at the LPG products and specifically at the propane and ibutane products. The field data from Plant C supported the results given by the models. They further indicated that mercury can be removed during processing at the MEG regeneration column, but also at the CO_2 removal unit and the dehydration unit, as it was expected (2.3.3). On the other hand, the simulation of Plant B indicated that almost all of the mercury entering the Demethanizer column ends up at the top of the column and consequently to the sales gas. It should be noted, though, that the uncertainty of the experimental data provided by Plant B is considered to be high. Another reason for deviation between Plant B field data and the model could be the fact that the model used is a pure thermodynamic model. As explained earlier, thermodynamic models are equilibrium models and require corrections for non-equilibrium conditions. It is known that the rate of condensation and dissolution of Hg^0 are slow in liquid at low temperatures and these conditions exist at the top of the Demethanizer [2]. Thus, it is possible that a correction should be applied for the model at these conditions to further improve the model. One such correction could be the use of corrected/adjusted tray efficiencies for the trays being at low temperatures, such as the top stage of the Demethanizer. It must also me noted that model used, does not take into account reactions, depositions and absorption effects, which are all reasons for deviation between the model and the field data. Finally, oil and gas installations form part of very dynamic systems where production rates often vary and new wells may come on-line. For this reason, it is likely that the mercury concentrations within gases and liquids arriving at the processing facility will fluctuate, thus creating deviations between the real mercury's concentration at the streams of the plant and the results provided by steady state simulations, such as the ones made using the Aspen HYSYS and PRO/II software packages.

6. Conclusions

In this thesis, an evaluation of mercury distribution models was made by comparing different models to solubility data of mercury in binary and multicomponent mixtures. These models were then used to perform simulations for two natural gas processing plants, Plant A and Plant B.

The analysis of mercury's solubility in binary and multicomponent hydrocarbon mixtures indicated:

- The SRK-Twu(Hg) and the UMR-PRMC were found to be the most accurate models of the eight models tested and are considered reliable for the prediction of mercury's distribution in a real process.

- The SRK-Twu(Hg) under-predicts mercury's solubility by 10% in the vapor phase, but it can accurately predict the solubility of mercury in the liquid phase. This results in the model tending to slightly favor the partitioning of mercury to the liquid phase. It must be noted though, that this deviation could well be due to the experimental uncertainty of the solubility data provided by Wiltec. Conclusively, the SRK-Twu(Hg) model is considered to be reliable.

- The PR PRO/II default model, was found to be the next best distribution model after the SRK-Twu(Hg) and the UMR-PRMC models, since it provided the next best predictions for the K values. The model under-predicts mercury's solubility by 30% and 10% in the vapor and liquid phase respectively. For that reasons it should be used with caution.

- The original SRK and PR models are not capable of accurately predicting mercury's solubility neither for the liquid nor for the vapor phase. The SRK PRO/II default model, improves the results for the liquid phase, comparing to the SRK, but the results of the K values are even worse than those of the SRK. The PRMC(Hg)-no k_{ij} and SRK-Twu(Hg)-no k_{ij} models can accurately describe the vapor phase but not the liquid phase of the systems tested. All these models strongly favor the partitioning of mercury to the liquid phase and are not considered to be reliable.

- It was found that if one uses for their model only vapor phase correction, by using an advanced expression for the alpha function such as Twu's or Mathias-Copeman expression, or only liquid phase correction, by using binary interaction parameters, they could possibly get worse results for the K values. That could result to worse predictions of mercury's distribution. It is strongly recommended that both vapor phase and liquid phase corrections should be applied at the same time.

For the simulations of Plant A and Plant B the Aspen HYSYS and PRO/II software packages were used. The SRK-Twu(Hg) model can be implemented directly in PRO/II but not in Aspen HYSYS. In Aspen HYSYS the SRK-Twu(All) model can be used instead, as it was found to give almost identical results with the SRK-Twu(Hg) model.

A new binary interaction parameter for the mercury-water system was calculated using the solubility data provided by AIChE [33]. This binary interaction parameter was necessary for the simulation of Plant B, since water was included in the simulation file.

The simulations performed using the SRK-Twu(All) and the UMR-PRMC models indicated that 10% and 6,5% respectively, of the mercury entering the Demethanizer follows the sales gas, while the remaining mercury concentrates at the propane and ibutane products. The field data from Plant C supported the results given by these models. On the other hand, the experimental data by Plant B indicated that almost all of the mercury entering the Demethanizer column follows the sales gas. The most possible reason for this deviation is the uncertainty of the experimental data provided by Plant B, which is considered to be high. Other reasons that could cause this deviation could be the following:

- The binary interaction parameters used for the SRK-Twu(All) model are not temperature depended. It is highly likely that the use of temperature depended binary interaction parameters would improve the predictions of the model at low temperature conditions, such as at the top of the Demethanizer.

- The SRK-Twu(All) and the UMR-PRMC models are pure thermodynamic/equilibrium models and require corrections for non-equilibrium conditions. It is known that the rate of condensation and dissolution of Hg^0 are slow in liquid at low temperatures [2].

- The SRK-Twu(All) and the UMR-PRMC models, do not take into account reactions, depositions and absorption effects.

- It is likely that the mercury concentrations within gases and liquids arriving at the processing facility will fluctuate, since oil and gas installations form part of very dynamic systems. Thus, the results provided by steady state simulations could deviate from the reality.

7. Future Work

The SRK-Twu(Hg) and UMR-PRMC models were found to be the most accurate models. However, the simulation of Plant B indicated deviations between the model and the field data. This indicates that there is room for the further improvement of the model and that additional verification of the results of the model via field data should be made. Possible actions to improve the model could be the following:

- Acquisition of solubility data for mercury in hydrocarbons, especially in methane, for low temperatures so that temperature depended binary interaction parameters can be developed. The binary interaction parameters that are now in use are not fitted to solubility data at low temperatures such as -60^0C that occur at the top of the Demethanizer.

- It is known that the rate of condensation and dissolution of Hg^0 are slow in liquid at low temperatures, such as at the top of the Demethanizer. Corrections could be applied for non-equilibrium conditions, since the model, being a pure thermodynamic/equilibrium model, considers only equilibrium conditions.

- It was stated earlier that for natural gas processes the reactions and species transformations of mercury are limited due to the low temperatures in a natural gas processing facility. Mercury remains mainly in the elemental form in natural gas, but reactions do take place and they should be considered in order to further improve the model. Deposition and absorption of mercury at the pipe walls can also take place and should also be considered.

- The acquisition of solubility data for mercury in other components that are of interest to the natural gas industry such as helium, could further improve the predictive ability of the model.

References

1. Abu El Ela, M., et al., *Egyptian gas plant employs absorbents for Hg removal.* Oil & Gas Journal, 2006. **104**(46): p. 52-58.
2. Wilhelm, S.M. and D.A. Kirchgessner, *Mercury in Petroleum and Natural Gas - Estimation of Emissions from Production, Processing, and Combustion*. 2001, Environmental Protection Agency, National Risk Management Research Laboratory.
3. Boschee, P., *Advancements in the Removal of Mercury from Crude Oil.* 2013.
4. Wilhelm, S.M. and N. Bloom, *Mercury in petroleum.* Fuel Processing Technology, 2000. **63**(1): p. 1-27.
5. Mokhatab, S., W.A. Poe, and J.G. Speight, *Handbook of natural gas transmission and processing*. 2006, Burlington, MA: Gulf Professional Pub. xxxi, 636 p.
6. Kidnay, A.J. and W.R. Parrish, *Fundamentals of natural gas processing*. Mechanical engineering. 2006, Boca Raton: CRC Press. 434 p.
7. Eckersley, N. and S. Mishra. *Mercury removal options in hydrocarbon processing facilities*. 2012; Available from: http://www.uop.com/mercury-removal-options-hydrocarbon-processing-facilities/.
8. Lang, D., M. Gardner, and J. Holmes, *Mercury arising from oil and gas production in the United Kingdom and UK continental shelf.* A report by University of Oxford, Department of Earth Sciences, United Kingdom, 2012.
9. Devold, H., *Oil and Gas Production Handbook An Introduction to Oil and Gas Production, Transport, Refining and Petrochemical Industry.* ABB Oil and Gas, 2013.
10. Gas Processors Association. and Gas Processors Suppliers Association (U.S.), *Engineering data book*. 12th ed. 2004, Tulsa, Okla. (6526 E. 60th St., Tulsa 74145): Gas Processors Suppliers Association.
11. Ezzeldin, M.F., *Mercury distribution in an Egyptian natural gas processing plant and its environmental impact*. 2012, University of Aberdeen.
12. Mentzelos, C., *Modelling of Mercury (Hg) Distribution in a Natural Gas Processing Plant.* 2014.
13. Salva, C.A. and D.L. Gallup. *Mercury Removal Process Is Applied to Crude Oil of Southern Argentina*. in *SPE Latin American and Caribbean Petroleum Engineering Conference*. 2010. Society of Petroleum Engineers.
14. Subirachs Sanchez, G., *Mercury in extraction and refining process of crude oil and natural gas*. 2013, University of Aberdeen.
15. CARNELL, P.J., A. FOSTER, and J. GREGORY, *Mercury matters.* Hydrocarbon engineering, 2005. **10**(12): p. 37-40.
16. Evans, M. and L. Brown, *CAPE-OPEN Models for Hg Speciation and Partitioning Flowsheet Development*, in *AIChE Annual Meeting*. 2012.
17. Carnell, P.J., V.A. Row, and R. McKenna, *A re-think of the mercury removal problem for LNG plants.* Johnson Matthey Catalysts, 2007.
18. Coade, R. and D. Coldham, *The interaction of mercury and aluminium in heat exchangers in a natural gas plants.* International Journal of Pressure Vessels and Piping, 2006. **83**(5): p. 336-342.
19. Corvini, G., J. Stiltner, and K. Clark, *Mercury removal from natural gas and liquid streams.* UOP LLC Houston, 2002.
20. Wilhelm, S.M., *Risk Analysis for Operation of Aluminum Heat Exchangers Contaminated by Mercury.* Process Safety Progress, 2009. **28**(3): p. 259-266.
21. Edmonds, B., R. Moorwood, and R. Szczepanski. *Mercury Partitioning in Natural Gases and Condensates*. in *GPA European Chapter Meeting, London*. 1996.
22. EPA. *Health Effects*. 29.12.2014; Available from: http://www.epa.gov/mercury/effects.htm.
23. Panduan, G., *Guidelines On Mercury Management in Oil and Gas Industry*, M.o.H.R. Department of Occupational Safety and Health, Malaysia, Editor. 2011.

24. Peng, J.J., et al., *A comparison of steady-state equilibrium and rate-based models for packed reactive distillation columns.* Industrial & Engineering Chemistry Research, 2002. **41**(11): p. 2735-2744.
25. Skouras-Iliopoulos, E., *Updated model parameters for mercury distribution at Plant A*. 2014: Statoil Internal Report.
26. Voutsas, E., et al., *Thermodynamic property calculations with the universal mixing rule for EoS/GE models: Results with the Peng–Robinson EoS and a UNIFAC model.* 2005.
27. Mentzelos, C., *Modelling of Mercury (Hg) Distribution in Natural Gas Mixtures*. 2015, National Technical University of Athens: Athens, Greece. p. 187.
28. Twu, C.H., et al., *A cubic equation of state with a new alpha function and a new mixing rule.* Fluid Phase Equilibria, 1991. **69**: p. 33-50.
29. Mathias, P.M. and T.W. Copeman, *Extension of the Peng-Robinson equation of state to complex mixtures: Evaluation of the various forms of the local composition concept.* Fluid Phase Equilibria, 1983. **13**(0): p. 91-108.
30. Miguens, A.C.M., et al., *Mercury Distribution in LPG and Natural Gas*. 2011: Statoil Internal Report.
31. Queimada, A., B. Salimi, and R. Barouni, *Simulation of Mercury Distribution In a Middle East Natural Gas Plant using Multiflash™ In Petro-SIM™*. 2014, GPA: Madrid, Spain.
32. *Elementary Mercury Phase Equilibrium in Selected Saturated Hydrocarbons Report*. 2014, Wiltec Research Company, Statoil confidential data.
33. Bloom, N.S. and D. Gallup. *On the Solubility of Mercury in Liquid Hydrocarbons*. 2010 06.02.2015]; Available from: https://aiche.confex.com/aiche/s10/webprogram/Paper175934.html.
34. Tassios, D.P., *Applied chemical engineering thermodynamics*. 1993, Berlin ; New York: Springer-Verlag. xxxi, 710 p.
35. *Mercury Survey - Statoil internal report*. 2013.
36. *Mercury Survey - Statoil internal report*. 2014.